

AD-A284 414



ATION PAGE

Form Approved

OMB No. 0704-0188

2

to supervise and/or coordinate, including the time for reviewing instructions, searching existing data sources, gathering the necessary information, and completing the report. Send comments regarding this burden estimate or any other aspect of this form, including suggestions for reducing the burden, to Washington Headquarters Services, Directorate for Information Operations and Reports, 1215 Jefferson Blvd., Management and Budget, Paperwork Project (0704-0188), Washington, DC 20503.

1. AGENCY USE ONLY (Leave blank)		2. REPORT DATE Aug 94		3. REPORT TYPE AND DATES COVERED	
4. TITLE AND SUBTITLE Impact of Air mass History on the Chemical, Microphysical, and Radiative Properties of clouds at Mt Mitchell, North Carolina				5. FUNDING NUMBERS	
6. AUTHOR(S) James C. Ullman				8. PERFORMING ORGANIZATION REPORT NUMBER AFIT/CI/CIA 94-121	
7. PERFORMING ORGANIZATION NAME(S) AND ADDRESS(ES) AFIT Students Attending: North Carolina State Univ				10. SPONSORING/MONITORING AGENCY REPORT NUMBER	
9. SPONSORING/MONITORING AGENCY NAME(S) AND ADDRESS(ES) DEPTMENT OF THE AIR FORCE AFIT/CI 2950 P STREET WRIGHT-PATTERSON AFB OH 45433-7765				11. SUPPLEMENTARY NOTES	
12a. DISTRIBUTION/AVAILABILITY STATEMENT Approved for Public Release IAW 190-1 Distribution Unlimited MICHAEL M. BRICKER, SMSgt, USAF Chief Administration				12b. DISTRIBUTION CODE Accession For NTIS GRA&I <input checked="" type="checkbox"/> DTIC TAB <input type="checkbox"/> Unannounced <input type="checkbox"/> Justification By Distribution Availability Codes Avail and/or Special Dist A-1	
13. ABSTRACT (Maximum 200 words) DTIC ELECTE SEP 15 1994 S B D 94-29929 14708				15. NUMBER OF PAGES 115 16. PRICE CODE	
14. SUBJECT TERMS				20. LIMITATION OF ABSTRACT	
17. SECURITY CLASSIFICATION OF REPORT		18. SECURITY CLASSIFICATION OF THIS PAGE		19. SECURITY CLASSIFICATION OF ABSTRACT	

DTIC QUALITY INSPECTED 3

94 9 14 075

**IMPACT OF AIR MASS HISTORY ON THE CHEMICAL,
MICROPHYSICAL, AND RADIATIVE PROPERTIES OF
CLOUDS AT MOUNT MITCHELL, NORTH CAROLINA**

by

JAMES CHARLES ULMAN


A thesis submitted to the Graduate Faculty of
North Carolina State University
in partial fulfillment of the
requirements for the Degree of
Master of Science

DEPARTMENT OF MARINE, EARTH, AND ATMOSPHERIC SCIENCES

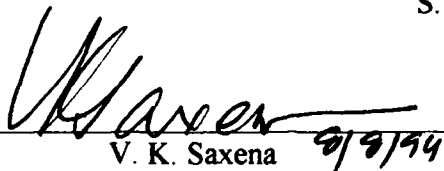
Raleigh

1994

APPROVED BY:



S. P. Arya



V. K. Saxena
Co-Chair of Advisory Committee



V. P. Aneja
Co-Chair of Advisory Committee

BIOGRAPHY

James Charles Ulman was born in Lexington, Kentucky, USA, on 1 August, 1966. He attended secondary school at Loyalsock Township Junior and Senior High School in Williamsport, Pennsylvania, USA from September, 1978 until graduation from High School in June, 1984.

Upon graduation from High School, James applied to and was accepted for Fall admission to the University of Pittsburgh, in Pittsburgh, Pennsylvania, USA. He started studies there in September of 1984, within the School of Engineering. He also at that time enrolled in the University's Air Force Reserve Officer Training Corps (AFROTC) commissioning program.

After transferring to the Department of Physics and Astronomy at Pitt in 1987, James received his Bachelor of Science degree in Physics with Astronomy Option in April of 1988. Upon graduation, he was subsequently commissioned a Second Lieutenant in the United States Air Force.

In December of 1988, James was sent on his first Air Force assignment to the Air Force Institute of Technology's (AFIT) Basic Meteorology Program (BMP) at Texas A&M University. His completion of this one year program resulted in the receipt of a Bachelor of Science degree in Meteorology in December, 1989.

When he completed the BMP, James was sent to become the Officer-in-Charge of a Cadre Weather Team (CWT) at Fort Polk, Louisiana, in January, 1990, and for the next two and half years was in charge of the weather unit's proficiency in combat-type training and field weather forecasting techniques, as well as for direct weather briefing support to the Commander of the Army's 5th Infantry Division (Mechanized). Completion of this tour of duty resulted in his return to an AFIT program at North Carolina State University to pursue a Master of Science degree in Atmospheric Sciences in August of 1992.

The author was married to the former Stephanie Lynn Russin on 25 July, 1992.

ACKNOWLEDGEMENTS

I would like to express my appreciation to the United States Air Force, particularly the Air Force Institute of Technology (AFIT), for providing the opportunity to further my education in pursuit of the Master of Science degree in meteorology. Without their assistance, not to mention their financial support, this endeavor would probably not have been possible.

Deep thanks must go to the members of my advisory committee: Drs. V. K. Saxena, V. P. Aneja, and S. P. Arya, for their support, guidance, and interest in seeing me succeed. I would also like to recognize Dr. G. F. Watson, who initially guided me on my way at N.C. State. I am indebted to Dr. Roland R. Draxler of the NOAA Air Resources Laboratory, for supplying the trajectory model code and background meteorological data used in this thesis. His patience with me while I sifted my way through the workings of his model, not to mention his great tolerance of my many phone calls and requests for data are very greatly appreciated. I would also like to thank some of my fellow students without whom my time at N.C. State would have seemed remarkably empty: Capt Benny D. Holbrook, Capt Craig A. Souza, Maj William H. Bauman, III, Lee Burns, John Anderson, Tom Keever, John Grovenstein, and all of the other members of Cloud Physics Group with whom I either "did time" at Mount Mitchell, or worked with in other ways.

I would especially like to thank my wife, Stephanie, for putting up with all of my odd working hours and derelictions of duty, not to mention the constant moves which military life has forced upon her. There were many times when she wanted to do things when I could not, and I appreciate her unending patience. Because of her, my time here has been a tremendously enjoyable experience.

This research work was supported through the Southeast Regional Center of the National Institute for the Global Environmental Change by the U.S. Department of Energy under cooperative agreement No. DE-FCO3-90ER61010.

TABLE OF CONTENTS

	Page
LIST OF TABLES.....	vi
LIST OF FIGURES.....	ix
 SECTION I: IMPACT OF AIR MASS HISTORIES ON THE CHEMICAL CLIMATE OF MOUNT MITCHELL, NORTH CAROLINA.....	 1
ABSTRACT.....	2
1. INTRODUCTION.....	4
2. METHODOLOGY.....	7
2.1. <i>Experimental Methods and Data Analysis</i>	7
2.2. <i>Cloud Event Characterization</i>	9
2.3. <i>Air Mass Categorization and Determination</i>	10
3. RESULTS AND DISCUSSION.....	14
3.1. <i>Air Mass Arrival Direction versus Local Wind Flow</i>	14
3.2. <i>Field pH Measurements</i>	15
3.3. <i>Summary of Field Results for Ionic Species in Cloud Water</i>	17
3.4. <i>Hydrogen Ion Concentration Analysis</i>	19
3.5. <i>Summary of HY-SPLIT Model Results of Back Trajectories</i>	22
3.6. <i>Summary of HY-SPLIT Model Results for Cloud Water Acidity</i>	23
3.7. <i>Summary of HY-SPLIT Model Results for Ionic Species in Cloud Water</i>	 24
4. CONCLUDING REMARKS.....	28
REFERENCES.....	31
 SECTION II. IMPACT OF EMISSIONS ON THE MICROSTRUCTURE, CHEMICAL COMPOSITION, AND ALBEDO OF CLOUDS AT MOUNT MITCHELL, NORTH CAROLINA.....	 56
ABSTRACT.....	57
1. Introduction.....	59
2. Methodology.....	63
a. <i>Cloud droplet size spectra and in situ cloud albedo</i>	64
b. <i>Cloud water acidity and chemical composition</i>	65
c. <i>Cloud condensation nuclei activation spectrum</i>	65

TABLE OF CONTENTS (continued)

	Page
<i>d. Air mass determination</i>	66
<i>e. Remotely sensed albedo</i>	67
3. Results and Discussion.....	67
<i>a. Cloud microstructure and acidity</i>	68
<i>b. Cloud albedo and cloud microphysics</i>	70
<i>c. Air mass history of AVHRR cases and cloud water chemistry</i>	72
4. Conclusions.....	74
REFERENCES.....	76
APPENDIX.....	91

LIST OF TABLES

SECTION I.

	Page
Table 1. Number and accrued duration of cloud events, by month, for the 1993 field season.....	35
Table 2. Mean pH values, precipitation occurrence, and event duration for each cloud event from the 1993 field season.....	36
Table 3. Average anthropogenic emission rates for SO _x and NO _x as determined from the U.S. EPA Emission Inventories for the air mass sectors relative to Mount Mitchell in units of 10 ³ kg km ⁻² yr ⁻¹	37
Table 4. Important characteristics and parameters of the HY-SPLIT back trajectory model and meteorological data sources used in this study.....	38
Table 5. Cloud water pH ranges with corresponding mean values of ionic constituents (μeq l ⁻¹) for the entire 1993 field season.....	39
Table 6. Mass concentration ratios of chlorine ion to sodium ion (Cl ⁻ /Na ⁺) for all pH ranges of cloud water samples collected from the entire 1993 field season.....	40
Table 7. Values of laboratory, field measured, and calculated (from the aggregate of ionic species) pH and hydrogen ion concentration (in μeq l ⁻¹) for June, August, and the entire 1993 field season..	41
Table 8. Average concentrations (in μeq l ⁻¹) of ionic constituents for June, August, and the entire 1993 field season. Correlation coefficients between the individual ionic species and derived hydrogen ion concentration are also shown.....	42
Table 9. Statistical summary of mean concentrations, in μeq l ⁻¹ , of ionic constituents for air mass trajectories calculated in the HY-SPLIT "Data" configuration for the entire 1993 field season.....	43

LIST OF TABLES (continued)

	Page
Table 10a. Mass concentration ratios of chlorine ion to sodium ion (Cl^-/Na^+) for all air mass sector categories calculated in the HY-SPLIT "Data" configuration from the entire 1993 field season.....	45
Table 10b. Mass concentration ratios of chlorine ion to sodium ion (Cl^-/Na^+) for all air mass sector categories calculated in the HY-SPLIT "Isobaric" configuration from the entire 1993 field season.....	45
Table 11. Statistical summary of mean concentrations, in $\mu\text{eq l}^{-1}$, of ionic constituents for air mass trajectories calculated in the HY-SPLIT "Isobaric" configuration for the entire 1993 field season.....	46

SECTION II.

Table 1. Population mean microphysical parameters and chemical parameters for three pH intervals. The \pm values represent standard errors.....	79
Table 2. Cloud pH, microphysical parameters, CCN, and albedos for nine cases coincident with AVHRR satellite reflectivity data. \pm values represent various instrument error possibilities (5% for pH, CCN, and AVHRR albedo, 17% for N and r_{avg} , and 34% for w). Cloud thicknesses (h) were estimated from skew T-log p plots.....	80
Table 3. Concentrations ($\mu\text{eq l}^{-1}$) of ionic constituents from the cloud water samples which corresponded with the observations of AVHRR satellite data. All quantities shown have a 5% instrument error potential.....	81

LIST OF TABLES (continued)

Page

APPENDIX.

Table A1. File of input parameters for running the HY-SPLIT trajectory model.....	93
Table A2. Cloud water pH ranges with corresponding mean values of ionic constituents ($\mu\text{eq l}^{-1}$) for the June, 1993 field season.....	94
Table A3. Cloud water pH ranges with corresponding mean values of ionic constituents ($\mu\text{eq l}^{-1}$) for the August, 1993 field season.....	95
Table A4. Statistical summary of mean concentrations, in $\mu\text{eq l}^{-1}$, of ionic constituents for trajectories calculated in the HY-SPLIT "Data" configuration for the June, 1993 field season.....	96
Table A5. Statistical summary of mean concentrations, in $\mu\text{eq l}^{-1}$, of ionic constituents for trajectories calculated in the HY-SPLIT "Isobaric" configuration for the June, 1993 field season.....	98
Table A6. Statistical summary of mean concentrations, in $\mu\text{eq l}^{-1}$, of ionic constituents for trajectories calculated in the HY-SPLIT "Data" configuration for the August, 1993 field season.....	100
Table A7. Statistical summary of mean concentrations, in $\mu\text{eq l}^{-1}$, of ionic constituents for trajectories calculated in the HY-SPLIT "Isobaric" configuration for the August, 1993 field season.....	102

LIST OF FIGURES

Page

SECTION I.

- Figure 1. The 1991 U.S. EPA Emissions Inventory of anthropogenic sulfur oxides (SO_x) for the eastern United States.....48
- Figure 2. The 1991 U.S. EPA Emissions Inventory of anthropogenic nitrogen oxides (NO_x) for the eastern United States.....49
- Figure 3. Plots of wind directions corresponding with all cloud events in which pH was measured.....50
- Figure 4. Relative frequencies of pH ranges for all cloud water samples retrieved during the entire 1993 field season.....51
- Figure 5a. HY-SPLIT model results of all pH-associated air mass trajectories calculated during cloud events for the entire 1993 field season.....52
- Figure 5b. Schematic diagram showing HY-SPLIT model results of all pH-associated trajectory calculations from the 1993 field season as in figure 5a, but with arrows representing relative numbers of trajectories in each category.....53
- Figure 6. Mean pH versus HY-SPLIT trajectory category crossed for samples from the entire 1993 field season calculated in the DATA configuration. Error bars represent the standard deviations of the pH within each category.....54
- Figure 7. Mean pH versus HY-SPLIT trajectory category crossed for samples from the entire 1993 field season calculated in the ISOBARIC configuration. Error bars represent the standard deviations of the pH within each category.....55

LIST OF FIGURES (continued)

Page

SECTION II.

- Figure 1. Frequency distributions of the 113 hourly cases for cloud acidity and microstructure measurements, subdivided to show the relative contributions from the various air mass sector origins.....82
- Figure 2. Cloud water pH versus cloud droplet number concentration (cm^{-3}). Least square line fit is shown (slope = -1.4×10^{-3} , intercept = 4.2, $r^2 = 0.64$). Error bars are omitted for clarity. Cloud water pH measurements are assumed accurate to within five percent and cloud droplet number concentrations are assumed accurate to within seventeen percent.....83
- Figure 3. Cloud water pH versus cloud droplet radius (μm). Least square line fit is shown (slope = 0.29, intercept = 2.3, $r^2 = 0.47$). Error bars are omitted for clarity. Cloud water pH measurements are assumed accurate to within five percent and cloud droplet radius concentrations are assumed accurate to within seventeen percent.....84
- Figure 4. AVHRR cloud albedo vs. cloud droplet number concentration (cm^{-3}) and average droplet radius (μm) for nine cases from the 1993 field season. Error bars represent instrument errors (5% for AVHRR albedo and 17% for both cloud droplet number concentration and average radius).....85
- Figure 5. *In situ* cloud albedo vs. cloud droplet number concentration (cm^{-3}) and average droplet radius (μm) for nine cases from the 1993 field season. Error bars represent instrument errors (17% for both cloud droplet number concentration and average radius).....86
- Figure 6. AVHRR cloud albedo vs. cloud water pH and cloud condensation nucleus concentration (cm^{-3}) for nine cases from the 1993 field season. Error bars represent instrument errors (5% for all quantities).....87

LIST OF FIGURES (continued)

	Page
Figure 7. <i>In situ</i> cloud albedo vs. cloud water pH and cloud condensation nucleus concentration (cm^{-3}) for nine cases from the 1993 field season. Error bars represent instrument errors (5% for both pH and CCN concentrations).....	88
Figure 8. 48-hour back trajectories of the nine cases of cloud albedo derived from the AVHRR satellite during the 1993 field season. Plot symbols represent 6-hour time increments along the trajectory.....	89

APPENDIX.

Figure A1. Relative frequencies of pH ranges for all samples retrieved during the June, 1993 field season.....	104
Figure A2. Relative frequencies of pH ranges for all samples retrieved during the August, 1993 field season.....	105
Figure A3. HY-SPLIT model results for all trajectories from the June, 1993 field season.....	106
Figure A4. HY-SPLIT model results for all trajectories from the August, 1993 field season.....	107
Figure A5. HY-SPLIT model results of all air mass trajectories calculated during cloud events for the entire 1993 field season.....	108
Figure A6. Schematic diagram showing HY-SPLIT model results of all trajectory calculations from the 1993 field season as in figure A5, but with arrows representing relative numbers of trajectories in each category.....	109
Figure A7. HY-SPLIT model results for all pH-associated trajectories from the June, 1993 field season.....	110
Figure A8. HY-SPLIT model results for all pH-associated trajectories from the August, 1993 field season.....	111

LIST OF FIGURES (continued)

	Page
Figure A9. Mean pH versus HY-SPLIT trajectory category crossed for samples from the June, 1993 field season calculated in the DATA configuration. Error bars represent standard deviations of the pH within each category.....	112
Figure A10. Mean pH versus HY-SPLIT trajectory category crossed for samples from the June, 1993 field season calculated in the ISOBARIC configuration. Error bars represent the standard deviations of the pH within each category.....	113
Figure A11. Mean pH versus HY-SPLIT trajectory category crossed for samples from the August, 1993 field season calculated in the DATA configuration. Error bars represent the standard deviation of the pH within each category.....	114
Figure A12. Mean pH versus HY-SPLIT trajectory category crossed for samples from the August, 1993 field season calculated in the ISOBARIC configuration. Error bars represent standard deviations of the pH within each category.....	115

IMPACT OF AIR MASS HISTORIES ON THE CHEMICAL CLIMATE OF MOUNT MITCHELL, NORTH CAROLINA

J. C. Ulman and V. K. Saxena*
North Carolina State University
Department of Marine, Earth, and Atmospheric Sciences
Raleigh, N.C. 27695-8208 U.S.A.

submitted for publication to
Atmospheric Environment, Part A

* To whom correspondence should be addressed

ABSTRACT

Cloud water acidity and ionic content, as measured at the Mount Mitchell State Park observing site (35° 44' 05" N, 82° 17' 15" W, 2038 m MSL--highest peak in the eastern U.S.), using a passive cloud water collector, are directly influenced by the trajectories of cloud forming air masses which pass over areas of varying levels of pollutant emission. Regions of the United States which are emitters of high levels of pollutants, such as SO_x and NO_x, will thus serve to reduce observed pH levels in cloud water samples and raise the levels of acidifying ions, such as sulfate and nitrate. Cloud water is one of the best indicators of pollution levels because all water soluble impurities in one cubic meter of air from an air mass are found condensed in typically one milliliter or less of the cloud water. The 48-hr backward trajectories for all 39 cloud events during the 1993 field season (15 May 1993 -14 October 1993) were computed using the Hybrid Single-Particle Lagrangian Integrated Trajectories (HY-SPLIT) model. Three sectors, identified as the polluted sector, from 290° to 65° azimuth relative to the site, the continental sector, 240° to 290° azimuth, and the marine sector, 65° to 240° azimuth, were used to classify the cloud forming air masses. The polluted sector was associated with the lowest overall pH averages, with the marine sector following closely behind. The highest average pH values were received from air masses indicated as having crossed the continental and the marine sectors (in combination), with the largest portions of those air mass trajectories passing through the continental sector (exclusively continental sector air masses were also the most frequent). These observations are in agreement with findings in Colorado where aerosols produced by wind erosion were responsible for neutralizing the precipitation acidity.

Key word index: back trajectories, sulfate, nitrate, cloud water acidity, regional climate change, clouds, aerosols.

1. INTRODUCTION

Cloud water acidity and cloud water chemical composition are strongly associated with the history of the air mass from which the cloud is formed (Castillo *et al.*, 1983, Kelly *et al.*, 1984, DeFelice and Saxena, 1990, Lin and Saxena, 1991a, Lin and Saxena, 1991b, Kim and Aneja, 1992, Aneja and Kim, 1993). Thus, knowledge of the pollutant emission characteristics of the geographic areas that are crossed by air masses will help in understanding the chemical makeup of clouds. Experimental methods of cloud water sampling (Saxena *et al.*, 1989) and subsequent methods of air mass analysis (Yeh, 1988, Saxena and Yeh, 1989, Lin and Saxena, 1991b, DeFelice and Saxena, 1991, Kim and Aneja, 1992, Aneja and Kim, 1993) and ionic analysis (Yeh, 1988, Saxena and Yeh, 1989, Saxena and Lin, 1989, Saxena and Lin, 1990, Kim and Aneja, 1992, Aneja and Kim, 1993), can be used to identify cloud water constituents and pollutants and aid in the determination of the air mass history. Pack *et al.* (1978), have shown that pollutants can be transported over long distances (500 kilometers and beyond) by experimenting with tetroon markers. As a result, changes in cloud water acidity and ionic composition can be documented along with concurrent observations of the directional changes of air masses transporting pollutant aerosols and precursors. Determination of air mass history, however, is not the only manner in which the source-receptor relationships between emissions and impacts of pollutant aerosols can be inferred. Fan *et al.* (1994) have recently used a model employing principal component analysis (Malm *et al.*, 1986, Hopke *et al.*, 1993), which combines both chemical and meteorological data at a site in southwestern Sweden to infer the source regions of aerosols impacting their observation site.

Interest in the transportation of pollutants has heightened recently due to their potential effects on the regional and global climate. Natural and anthropogenic pollutants such as sulfate have the potential to act as effective cloud condensation nuclei (CCN), and the increased number concentrations of cloud droplets resulting from an increase of CCN can potentially counteract the greenhouse warming of the earth-troposphere system. Charlson *et al.* (1992) have shown that an approximate doubling of CCN would be sufficient to counteract the greenhouse warming effect due to a doubling of carbon dioxide. We therefore have conducted research during a 1993 field campaign to fulfill a number of objectives related to these potential climatic implications. We have sought to establish a preliminary relationship between the chemical properties of the observed clouds as well as precursor aerosols and/or trace gases by identifying the history of the cloud forming air masses via back trajectory analysis. In order to limit the uncertainty inherent in back trajectory analysis, we have accomplished the back trajectory calculations using a diagnostic computer model with two distinctly different treatments of vertical motion for every cloud water sample in which the pH was measured. Thus, a season-long statistical analysis of air mass history for the Mount Mitchell site was achieved. To the authors' knowledge, this is the first time that a detailed analysis of air mass history will be reported for each and every cloud water sample retrieved during an entire field season at remote sampling location. As a result of accomplishing the statistical survey of the air mass history versus the cloud water chemistry, we have concurrently added to the growing base of Mount Mitchell observational data, from which comparisons can be made with previous data in order that a continuing assessment of long-term regional climate change can be accomplished. It is the monitoring and assessment of the regional climate that is the

long-term goal of this research. In this paper, we will also explain how the experiments were conducted, what experimental platforms were utilized, and what conclusions may be drawn.

One of the ways through which a study of the long-range transport of pollutants can be launched is to establish an experimental location that is remote enough so as to be essentially immune to the effects of local pollution sources and to be high enough topographically such that it can be considered to be residing in the "free" troposphere. The location should be accessible to retrieve cloud water samples which have been subjected to long-range transport. Also, most importantly, the site must be a plentiful source of cloud water. It is for these reasons that an experimental site in the Mount Mitchell State Park ($35^{\circ} 44' 05''$ N, $82^{\circ} 17' 15''$ W) -- a United Nations Biosphere Reserve and home of the highest peak (2,038 m or 6,684 ft MSL) in the eastern U.S. -- was chosen. The elevation of the actual experimental site (Mount Gibbs) is 2006 m MSL, and it is located approximately 4 km southwest of Mount Mitchell. The ridge line upon which the site resides runs north-northeast to south-southwest. A diagram of the observation site is given elsewhere (Lin and Saxena, 1991b and Aneja and Kim, 1993). Climatologically, the fact that the site is immersed in clouds on 71% of the summer days (Saxena *et al.*, 1989), with 28-41% actual immersion time, measured over the years 1986-1988 (Lin and Saxena, 1991a), is particularly important, because it allows sampling of fairly substantial amounts of cloud water over short periods of time. Thus, statistically significant datasets can be assembled in one summer sampling period. Relevant climatological statistics regarding the observing site at Mount Mitchell are given in Yeh (1988) concerning mean temperatures, expected dates for the onset of frost, riming, snow, fog, precipitation frequency, and other criteria.

2. METHODOLOGY

2.1. *Experimental Methods and Data Analysis*

Cloud water samples were taken at Mount Mitchell during two month-long campaigns in June and August of 1993. In addition, cloud water samples were obtained on one day each in the months of July and October. Lin and Saxena (1991b) give a description of the guidelines used for the onset and termination of cloud events.

Ambient meteorological data were obtained by instruments located on the main observational platform, a 16.5 meter walk-up tower instrumented at the top with an R.M. Young wind speed and direction windbird, a temperature/humidity probe, and a barometric pressure transducer. All of these instruments were wired to a recording device located at the base of the tower which could give instantaneous readouts, 5-, and/or 15-minute averages of wind speed/direction, temperature, relative humidity, and barometric pressure. The person making measurements at any given time hand-recorded 5-minute average readings whenever samples were to be retrieved from the tower (typically at the top of every hour during a cloud event).

The Atmospheric Sciences Research Center (ASRC) (Kadlecek *et al.*, 1983) passive cloud water collector was located on the tower's vertically movable carriage, for the receipt of cloud water droplets during cloud events. Clouds, transported by the ambient winds, would deposit the droplets upon the strings on the collector, where they would drip down by gravity into a replaceable nalgene bottle at the base of the collector. These collection bottles would be replaced every hour during a cloud event and the resulting sample would be taken to an examination point where preliminary analysis would be undertaken. Preliminary analysis consisted of a check

and double-check of the pH with a standard pH probe and weighing of the sample. The remainder of the sample, if any, was then bottled, sealed, and refrigerated for further analysis of ionic composition and a re-check of the pH. A Forward-Scattering Spectrometer Probe, or FSSP (Knollenberg, 1981), was deployed upon the same vertically movable carriage as the ASRC, and had the versatility of rotational movement, so as to be horizontally trained into any ambient winds. This device was used to obtain number counts and size distributions of cloud particles over specific time periods, such that calculations of average radius, droplet number concentration, and liquid water content (LWC) would be possible upon further analysis. During a cloud event, the FSSP would be activated and would continuously intake cloud water droplets, while being pointed into the prevailing wind direction. The cloud microphysical parameters received by the FSSP were then instantaneously transmitted to an analog receiver where the droplet sizes and counts were subdivided into size bins. The continuous receipt of droplet data were then sent to a desktop computer where the data were saved to floppy disk for subsequent data reduction.

Excess cloud water samples, which were bottled, sealed, refrigerated, and returned to N.C. State, underwent subsequent ion chromatography analysis at the North Carolina State University Department of Soil Sciences for aerosol content of the following ionic species: $\text{SO}_4^{=}$, NO_3^- , NH_4^+ , Cl^- , Na^+ , K^+ , Mg^{++} , and Ca^{++} . Kim and Aneja (1992) provide a more detailed discussion of how these ions are measured and analyzed. Mass, molar, and equivalent concentrations for these ionic constituents were tabulated for a total of 234 cloud water samples for the entire field season, 138 for June, 2 for July, and 94 for August of 1993.

2.2. *Cloud Event Characterization*

Markus *et al.* (1991) have stated that there are three primary mechanisms responsible for the formation of clouds in mountainous areas. These are: large-scale weather systems, resulting in widespread regional cloudiness; orography, resulting in localized cap clouds; and solar heating, which gives rise to cumulus-type clouds. The cloud events as seen at Mount Mitchell were primarily of the first two types, with a resulting impact on the cloud event lengths. Thus, for the characterization of cloud events, two categories were used: long and short. Long events were those of greater than 8 hours duration, usually associated with synoptic-scale (frontal or upper-level) disturbances (Lin and Saxena, 1991b). Short events were those of 8 hours duration or less, generally ascribed to local or regional orographic forcing mechanisms (Lin and Saxena, 1991b). Of the 37 cloud events registered during June and August of 1993, 8 events were long events and 29 events were of the short variety (there were 2 additional short events observed in July and October of 1993, one in each month, for a grand total of 39 cloud events registered for the entire 1993 field season). Table 1 gives the number of events for each month as well as the total time, by event category, of all events occurring within each individual month of sampling for the entire field season. The actual immersion time for the site in clouds during potential sampling periods was somewhat difficult to assess since the site, for periods of time, was not always manned. However, based on a rough estimate of the total number of possible sampling days versus the estimate of total number of hours of sampling given in table 1, immersion time of clouds at Mount Mitchell for our field study was approximately 17%. For each of the individual cloud events, we have compiled a list of the mean pH values observed for those events, the corresponding event length type, and whether or not liquid

precipitation was observed in the event. This listing is given in table 2, and shows that the mean pH values for short events ranged from 2.51 to 4.76, the mean pH for long events ranged from 3.02 to 3.76 and liquid precipitation was observed during both types of events, but more commonly for long events (50% of long events contained liquid precipitation).

2.3. *Air Mass Categorization and Determination*

Categorization of air masses traversing the Mount Mitchell observation site was accomplished by utilizing anthropogenic emissions data of SO_x and NO_x provided by the Environmental Protection Agency (EPA, 1993). Because of the importance these pollutants have regarding atmospheric chemistry on local, regional, and global scales (Dignon, 1992), we were able quantify the emission patterns of these pollutants, by converting the raw data from the Regional Emission Inventories into a format whereby any given state in the eastern U.S. falls within a certain *range* of values as given in figures 1 and 2. Clearly, air masses traversing the Ohio Valley regions of the United States for both SO_x and NO_x and also the northeast Atlantic coast in the case of NO_x , are shown in the figures to be areas of highest average emissions of these pollutants.

In a manner similar to Ogren and Rohde (1986) and Hansen *et al.* (1990), we have been able to put each of the states in the eastern half of the U.S. into a particular anthropogenic emission range category. A pollutant region (sector) label was assigned to certain geographic areas relative to the Mount Mitchell observing site. Figures 1 and 2 show that all geographic areas in relative azimuthal proximity to Mount Mitchell, have been divided into three primary regimes (Yeh, 1988, Saxena and Yeh, 1989, Lin and Saxena, 1991b, Kim and Aneja, 1992). The system

characterizes cloud forming air masses as being "polluted" if they are transported from a region bounded by 290° to 65° (Sector 1) azimuth relative to Mount Mitchell, "marine" if transported from a region bounded by 240° to 65° (Sector 2), and "continental" if transported from a region bounded by 240° to 290° (Sector 3). Obviously, considerable cross-over from region to region is possible and expected, and for data which will be subsequently presented, the crossover characteristics will be duly annotated by giving a dual or even triple representation of the air mass sectors crossed. For example, in situations where over 50% of a calculated back trajectory falls within one sector and the remainder falls within another, the air mass characterization will be listed as primary air mass sector (over 50% of the trajectory) followed by the secondary air mass sector (less than 50% of the trajectory).

By taking a circular 1200 kilometer radius (assumed for air parcels averaging 25 km/hr for 48 hours) around the observation site, we have assessed the anthropogenic air mass sector emissions relative to Mount Mitchell, which are given in table 3 for both SO_x and NO_x. From this table, which includes data from a previous EPA emission inventory in 1985, it is evident that Sector 1 has the highest overall anthropogenic emissions followed by Sector 2 and Sector 3 in descending order for both types of pollutants. However, a comparison between the two inventories indicates that Sector 1 SO_x emissions have been reduced 8.0%, Sector 2 emissions were lower by 11.6%, with NO_x emissions actually shown to rise over the six-year period (15.8% for Sector 1, 12.4% for Sector 2, and 13.7% for Sector 3). The large discrepancy between the Sector 3 SO_x emissions for the two inventories is unexplained, but probably has to do with either differing calculation methods or the overall areas within the sector being considered. If there has been such a substantial increase in SO_x emissions from the continental sector during the six-year period

between the inventories, an in-depth investigation of the emissions should be undertaken to explain the causes.

Sulfate aerosols have been hypothesized to be effective CCN (Hegg *et al.*, 1984, Hegg *et al.*, 1991, Parungo, *et al.*, 1994), and will be shown later to be the main aerosol responsible for acidifying the cloud water. Twomey and Wojciechowski (1969) have stated that CCN over marine areas generally have a residence time on the order of three days, while Charlson *et al.*, (1992) have asserted that the residence time of sulfate aerosol is "several" days. Based on these statements and assumptions, and the realization that the error in characterization of air mass movement beyond at least three days can become substantial, we have chosen to investigate the long-range transport of aerosols in cloud forming air masses by calculating 48-hour back trajectories.

The Hybrid Single-Particle Lagrangian Integrated Trajectories (HY-SPLIT) (Draxler, 1992) model was chosen for the determination of the 48-hour air mass back trajectories in this study due its compatibility with desktop computers and high-resolution Nested Grid Model (NGM) meteorological data sources (see table 4 for a summary of the HY-SPLIT model's most important facts and assumptions). This model is an analytical algorithm which provides the user many options for calculated output; everything from forward and backward trajectories to dispersion of air concentrations to surface and upper level maps of many meteorological parameters (relative humidity, vertical velocities, wind patterns, and many more). For the purposes of this investigation, we were interested in calculations of backward trajectories, as these are the best indicators, without the aid of tracers, balloons, and even aircraft, of the origins and subsequent pathways of air masses forming clouds at the Mount Mitchell observation site. The actual calculation

routines for the generation of back trajectories are explained and demonstrated in Draxler (1992) and will not be discussed here. The mathematics involved in the calculations are all based on finite differencing and interpolation approximations of the primary meteorological equations of motion and meteorological thermodynamics.

There are four ways in which the HY-SPLIT model can be used to calculate back trajectories of cloud forming air masses, and all four differ only in the manner in which the vertical motion of the trajectories are treated. The four calculation options are: (1) a "data" option, in which air parcel trajectories utilize vertical motion calculations already provided within the framework of the NGM meteorological data, (2) an "isobaric" option which allows for no vertical motion at all, (3) an "isosigma" option, where air parcels are forced to maintain a constant ratio of their pressure level value to a model surface pressure level value, and (4) a "divergence" option, which calculates the vertical motion of air parcels along a trajectory by using an integrated form of the continuity equation, instead of including vertical velocity data from the NGM as in (1). The data option and the isobaric option were used to calculate back trajectories for every sample in which cloud water resulted in at least an observation of pH, whether or not any remainder was available for further ionic analysis. The isosigma and divergence options were employed for some special cases, such as cases where the observed pH was found to be below a threshold of 3.0 or greater than 4.0, for cases of special interest, such as observations which coincided with remote observational methods, or cases where there occurred some ambiguity as to the categorization of the back trajectory, e.g., back trajectories which ran along sector lines.

3. RESULTS AND DISCUSSION

3.1. *Air Mass Arrival Direction versus Local Wind Flow*

Local winds at Mount Mitchell in previous years and in our study have been shown to arrive in two distinct regimes relative to the ridge line upon which the observation site resides. 92.2% of all cloud event samples resulting in an observation of pH were found to coincide with observed winds arriving either from a zone of 90° to 150° or from a zone of 240° to 330° azimuth relative to the observation site (see figure 3). These regimes are approximately perpendicular to the north-northeast to south-southwest ridge line upon which the site resides, and this occurrence has also been documented for a similar topographical scenario by Mohnen *et al.* (1987) at Whiteface Mountain, New York. It is therefore of further interest to note the approximate percentages of air masses which are shown to arrive at Mount Mitchell in roughly the same direction as the observed winds, to help determine the actual requirement for a detailed set of air mass back trajectory analyses. The percentage of air masses found to arrive at the site from HY-SPLIT calculations within 30° on either side of the observed wind direction for the same time period was 60.6 % for trajectories calculated with the NGM data option and 61.7 % for back trajectories calculated in the isobaric format. Thus, we see that only approximately 3 out of 5 air mass inflow directions, based on our field results, coincide with *in situ* wind observations using a 30° margin-of-error to account for uncertainties in the wind direction and air mass inflow direction. Because of the regimented nature of the wind observations, and the fact that air masses have been shown via HY-SPLIT to arrive from virtually all circumferential directions relative

to the site, we have demonstrated a substantial need for determining air mass history by back trajectory analysis as opposed to inference from *in situ* wind observations.

3.2. Field pH Results

From the entire field season, 192 cloud water samples were retrieved which allowed a measurement of pH. From these, a total of 234 individual samples of cloud water remained available for subsequent ionic concentration analysis. The discrepancy between the two amounts is a result of the fact that cloud water sample receipts were of many different amounts. These amounts ranged from samples which were barely large enough to measure the pH to samples which overflowed the nalgene sampling bottle and resulted in more than one ionic testing sample from one measured pH. Thus, we had situations where multiple ionic results may have been gained from one sample, or, in opposite fashion, an observed pH may have had no ionic composition data associated with it. Nevertheless, the choice for determining when to calculate a back trajectory with HY-SPLIT rested with the observation of whether or not a pH was measured from a particular sample. Thus, there were cases where one set of trajectories were represented for more than one set of ionic data, and vice versa, where trajectories were calculated, but have no associated ionic composition results.

Similar to methods employed by Falconer and Falconer (1980) at Whiteface Mountain, we have subdivided the entire range of pH data from all sampling periods into subranges which demonstrate the relative frequencies of pH values. Figure 4 is a piechart representing the summary of all the pH values from the entire field season. The range of 3.26 to 3.45 is shown to be the largest slice. This range was not only most common for the entire field season, but also included the pH averages for both

of the primary sampling months of the campaign (3.33 ± 0.34 for June, 3.41 ± 0.40 for August, and 3.37 ± 0.45 overall). For figure 4, the relative frequencies of the pH values were taken from the previously mentioned database of 192 overall pH measurements, not from data taken in concert with the ionic concentrations.

In terms of relative pH statistics, a summary of the extreme pH values observed from the data is given as follows:

Highest observed pH: 4.78; 3 October 1993, 1230 GMT

Lowest observed pH: 2.47; 20 August 1993, 1700 GMT

Highest average pH for a cloud event: 4.76 ± 0.03 ; 3 October 1993

Lowest average pH for a cloud event: 2.51; 10 June 1993 (one observation only)

High pH receipts such as that from 3 October (but not specifically from that event) were usually not a result of cloud water only, but from either cloud water mixed with rain and/or drizzle or exclusively from rain. This phenomenon has been previously observed and can be attributed to the dilution effects of higher amounts of available liquid water (Mohnen, 1990, Saxena and Lin, 1990, Markus *et al.*, 1991). Cloud events containing rain mixed with cloud water or rain only were very common, particularly with long events. 11 of the 39 total events contained some sort of liquid precipitation and 4 of the 8 long events (3 in June, 1 in August) contained the same. Second, the low 2.47 pH value occurred at the end of a cloud event, which was very common, since both at the beginning and at the end of many cloud events, the clouds involved tended to have very low liquid water contents. This situation resulted in smaller droplet sizes and higher acidity due to the loss of water to the local canopy, evaporation, and nucleation scavenging (Saxena *et al.*, 1989, DeFelice and Saxena, 1990). Third, the lowest average pH for a cloud event

(2.51) was the only observation during that short event, and thus had no standard deviation, although it must be remembered for this and all other observations, that there existed an approximate 5% pH instrument error possibility. Though this factor was not included in the pH statistics, it must be considered when assessing overall pH patterns and for individual pH measurements.

3.3. *Summary of Field Results for Ionic Species in Cloud Water*

Upon return of refrigerated sample residuals ("splits") to the Department of Soil Sciences at North Carolina State, the samples were analyzed for ionic content of SO_4^- , NO_3^- , NH_4^+ , Cl^- , Na^+ , Ca^{++} , K^+ , and Mg^{++} . Results of this analysis were provided for a total of 234 samples from the entire field season (138 in June, 2 in July, and 94 in August).

Concerning the cloud water pH, it was our expectation that the sulfate and nitrate aerosols, and particularly the sulfate, would be responsible for the substantial reduction in the acidity. Hegg and Hobbs (1979, 1981) have demonstrated that oxidation of SO_2 is the primary mechanism for the production of sulfate in clouds, and previous work at Mount Mitchell has clearly indicated that the SO_2 precursor gas and the resulting sulfate is the primary contributor to the acidity of cloud water at that location (Yeh, 1988, Saxena and Yeh, 1989, Saxena *et al.*, 1989, Saxena and Lin, 1990, Lin and Saxena, 1991b, Kim and Aneja, 1992, Aneja and Kim, 1993).

Table 5 shows the mean concentrations, in $\mu\text{eq l}^{-1}$, of all major ionic constituents of the cloud and rain water received at Mount Mitchell for the 1993 field season. Inspection of the table demonstrates, that for the chosen pH ranges, both sulfate and nitrate concentrations are inversely proportional to the cloud water

pH. For the entire field season, the inverse correspondence for both ions is clear, with a minor deviation from the pattern in the nitrate/pH range of 2.86 to 3.05. Also of note however, is that the standard deviations for all ionic constituents were at least an appreciable fraction of, or in some cases greater than, the mean concentrations shown for a given species. The high deviation values are the results of fairly wide spreads in observed concentrations within the respective pH ranges. The ammonium ion is thought to be the primary aerosol of neutralization for the sulfate and nitrate, and is often in chemical combination as either ammonium sulfate or ammonium nitrate. Thus, its pattern of concentration for the various pH ranges should somewhat mirror those of the sulfate and particularly the nitrate. The ammonium does, in fact, sequentially decrease along with decreasing levels of both sulfate and nitrate, except for the 2.86 to 3.05 and 3.06 to 3.25 pH ranges, where also the nitrate displays a similar characteristic. This is indicative of close chemical associations between the nitrate ions and the ammonium ions. Comparisons of the relative concentrations of sodium and chlorine ions indicate contradictory patterns. Though some sequential decrease is observed for these ions with sequentially increasing pH ranges, there are obvious exceptions to this pattern for the 3.06 to 3.25 range in the case of chlorine and for the three pH ranges covering 3.06 to 3.65 in the sodium examples. Also, the range for pH values greater than 4.25 are extremely high for both ions when measured against all of the other ions. Table 6 gives the results of Cl^-/Na^+ mass concentration ratios for each of the pH ranges discussed in table 5. We would expect that higher ratios would be observed coincident with lower pH ranges, assuming that industrial emissions of chlorine, if emitted for example as HCl, would be coincident with expected low pH values in air masses passing through more polluted regions. However, even though a general

decreasing ratio pattern is observable as the pH ranges increase, which would be consistent with the assumption of higher pH's being associated with cleaner air masses, there are deviations from the pattern in a number of ranges (see pH < 2.66, pH 2.66-2.85, pH 3.46-3.65 and pH > 4.25). Reasons for these pattern deviations could include small errors in the chlorine and/or sodium ion concentrations, errors in the actual measurements of the cloud water pH and/or large numbers of pH values being concentrated near the range bounds for certain cases. Regarding the other analyzed ions, it is shown that concentrations of the calcium and magnesium ions decrease with increasing levels of pH. The same observation is also true of the potassium ion, but since this ion is most closely associated with cloud forming air masses containing marine sector origin, expectations of decreasing concentrations with increased pH ranges would not be as strongly correlated, due to the marine sector having intermediate levels of pH-reducing anthropogenic emissions.

3.4. *Hydrogen Ion Concentration Analysis*

It is essentially the hydrogen ion concentrations, along with the ammonium ions, that must be neutralized and/or overcompensated for, mainly by sulfate and nitrate, in order for cloud water pH values to become as low as has been observed in the 1993 field season and previous field seasons. However, since the hydrogen ion concentrations cannot, as yet, be measured directly from cloud water samples either at the field site or as a result of ionic analysis, the hydrogen ion concentrations had to be either inferred or approximated by calculations of ion balance.

From both the field-measured values of acidity and subsequent laboratory analysis of the pH, a direct calculation of the hydrogen ion concentration was found with the following relationship:

$$\text{pH} = -\log [\text{H}^+]. \quad (1)$$

From all field-measured and laboratory-measured pH values was calculated a corresponding hydrogen ion concentration value using this formula. Additionally, the method of using a summation of all analyzed ions (electroneutrality) to approximate the hydrogen ion concentration was used. The electroneutrality result was necessarily an approximation since not all possible ions could be analyzed for, but there are many instances in the literature where the eight ions which were analyzed from the cloud water in this study have been used to provide an accurate assessment of cloud water acidity and hydrogen ion concentration (Castillo *et al.*, 1983, Lazrus *et al.*, 1983, Waldman *et al.*, 1985, Collett *et al.*, 1989, Collett *et al.*, 1990, to name a few). Therefore, the electroneutrality calculation was made using the following relationship:

$$[\text{H}^+] = \{2 \times [\text{SO}_4^{2-}]\} + [\text{NO}_3^-] + [\text{Cl}^-] - [\text{NH}_4^+] - [\text{Na}^+] - [\text{K}^+] \quad (2) \\ - \{2 \times [\text{Ca}^{++}]\} - \{2 \times [\text{Mg}^{++}]\}.$$

The results of calculations made using this equation have also been tabulated from the analyzed ionic data, and from those, a calculated pH. Results of both methods have been averaged for June, August, and the entire field season and those summaries are given in table 7. The variability in the June data, particularly regarding the average pH generated from the "calculated" hydrogen ion concentration, resulted in an average pH which was much higher than the average field pH. This was the result of errors in the pH and ionic data from early June. The

net effect of this problem was that acidity averages from the first half of June were consistently elevated above the field values, which, for our purposes, had to be considered the most reliable, since they were measured *in-situ* with no lag time between retrieval and measurement (laboratory samples may have been refrigerated for long periods of time before pH testing). Also of note from the June data were the large standard deviations of the "calculated" and laboratory pH values. These are indicative of a much wider range of values compared to the field values and reflect a certain inconsistency in the data which is not seen in August for any of the categories.

Perhaps the best indicators of not only the validity of the ionic data but also the dependence of the pH on the sulfate concentrations are correlation coefficients between the various ionic constituents and the respective hydrogen ion concentrations. Table 8 gives all of the correlation coefficients between these parameters. A high correlation (at or greater than about 0.90) between the sulfate and the hydrogen ion concentration has been shown (Yeh, 1988, Saxena and Yeh, 1989) to prove that the sulfate is the dominant ion responsible for the reduction in overall pH levels at Mount Mitchell. Correlation coefficients should also be high, but not necessarily as high, for nitrate and oppositely, ammonium, which serves to counteract the effects of the sulfate and nitrate. Table 8 shows however that there was a significant deviation from this pattern in June for all three of these ions, where the unusually low correlation between these ions and the hydrogen ion concentration is seen only for the *field* pH values. There is however, an extremely strong correlation between sulfate, nitrate, and ammonium ions with the hydrogen ion concentration for both the laboratory and calculated categories. There is no such disagreement in August, where correlation coefficients for all ionic species are in

excellent agreement. Based on these correlations therefore, and assuming an error in some of the June data, there is little question that the sulfate and nitrate were primary contributors to the reduction in cloud and rain water pH, and that the ammonium and hydrogen ion concentrations were the most significant neutralizing agents. It would also appear that the other ions, due mainly to their much lower overall concentrations, did not contribute appreciably to the acidity levels of the cloud/rain water observed at Mount Mitchell for the 1993 field season.

3.5. Summary of HY-SPLIT Model Results of Back Trajectories

Overall, we calculated 572 individual trajectories for all cloud events in all four trajectory calculation regimes (270 trajectories in June, 4 in July, 288 in August, and 10 in October), regardless of the presence of an indicated pH value. As mentioned previously, the large majority of these trajectory calculations were made in both the data and isobaric configurations, with a few extras calculated in the isosigma and divergence modes. From the total number of trajectories presented above, we decided to further break down the numbers of trajectories by reporting only those trajectories which actually matched in time with a reported pH value (not all trajectories run necessarily coincided with a pH receipt, but were sometimes calculated in order to maintain the temporal continuity within a given cloud event). This resulted in the reduction of the numbers of trajectories to a total of 480 trajectories (238 in June, 4 in July, 230 in August, and 8 in October). The results of producing this subset of trajectory categories, shown in figure 5a, yielded no appreciable changes in the overall pattern of trajectory frequencies. The continental air mass regime represented the most of all types (34.2%) followed by the marine (18.8%) and C/M categories (10.6%) for the aggregate of the field season. Shown

in figure 5b is a schematic representation of figure 5a (minus the M/C/P and M/P/C sector categories). This figure gives the representations (by the relatively-sized arrows--not drawn to actual scale) of the numbers of each type of air mass back trajectory calculated for the whole field season for all cloud events, regardless of pH observation. This figure is presented to provide a visual account of the relative air mass incursions at Mount Mitchell for our field study.

3.6. *Summary of HY-SPLIT Model Results for Cloud Water Acidity*

For field pH data which was matched in time with ionic composition data (234 observations from the field season), we have taken the pH values which corresponded with the trajectories generated for the same observation times and assessed the variance in pH level with air mass sector categories, as shown in figures 6 and 7 for the entire field season (laboratory and calculated pH values were ignored for this analysis, since field values were deemed the most reliable). Because all trajectories were generated in the data and isobaric vertical motion options for all pH and ionic data, plots of the mean and deviations of these quantities were generated for both types of calculations.

Very little overall difference between figures 6 and 7 is evident, as it clear in both that the highest mean pH values were found associated with trajectories from the C/M trajectory category, which had an mean pH value of 3.89 ± 0.42 for the season when trajectories were calculated with data option as opposed to a mean of 3.82 ± 0.38 when isobaric trajectories were generated. For both types of back trajectories, this occurrence can be explained by the fact that a large number of the pH receipts obtained associated with C/M trajectories were found during periods where both cloud and rain water (or rain by itself) were observed at the tower,

particularly during the long event in August. High mean pH values (3.57 ± 0.37 for the data trajectories and 3.63 ± 0.41 for isobaric trajectories) were also observed in cases where the cloud forming air masses were shown to come from the continental sector exclusively. Elevated pH levels for air masses from the continental sector are consistent with the low average anthropogenic emissions of SO_x and NO_x from the continental sector as compared to Sectors 1 and 2. All other pH averages for the remaining trajectory/sector combinations were at or below the seasonal mean of 3.37. Trajectories shown to be either marine exclusively or where the trajectories passed primarily within the marine sector (marine, M/C, and M/P) were all very similar independent of vertical motion option, and all of these types were associated with mean pH values below the seasonal mean. Air masses moving through the polluted sector corresponded with variable results. Exclusively polluted sector trajectories were allied with some of the lowest averages for both types of trajectories, and the same is true of the C/P category, where the concurrent low pH averages indicate that despite air masses in this category being mostly continental in nature, even a small amount of air mass movement through the polluted sector can impact the pH of the cloud water transported by the air mass. Similar arguments can be applied, regarding the secondary air mass, to the P/C category in both calculation options, as the mean pH for this category is higher than for all other categories indicating polluted sector passage, regardless of whether or not the polluted sector was the primary or the secondary sector.

3.7. *Summary of HY-SPLIT Model Results for Ionic Species in Cloud Water*

Table 9 gives the mean ionic concentrations for each of the sector categories from the entire field season when back trajectories were calculated in the HY-SPLIT

data option. Tabular format was chosen over graphical format in this case due to the extremely large standard deviations of the calculated values in some cases. In this table, we see that equivalent sulfate concentrations dominate all equivalent ionic concentrations in every associated trajectory category. Since all pH values for the entire field season were below the CO₂-equilibrated value of 5.60, this observation was certainly expected. However, it is of interest that all sulfate concentrations over 1000 $\mu\text{eq l}^{-1}$ were matched with trajectory categories shown to have polluted sector air mass influence, regardless of whether or not the polluted sector was primary or secondary when in combination with other sectors. Similarly, all nitrate concentrations over 58 $\mu\text{eq l}^{-1}$, except for the marine air mass sector, were shown to be associated with polluted sector influence. The mean values for both ions are thus consistent with the expectation of higher anthropogenic emissions of sulfur and nitrogen-based anthropogenic pollutants from Sector 1. Ammonium, which along with hydrogen ion, is primarily responsible for the neutralization of the sulfates and nitrates, had the second highest mean equivalent concentrations throughout the field season of all eight analyzed ions. Ammonium ion concentrations, when related with various air mass regimes, showed very similar traits to that of the sulfate and nitrate, with the higher concentrations associated with air masses shown to have passed at least partially through the polluted sector. Sodium and chlorine ion concentrations are shown to be most closely associated with the marine sector, as would be expected. However, since some high values of chlorine and sodium were both observed with continental and polluted sector combinations, an investigation of the $\text{Cl}^{-}/\text{Na}^{+}$ ratio was conducted to determine which ion is more closely associated with land-based industrial emission. Industrial ejection of gaseous chlorine has been postulated by Petrenchuk and Drozdova (1966) and Saxena and Lin (1990); thus, it

would be expected that the Cl^-/Na^+ mass concentration ratio would be elevated over more highly polluted areas, while the ratio would be expected to be closer to the 1.80 sea-water value (Millero, 1974) for air masses shown to be mainly marine in origin. Table 10a gives the respective ratios for each sector category, where it is observed that the ratios are much higher where the polluted sector category is represented (P/M, C/P, and M/P), indicating that chlorine, moreso than sodium, was associated with anthropogenic emission areas on land. Values closer to 1.80, such as for the marine, M/C, and C/M categories, all have the marine air mass sector represented, which indicates the likelihood of maritime air contributing to the reduced ratio. The potassium ion concentration is shown in table 9 to be weakly correlated with marine air masses and air masses where the marine sector is represented in combination. Calcium ion concentrations show a moderately strong correlation with polluted air masses (P/C, C/P, and polluted categories yielded the highest values), which is also chemical behavior we would expect given that this ion is usually associated with anthropogenic activities such as cultivation and construction (Gorham *et al.*, 1984, Lin and Saxena, 1991b). The magnesium ion is shown to have the highest concentrations paired with the C/P and P/C sector categories, although high averages were also associated with marine sector categories as well. Magnesium, which is an ion most closely linked with agricultural activities, shows higher concentrations from air masses which have crossed land areas, but the high values for air masses of marine area passage were not expected. It is true, however, that nearly all marine sector air masses crossed substantial amounts of land prior to arrival at the observation site, thus, some land-based ionic constituents could have been represented in air masses indicated to have crossed areas falling within the marine sector.

Table 11 provides the same information as table 9, but for air mass back trajectories which were calculated isobarically. With minor variations, the sulfate and nitrate ions again are shown to have their highest concentration levels associated with air masses of both primary and secondary polluted sector influence, with some of the lowest levels associated with continental air mass influence. The ammonium concentrations are also similar in this regard. Chlorine and sodium ion concentrations for air mass trajectories calculated isobarically again reflect expected higher concentrations for air masses shown to be mainly marine in origin. The Cl^-/Na^+ mass concentration ratios for isobaric back trajectories are given in table 10b, and differ little from those given for data trajectories, except for small increases upward for some of the categories (marine, polluted, C/P, P/C, and M/C/P categories). Otherwise, the ratios all again reflect overall increases for air masses containing non-marine influence (M/P category excepted). Potassium concentrations also varied little with calculation option and were again shown to have high concentrations correlated with marine air masses or air masses indicated to have passed through the marine sector (marine and M/P had the highest mean potassium concentrations). The calcium ion concentrations were found to be highest when paired with the C/P and P/C sector categories, as with the data calculations. The highest equivalent concentration of magnesium ion was again linked with the C/P category, but the second highest value was found associated with the marine category, which, as in table 9, is not an expected result for an ion most commonly linked with anthropogenic processes.

4. CONCLUDING REMARKS

For both types of trajectory calculation routines, air masses which were found via HY-SPLIT to be of polluted origin were correlated with the lowest mean pH values. Highly polluted (exclusively Sector 1) air masses however, were rare for the entire field season (less than 3% of the total in the data configuration and less than 4% of the total in the isobaric configuration). Marine sector air masses (singly and in combinations), resulted in cloud water pH values lower than from previous years. A possible explanation is that heavy pollutant emitters near Mount Mitchell to the south, southeast, or east, may have emerged. However, it is also possible that the use of a different trajectory model, and/or a re-defined manner of assessing the air mass origin, may have resulted in the downward pH trend. These trends were observed regardless of the trajectory calculations used. Continental air masses, and air masses containing either primary or secondary continental influence yielded mixed results. Exclusively continental air masses were the single most commonly observed air mass from the field season and also were correlated with some of the highest pH observations and corresponding low values of acidifying ion concentrations. Elevated levels of cloud water acidity for cases coincident with continental sector influence can be attributed to a combination of low pollutant aerosol emissions from Sector 3, as well as from the neutralizing impact of medium-to-high levels of alkaline soil aerosol particles such as calcium and magnesium ions. Nagamoto *et al.* (1983), have shown that soil-based aerosols produced by wind erosion can result in the neutralization of cloud water near Denver, Colorado. For land-crossed air mass categories which we have shown to display high average

concentrations of alkaline cations, a net increase in cloud water acidity may have been enhanced due to these aerosols.

Results of the averages of both pH and ionic data indicated that there was little difference between the two types of trajectory calculation routines. Small variations were evident, but the large majority of back trajectories resulted in air masses crossing the same sectors for the same ending times at Mount Mitchell, independent of vertical motion option. For the 234 cases which included ionic data, the air mass sectors were identical 85.5% of the time.

Correlations between sulfate and hydrogen ion concentrations for field, laboratory, and calculated values based on electroneutrality showed that the sulfate continued to be the primary contributor to the acidity of cloud and rain water at Mount Mitchell, with nitrate, ammonium, and hydrogen ions essentially controlling the observed acidity levels. Since the sulfate and nitrate were the ions mainly responsible for reducing cloud water pH values, and since these ions were found to have their highest average concentrations associated with polluted sector air masses, we have demonstrated that air masses originating from, or passing through the urban-industrial regions of the U.S. can impact the chemical properties of clouds at remote, rural locations. Because these aerosols (both natural and anthropogenic) can be very efficient CCN, extrapolation of our observations would indicate that anthropogenic emission of the precursor aerosols and gases of sulfate and nitrate from all areas can impact the regional and possibly global climate. It is thus of considerable importance to continue the monitoring of not only the emission patterns of these pollutants, but also the physico-chemical effects of these pollutants as well.

Acknowledgments--This study was supported through the Southeast Regional Center of the National Institute for the Global Environmental Change by the U.S. Department of Energy under cooperative agreement No. DE-FCO3-90ER61010. Dr W. Robarge was responsible for the chemical analysis of the cloudwater samples and for the QA/QC of the data. We are indebted to Dr Roland R. Draxler from the NOAA Air Resources Laboratory for providing the trajectory model code, meteorological background data, and for useful hints and discussions which aided in the production of the back trajectories.

REFERENCES

- Aneja V. P. and Kim D.-S. (1993) Chemical dynamics of clouds at Mount Mitchell, North Carolina. *J. Air & Waste Mgmt. Assoc.* **43**, 1074-1083.
- Castillo R. A., Justo J. E. and McLaren E. (1983) The pH and ionic composition of stratiform cloud water. *Atmos. Environ.* **17**, 1497-1505.
- Charlson R. J., Schwartz S. E., Hales J. M., Cess R. D., Coakley J. A., Jr., Hansen J. E. and Hofmann D. J. (1992) Climate forcing by anthropogenic aerosols. *Nature* **255**, 423-430.
- Collett J. L., Jr., Daube B. C., Jr., Munger J. W. and Hoffmann M. R. (1989) Cloudwater chemistry in Sequoia National Park. *Atmos. Environ.* **23**, 999-1007.
- Collett J. L., Jr., Daube B. C., Jr. and Hoffmann M. R. (1990) The chemical composition of intercepted cloudwater in the Sierra Nevada. *Atmos. Environ.* **24A**, 959-972.
- DeFelice T. P. and Saxena V. K. (1990) Temporal and vertical distributions of acidity and ionic composition in clouds: comparison between modeling results and observations. *J. Atmos. Sci.* **47**, 1117-1126.
- DeFelice T. P. and Saxena V. K. (1991) The characterizations of extreme episodes of wet and dry deposition of pollutants on an above cloud-base forest during its growing season. *J. Appl. Meteor.* **30**, 1548-1561.
- Dignon J. (1992) NO_x and SO_x emissions from fossil fuels: a global distribution. *Atmos. Environ.* **26A**, 1157-1163.
- Draxler R. R. (1992) Hybrid Single-Particle Lagrangian Integrated Trajectories (HY-SPLIT): Version 3.0--User's Guide and Model Description. NOAA Technical Memo ERL ARL-195, Air Resources Laboratory, Silver Spring, MD, U.S.A., 26 pp.
- Environmental Protection Agency (1993) Regional Emission Inventories (1987-1991): Volume II--Emission Summaries. Office of Air Quality Planning and Standards, Research Triangle Park, NC, 27711.
- Falconer R. E. and Falconer P. D. (1980) Determination of cloud water acidity at a mountain observatory in the Adirondack Mountains of New York state. *J. Geophys. Res.* **85**, 7465-7470.

- Fan A., Hopke P. K. and Raunemaa T. M. (1994) A study on the sources of air pollutants observed at Tjorn, Sweden. *J. Aerosol Sci.* **25** Supp. 1, S31-S32.
- Gorham E., Martin F. B. and Litzau J. T. (1984) Acid rain: ionic correlations in the eastern United States. *Science* **225**, 407-409.
- Hansen A. D. A., Artz R. S., Pszenny A. A. P., and Larson R. E. (1990) Aerosol black carbon and radon as tracers for air mass origin over the North Atlantic Ocean. *Global Biogeochemical Cycles* **4**, 189-199.
- Hegg D. A. and Hobbs P. V. (1979) The homogeneous oxidation of sulfur dioxide in cloud droplets. *Atmos. Environ.* **13**, 981-987.
- Hegg D. A. and Hobbs P. V. (1981) Cloud water chemistry and the production of sulfates in clouds. *Atmos. Environ.* **15**, 1597-1604.
- Hegg D. A., Hobbs P. V. and Radke L. F. (1984) Measurements of the scavenging of sulfate and nitrate in clouds. *Atmos. Environ.* **18**, 1939-1946.
- Hegg D. A., Radke L. F. and Hobbs P. V. (1991) Measurements of Aitken nuclei and cloud condensation nuclei in the marine atmosphere and their relation to the DMS-cloud-climate hypothesis. *J. Geophys. Res.* **96**, 18,727-18,733.
- Hopke P. K., Gao N. and Cheng M. D. (1993) Combining chemical and meteorological data to infer source areas of airborne pollutants. *Chemometrics and Intel. Lab. Sys.* **19**, 187-199.
- Kadlecek J., McLaren S., Camarota N., Mohnen V. A. and Wilson J. (1983) Cloud water chemistry at Whiteface Mountain. In: *Precipitation Scavenging, Dry Deposition and Resuspension* (edited by Pruppacher H. R., Semonin R. G. and Slinn W. G. N.), pp. 103-114. Elsevier, New York, NY.
- Kelly T. J., Tanner R. L., Newman L., Galvin P. J. and Kadlecek J. A. (1984) Trace gas and aerosol measurements at a remote site in the northeast U.S. *Atmos. Environ.* **18**, 2565-2576.
- Kim D.-S. and V. P. Aneja (1992) Chemical composition of clouds at Mount Mitchell, North Carolina. *Tellus* **44B**, 41-53.
- Knollenberg, R. G. (1981) Techniques for probing cloud microstructure. In: *Clouds: Their Formation, Optical Properties, and Effects* (edited by Hobbs P. V. and Deepak A.), pp. 15-19. Academic Press, Inc., San Diego, CA.

- Lazrus A. L., Haagenson P. L., Kok G. L., Huebert B. J., Kreitzberg C. W., Likens G. E., Mohnen V. A. and Wilson W. E. (1983) Acidity in air and water in a case of warm frontal precipitation. *Atmos. Environ.* **17**, 581-591.
- Lin N.-H. and V. K. Saxena (1991a) Short communication: interannual variability in acidic deposition on the Mount Mitchell area forest. *Atmos. Environ.* **25A**, 517-524.
- Lin N.-H. and V. K. Saxena (1991b) In-cloud scavenging and deposition of sulfates and nitrates: case studies and parameterization. *Atmos. Environ.* **25A**, 2301-2320.
- Malm W. C., Hohnson C.E. and Bresch J. F. (1986) Applications of principal component analysis for purpose of identifying source-receptor relationships. In: *Receptor Methods for Source Apportionment* (edited by Pace T. G.), pp. 127-148, Air Pollut. Control Assoc., Pittsburgh, PA.
- Markus M. J., Bailey B. H., Stewart R., and Samson P. J. (1991) Low-level cloudiness in the Appalachian region. *J. Appl. Meteor.* **30**, 1147-1162.
- Millero F. J. (1974) The physical chemistry of seawater. *Ann. Rev. Earth Planet Sci.* **2**, 101-150.
- Mohnen V. A., Leonard K., and Bailey B. H. (1987) Cap cloud frequency and chemistry at Whiteface Mountain, *Preprint of AMS Annual Meeting*, pp. 51-54, January 1987, New Orleans, LA. Amer. Met. Soc., Boston, MA.
- Mohnen V. A. (1990) An Assessment of Atmospheric Exposure and Deposition to High Elevation Forests in the eastern United States. Technical Report, EPA 600/3-90/058 (U.S. Environmental Protection Agency, Washington, D.C., U.S.A.).
- Nagamoto C. T., Parungo F., Reinking R., Pueschel R. and Gerish T. (1983) Acid clouds and precipitation in eastern Colorado. *Atmos. Environ.* **17**, 1073-1082.
- Ogren J. and Rohde H. (1986) Measurements of the chemical composition of cloudwater at a clean air site in central Scandinavia. *Tellus* **38B**, 190-196.
- Pack D. H., Ferber G. J., Heffter J. L., Telegadas K., Angell J. K., Hoecker W. H. and Machta L. (1978) Meteorology of long-range transport. *Atmos. Environ.* **12**, 425-444.

- Parungo F., Boatman J. F., Sievering H., Wilkison S. W. and Hicks B. B. (1994) Trends in global marine cloudiness and anthropogenic sulfur. *J. Climate* 7, 434-440.
- Petrenchuk O. P. and Drozdova V. M. (1966) On the chemical composition of cloud water. *Tellus* 18, 280-286.
- Saxena V. K. and Lin N.-H. (1989) Contribution of acidic deposition on high elevation forest canopy to the hydrologic cycle. In: *Acidic Deposition*, pp. 193-201, Publ. No. 179. International Association of Hydrological Sciences (IAHS).
- Saxena V. K., Stogner R. E., Hendler A. H., DeFelice T. P., Yeh J.-Y. R. and Lin N.-H. (1989) Monitoring the chemical climate of the Mount Mitchell State Park for evaluation of its impact on forest decline. *Tellus* 41B, 92-109.
- Saxena V. K. and J.-Y. R. Yeh (1989) Temporal variability in cloud water acidity: physico-chemical characteristics of atmospheric aerosols and windfield. *J. Aerosol Sci.* 19, 1207-1210.
- Saxena V. K. and Lin N.-H. (1990) Cloud chemistry measurements and estimates of acidic deposition on an above cloudbase coniferous forest. *Atmos. Environ.* 24A, 329-352.
- Twomey S. A. and Wojciechowski T. A. (1969) Observations of the geographical variation of cloud nuclei. *J. Atmos. Sci.* 26, 684-688.
- Waldman J. M., Munger J. W., Jacob D. J., and Hoffmann M. R. (1985) Chemical characterization of stratus cloudwater and its role as a vector for pollutant deposition in a Los Angeles pine forest. *Tellus* 37B, 91-108.
- Yeh, J.-Y. R. (1988) Measurements of cloud water acidity and windfield for evaluating cloud-canopy interactions in Mt. Mitchell State Park. MS thesis (available from D. H. Hill Library, North Carolina State University).

Table 1. Number and accrued duration of cloud events, by month, for the 1993 field season.

MONTH	EVENT TYPE	NUMBER OF EVENTS	COMBINED EVENT DURATION (Approx. hr:min)
JUNE	Long	4	61:20
	Short	17	37:30
JULY	Long	0	0:00
	Short	1	2:00
AUGUST	Long	4	71:00
	Short	12	47:30
OCTOBER	Long	0	0:00
	Short	1	2:00
TOTALS	Long	8	132:20
	Short	31	89:00
GRAND TOTAL		39	221:20

Table 2. Mean pH values, precipitation occurrence, and event duration for each cloud event from the 1993 field season.

1993			1993						
Cloud Event	Mean pH	St. Dev.	Liquid Precip.	Event Category	Cloud Event	Mean pH	St. Dev.	Liquid Precip.	Event Category
June 3 (a)	3.07	0.19	No	Short	June 30 (a)	3.20	0.09	No	Short
June 4 (a)	2.87	0.06	No	Short	July 1 (a)	3.09	0.23	No	Short
June 8 (a)	3.07	0.00	No	Short	August 5 (a)	3.73	0.11	Yes	Short
June 10 (a)	2.51	0.00	No	Short	August 5 (b)	3.44	0.28	No	Long
June 10 (b)	3.25	0.00	Yes	Short	August 6-7 (a)	3.76	0.43	Yes	Long
June 13 (a)	3.23	0.19	Yes	Long	August 8 (a)	3.64	0.13	No	Short
June 13-14 (a)	3.19	0.33	Yes	Short	August 8 (b)	4.00	0.13	Yes	Short
June 14 (b)	2.96	0.20	No	Short	August 9 (a)	3.25	0.00	No	Short
June 15 (a)	3.28	0.16	No	Short	August 9-10 (a)	3.22	0.13	No	Long
June 15 (b)	3.06	0.06	No	Short	August 11 (a)	3.07	0.00	No	Short
June 16 (a)	3.44	0.01	No	Short	August 12 (a)	3.36	0.07	Yes	Short
June 18 (a)	3.37	0.00	No	Short	August 13 (a)	3.68	0.22	Yes	Short
June 18 (b)	3.74	0.00	No	Short	August 14 (a)	3.82	0.23	Yes	Short
June 18-19 (a)	3.78	0.04	Yes	Short	August 17-18 (a)	2.91	0.05	No	Short
June 19 (a)	3.19	0.04	No	Short	August 18 (a)	3.33	0.11	No	Short
June 21-22 (a)	3.61	0.42	Yes	Long	August 19 (a)	2.96	0.08	No	Short
June 24 (a)	3.25	0.11	No	Long	August 20 (a)	3.02	0.20	No	Long
June 24-25 (a)	3.27	0.21	Yes	Long	August 24 (a)	3.37	0.06	No	Short
June 26 (a)	3.30	0.00	No	Short	October 3 (a)	4.76	0.03	No	Short
June 29 (a)	3.28	0.28	No	Short					

Table 3. Average anthropogenic emission rates for SO_x and NO_x as determined from the U.S. EPA Emission Inventories for the air mass sectors relative to Mount Mitchell in units of 10³ kg km⁻² yr⁻¹.

Air Mass Sector	Sector Range	1991		1985 **		1985 **	
		SO _x	NO _x	SO _x	NO _x	SO _x	NO _x
Sector 1	290°-65°	6.86	5.95	7.46	5.01		
Sector 2	65°-240°	4.40	4.42	4.98	3.87		
Sector 3	240°-290°	3.60	3.51	1.23	3.03		

** - taken from Saxena and Yeh, 1989 and Lin and Saxena, 1991.

Table 4. Important characteristics and parameters of the HY-SPLIT back trajectory model and meteorological data sources used in this field study.

Back Trajectory Model	Trajectory Output Options (Vertical Motion)
HY-SPLIT (Hybrid Single-Particle Lagrangian Integrated Trajectories)	NGM Data, Isobaric, Isosigma, Divergence Calculated
Model Developer	NGM Vertical Layers
Roland R. Draxler (1992)	10
Model Type	NGM Data Resolution
Multiple-Layer Lagrangian-Eulerian Hybrid	182.9 km spatial, 2 hour temporal
Possible Meteorological Background	Major Input Parameters
Data Formats	Start Date and Time (GMT)
Nested Grid Model (NGM) **	Days to Run
Limited Fine-Mesh (LFM)	Surface Pressure or Height (mb or meters)
Rawinsonde (Non-gridded)	NGM Data File
Medium-Range Forecast (MRF)	Vertical Motion Option
Persian Gulf (PEG)	Decimal Latitude/Longitude of End Point
Trajectory Output Frequency	Trajectory Time Step (Hours)
1 per hour	
** - Meteorological Data Used for this Study	

Table 5. Cloud water pH ranges with corresponding mean values of ionic constituents ($\mu\text{eq l}^{-1}$) for the entire 1993 field season.

pH Range	Number of samples	Ionic Constituents							
		$\mu\text{eq l}^{-1}$ SO ₄ =	$\mu\text{eq l}^{-1}$ NO ₃ -	$\mu\text{eq l}^{-1}$ NH ₄ ⁺	$\mu\text{eq l}^{-1}$ Cl ⁻	$\mu\text{eq l}^{-1}$ Na ⁺	$\mu\text{eq l}^{-1}$ Ca ⁺⁺	$\mu\text{eq l}^{-1}$ Mg ⁺⁺	$\mu\text{eq l}^{-1}$ K ⁺
pH < 2.66	1	Mean 1889.79 St. Dev. 0.00	157.10 0.00	476.72 0.00	117.35 0.00	90.00 0.00	174.75 0.00	50.68 0.00	20.05 0.00
pH 2.66-2.85	5	Mean 1225.29 St. Dev. 609.99	68.33 26.29	264.24 115.15	51.12 19.64	23.80 20.07	116.29 144.22	20.86 17.54	11.46 10.07
pH 2.86-3.05	26	Mean 1182.64 St. Dev. 679.75	84.34 40.17	289.59 166.50	46.08 22.47	15.08 10.59	62.19 52.79	15.07 10.26	6.67 4.32
pH 3.06-3.25	44	Mean 929.48 St. Dev. 311.15	68.08 24.03	277.08 116.39	59.81 40.10	27.42 39.85	45.03 26.83	17.45 11.84	8.20 8.13
pH 3.26-3.45	74	Mean 596.32 St. Dev. 198.50	47.37 17.64	185.37 85.30	44.26 27.47	24.89 25.43	32.80 20.22	13.13 8.68	5.57 3.39
pH 3.46-3.65	18	Mean 391.65 St. Dev. 151.94	30.57 11.69	120.13 77.50	35.71 24.24	15.99 15.67	21.02 14.89	7.47 6.50	3.76 3.73
pH 3.66-3.85	17	Mean 202.46 St. Dev. 63.26	14.58 8.40	52.75 37.63	14.69 15.75	10.63 14.32	12.98 8.30	4.90 4.15	4.06 6.23
pH 3.86-4.05	21	Mean 122.63 St. Dev. 21.92	6.96 3.60	24.86 12.04	7.97 11.00	9.96 5.50	9.05 10.03	4.09 5.79	3.66 4.42
pH 4.06-4.25	25	Mean 70.96 St. Dev. 16.55	3.48 1.43	13.01 5.01	1.04 1.33	6.50 4.58	4.91 2.15	1.94 0.93	2.15 1.57
pH > 4.25	3	Mean 43.58 St. Dev. 36.36	3.59 1.48	15.22 6.12	30.90 36.56	21.52 36.21	4.79 6.83	1.45 1.73	4.94 8.55

Total number of observations = 234

Table 6. Mass concentration ratios of chlorine ion to sodium ion (Cl^-/Na^+) for all pH ranges of cloud water samples collected from the entire 1993 field season.

pH Ranges	< 2.66	2.66-2.85	2.86-3.05	3.06-3.25	3.26-3.45
Cl^-/Na^+ Ratio	1.30	2.15	3.06	2.18	1.78
pH Ranges	3.46-3.65	3.66-3.85	3.86-4.05	4.06-4.25	>4.25
Cl^-/Na^+ Ratio	1.91	1.38	0.80	0.16	1.44

Table 7. Values of laboratory, field measured, and calculated (from the aggregate of ionic species) pH and hydrogen ion concentration (in $\mu\text{eq l}^{-1}$) for June, August, and the entire 1993 field season.

	Lab pH	Field pH	Calc. pH	[H] ⁺ (Lab)	[H] ⁺ (Field)	[H] ⁺ (Calc.)
Averages for June	3.51	3.47	3.67	506.63	482.75	372.92
Standard Deviation	0.50	0.40	0.56	405.27	409.77	335.01
Averages for August	3.32	3.42	3.42	538.04	513.30	530.49
Standard Deviation	0.35	0.39	0.41	365.24	346.91	391.87
Averages for Field Season	3.43	3.45	3.56	523.57	497.43	439.88
Standard Deviation	0.45	0.39	0.52	390.55	385.24	370.11

Table 8. Average concentrations (in $\mu\text{eq l}^{-1}$) of ionic constituents for June, August, and the entire 1993 field season. Correlation coefficients between the individual ionic species and derived hydrogen ion concentration are also shown.

	Ionic Constituents							
	SO ₄ =	NO ₃ -	NH ₄ +	Cl-	Na+	Ca++	Mg++	K+
Averages for June	527.18	38.73	153.57	39.91	26.78	31.61	13.57	7.38
Standard Deviation	449.41	33.26	136.58	39.21	29.14	41.71	11.87	6.30
Correlation Coefficients for Hydrogen Ion Conc. versus Ionic Species								
Lab [H] ⁺ vs. Ionic Species	0.92	0.90	0.89	0.79	0.47	0.48	0.71	0.44
Field [H] ⁺ vs. Ionic Species	0.68	0.68	0.59	0.46	0.83	0.59	0.53	0.46
Calculated [H] ⁺ vs. Ionic Species	0.99	0.91	0.89	0.71	0.40	0.53	0.66	0.42
Correlation Coefficients for Hydrogen Ion Conc. versus Ionic Species								
Averages for August	691.53	50.98	188.18	32.93	9.05	34.84	8.03	3.04
Standard Deviation	508.98	33.81	136.62	19.61	12.36	33.38	7.00	2.69
Correlation Coefficients for Hydrogen Ion Conc. versus Ionic Species								
Lab [H] ⁺ vs. Ionic Species	0.96	0.90	0.85	0.64	0.15	0.70	0.71	0.41
Field [H] ⁺ vs. Ionic Species	0.95	0.89	0.83	0.64	0.10	0.67	0.67	0.40
Calculated [H] ⁺ vs. Ionic Species	0.98	0.84	0.85	0.67	0.15	0.74	0.72	0.39
Correlation Coefficients for Hydrogen Ion Conc. versus Ionic Species								
Averages for Field Season	600.61	44.40	168.67	38.10	21.30	34.89	11.94	5.69
Standard Deviation	489.16	34.96	137.50	34.90	32.89	43.98	12.81	5.63
Correlation Coefficients for Hydrogen Ion Conc. versus Ionic Species								
Lab [H] ⁺ vs. Ionic Species	0.92	0.89	0.87	0.72	0.35	0.54	0.61	0.38
Field [H] ⁺ vs. Ionic Species	0.77	0.74	0.68	0.48	0.23	0.57	0.48	0.39
Calculated [H] ⁺ vs. Ionic Species	0.98	0.88	0.87	0.61	0.27	0.58	0.55	0.28

Table 9. Statistical summary of mean concentrations, in $\mu\text{eq l}^{-1}$, of ionic constituents for air mass trajectories calculated in the HY-SPLIT "Data" configuration for the entire 1993 field season.

Sectors Crossed by Trajectory										
Marine (N=56)	Field pH	SO ₄ =	NO ₃ -	NH ₄ +	Cl-	Na+	Ca++	Mg++	K+	
Mean	3.28	648.06	58.60	223.79	60.56	36.35	28.47	16.52	8.58	
Standard Deviation	0.16	328.11	30.68	110.02	38.64	32.70	15.69	10.24	4.95	
pH Range	2.93-3.57									
Continental (N=69)	Field pH	SO ₄ =	NO ₃ -	NH ₄ +	Cl-	Na+	Ca++	Mg++	K+	
Mean	3.57	411.12	30.90	105.67	28.83	12.29	28.52	7.51	4.42	
Standard Deviation	0.37	298.26	23.17	82.93	24.52	14.63	49.89	9.43	5.11	
pH Range	2.83-4.33									
Polluted (N=6)	Field pH	SO ₄ =	NO ₃ -	NH ₄ +	Cl-	Na+	Ca++	Mg++	K+	
Mean	3.12	1141.15	83.56	310.15	32.27	11.57	69.09	16.25	6.01	
Standard Deviation	0.22	636.88	44.37	193.56	17.74	2.99	44.92	8.81	3.21	
pH Range	2.91-3.39									
Marine/Continental (N=21)	Field pH	SO ₄ =	NO ₃ -	NH ₄ +	Cl-	Na+	Ca++	Mg++	K+	
Mean	3.34	649.63	41.45	189.03	44.88	34.39	35.65	14.37	5.88	
Standard Deviation	0.34	463.74	25.68	164.99	36.13	41.45	33.42	11.53	5.75	
pH Range	2.74-4.08									
Marine/Polluted (N=16)	Field pH	SO ₄ =	NO ₃ -	NH ₄ +	Cl-	Na+	Ca++	Mg++	K+	
Mean	3.17	1054.28	75.76	279.43	53.59	15.18	47.25	16.19	10.85	
Standard Deviation	0.16	468.95	29.76	95.77	17.60	8.61	28.29	8.68	9.45	
pH Range	2.88-3.38									

Table 9. (continued)

Contin./Marine (N=39)	Field pH	SO ₄ =	NO ₃ -	NH ₄ +	Cl-	Na+	Ca++	Mg++	K+
Mean	3.89	226.23	12.66	50.15	8.10	9.35	12.74	4.11	2.71
Standard Deviation	0.42	451.96	29.12	113.98	20.33	14.45	32.02	8.24	3.23
pH Range	2.51-4.68								
Contin./Polluted (N=11)	Field pH	SO ₄ =	NO ₃ -	NH ₄ +	Cl-	Na+	Ca++	Mg++	K+
Mean	3.05	1383.33	80.25	352.21	47.12	11.01	87.03	22.18	4.23
Standard Deviation	0.17	450.08	11.31	66.04	10.11	1.94	22.21	5.45	0.68
pH Range	2.85-3.26								
Polluted/Marine (N=1)	Field pH	SO ₄ =	NO ₃ -	NH ₄ +	Cl-	Na+	Ca++	Mg++	K+
Mean	2.99	1110.21	107.11	218.33	38.87	3.91	30.79	9.54	2.48
Standard Deviation	0.00	0.00	0.00	0.00	0.00	0.00	0.00	0.00	0.00
pH Range	2.99								
Polluted/Contin. (N=9)	Field pH	SO ₄ =	NO ₃ -	NH ₄ +	Cl-	Na+	Ca++	Mg++	K+
Mean	3.36	789.91	59.27	180.60	44.35	43.44	90.39	19.84	3.19
Standard Deviation	0.09	525.92	44.24	77.67	63.58	107.85	79.02	36.97	6.42
pH Range	3.28-3.47								
Marine/Con./Poll. (N=3)	Field pH	SO ₄ =	NO ₃ -	NH ₄ +	Cl-	Na+	Ca++	Mg++	K+
Mean	3.01	1063.19	58.48	303.96	36.23	17.53	33.95	11.35	5.14
Standard Deviation	0.16	427.62	17.03	152.22	4.65	8.36	19.27	1.87	2.29
pH Range	2.84-3.16								
Marine/Poll./Con. (N=2)	Field pH	SO ₄ =	NO ₃ -	NH ₄ +	Cl-	Na+	Ca++	Mg++	K+
Mean	3.18	929.17	61.69	276.36	31.20	13.33	27.62	8.89	3.27
Standard Deviation	0.00	19.45	0.09	0.04	1.95	0.03	0.53	0.00	0.11
pH Range	3.18								

Note: Samples might include liquid precipitation as well as cloud water.

Table 10a. Mass concentration ratios of chlorine ion to sodium ion (Cl^-/Na^+) for all air mass sector categories calculated in the HY-SPLIT "Data" configuration from the entire 1993 field season.

Air Mass Sector Categories	M	C	P	M/C	M/P	C/M	C/P	P/M	P/C	M/C/P	M/P/C
Cl^-/Na^+ Ratio	2.57	4.13	4.30	2.01	5.45	1.34	6.60	15.30	4.28	3.19	3.61

45

Table 10b. Mass concentration ratios of chlorine ion to sodium ion (Cl^-/Na^+) for all air mass sector categories calculated in the HY-SPLIT "Isobaric" configuration from the entire 1993 field season.

Air Mass Sector Categories	M	C	P	M/C	M/P	C/M	C/P	P/M	P/C	M/C/P
Cl^-/Na^+ Ratio	2.71	3.37	4.39	1.72	5.26	1.29	6.64	15.30	5.34	3.99

Table 11. Statistical summary of mean concentrations, in $\mu\text{eq l}^{-1}$, of ionic constituents for air mass trajectories calculated in the HY-SPLIT "Isobaric" configuration for the entire 1993 field season.

Sectors Crossed by Trajectory		Field pH	SO ₄ =	NO ₃ -	NH ₄ +	Cl-	Na+	Ca++	Mg++	K+
Marine (N=47)										
Mean		3.29	726.98	59.71	244.70	80.37	53.79	32.41	21.75	10.93
Standard Deviation		0.15	328.79	27.80	107.41	39.89	29.14	12.01	8.83	5.15
pH Range		3.01-3.57								
Continental (N=74)										
Mean		3.63	382.16	29.35	100.87	27.69	12.67	26.09	7.11	4.20
Standard Deviation		0.41	299.75	23.67	83.67	24.66	15.70	48.07	9.21	5.05
pH Range		2.83-4.68								
Polluted (N=9)										
Mean		3.17	999.79	72.17	263.23	28.98	10.19	64.75	13.78	4.58
Standard Deviation		0.19	546.40	39.02	168.45	15.00	3.22	36.13	7.94	3.39
pH Range		2.91-3.39								
Marine/Continental (N=19)										
Mean		3.24	412.70	28.92	95.07	45.48	42.00	21.16	13.58	6.97
Standard Deviation		0.29	367.55	22.91	84.24	39.19	41.23	16.72	12.38	5.95
pH Range		2.74-3.82								
Marine/Polluted (N=18)										
Mean		3.18	1040.38	74.19	279.09	51.10	14.97	45.07	15.38	10.00
Standard Deviation		0.15	442.38	28.32	89.96	18.05	8.11	27.32	8.49	9.21
pH Range		2.88-3.38								

Table 11. (continued)

Contin./Marine (N=38)	Field pH	SO4=	NO3-	NH4+	Cl-	Na+	Ca++	Mg++	K+
Mean	3.82	229.43	15.44	51.03	9.72	11.64	12.98	4.85	3.13
Standard Deviation	0.38	335.61	30.44	92.04	21.48	17.65	30.23	9.02	3.41
pH Range	2.51-4.24								
Contin./Polluted (N=16)	Field pH	SO4=	NO3-	NH4+	Cl-	Na+	Ca++	Mg++	K+
Mean	3.11	1331.38	80.50	382.38	53.55	30.02	97.62	27.31	5.45
Standard Deviation	0.15	494.39	29.45	110.94	44.23	80.30	56.93	24.90	4.08
pH Range	2.85-3.28								
Polluted/Marine (N=1)	Field pH	SO4=	NO3-	NH4+	Cl-	Na+	Ca++	Mg++	K+
Mean	2.99	1110.21	107.11	218.33	38.87	3.91	30.79	9.54	2.48
Standard Deviation	0.00	0.00	0.00	0.00	0.00	0.00	0.00	0.00	0.00
pH Range	2.99								
Polluted/Contin. (N=9)	Field pH	SO4=	NO3-	NH4+	Cl-	Na+	Ca++	Mg++	K+
Mean	3.23	994.86	57.91	227.76	30.63	8.84	81.44	11.23	1.95
Standard Deviation	0.24	621.04	23.37	116.87	13.18	2.20	25.33	5.86	1.36
pH Range	2.89-3.47								
Marine/Con./Poll. (N=2)	Field pH	SO4=	NO3-	NH4+	Cl-	Na+	Ca++	Mg++	K+
Mean	3.12	1154.58	65.51	325.53	39.31	15.18	29.34	10.08	3.67
Standard Deviation	0.06	203.29	7.74	41.05	5.13	2.83	6.35	1.22	0.49
pH Range	3.07-3.16								

Note: Samples might include liquid precipitation as well as cloud water.

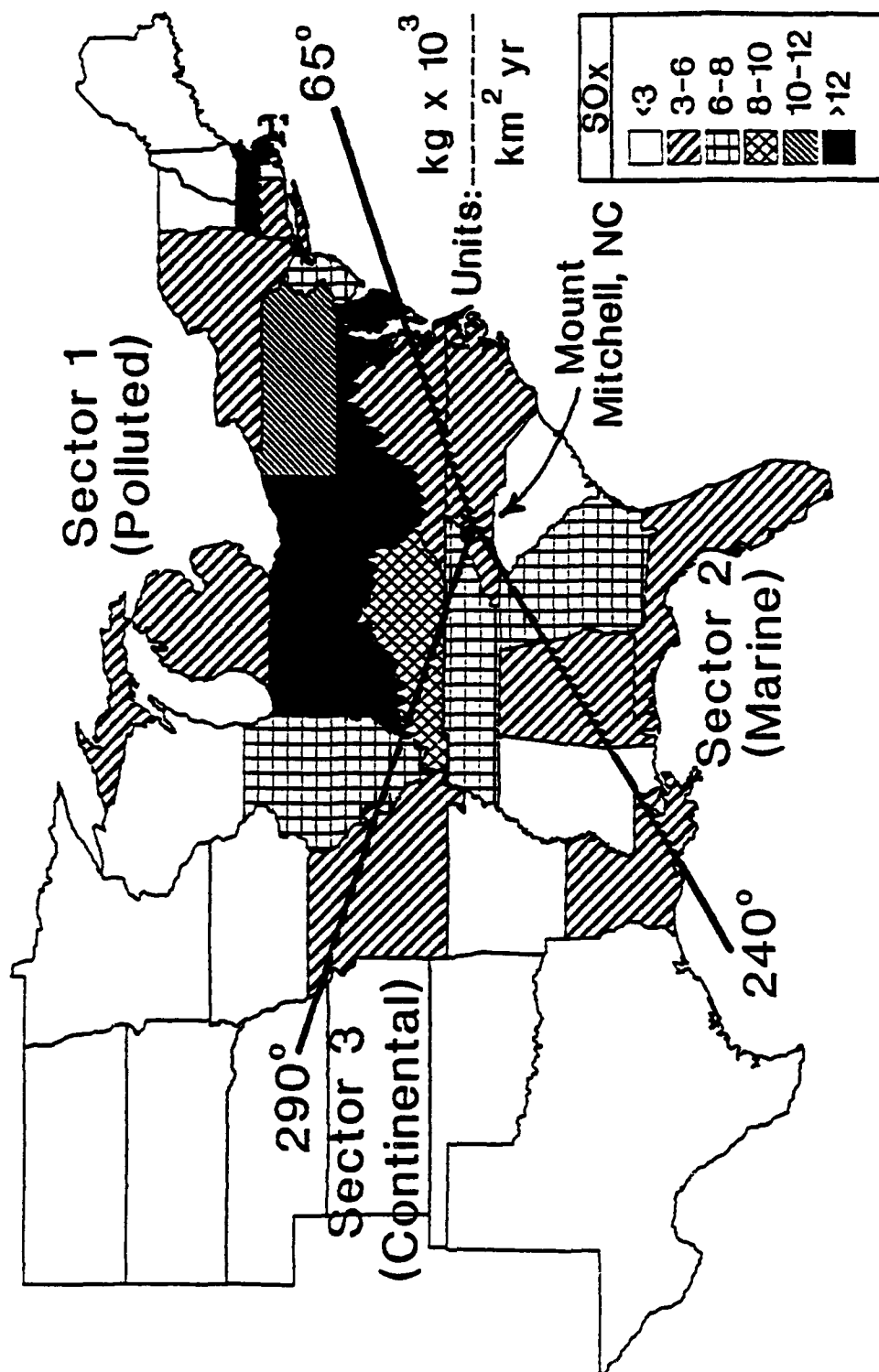


Figure 1. The 1991 U.S. EPA Emissions Inventory of anthropogenic sulfur oxides (SO_x) for the eastern United States.

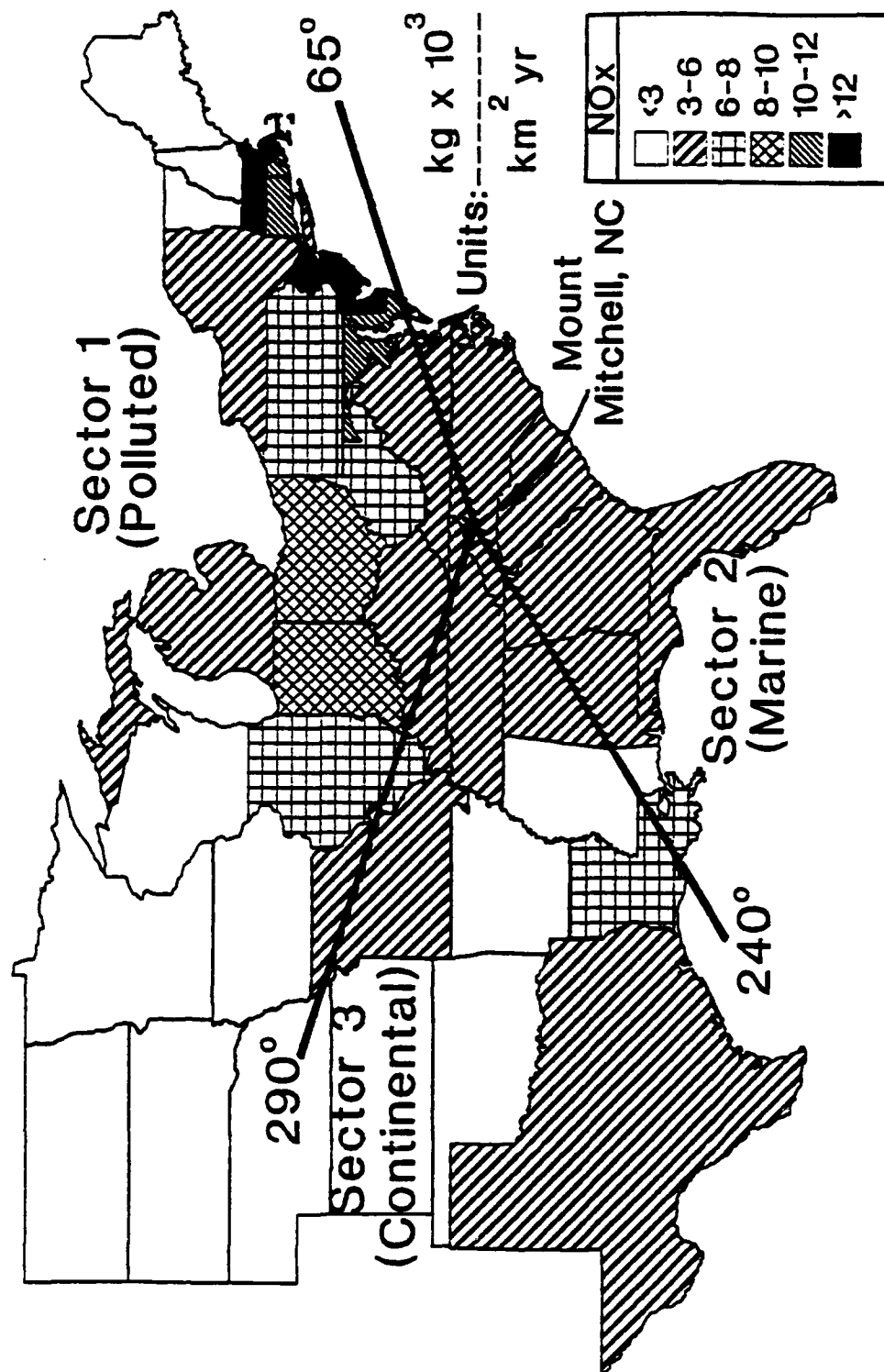


Figure 2. The 1991 U.S. EPA Emissions Inventory of anthropogenic nitrogen oxides (NO_x) for the eastern United States.

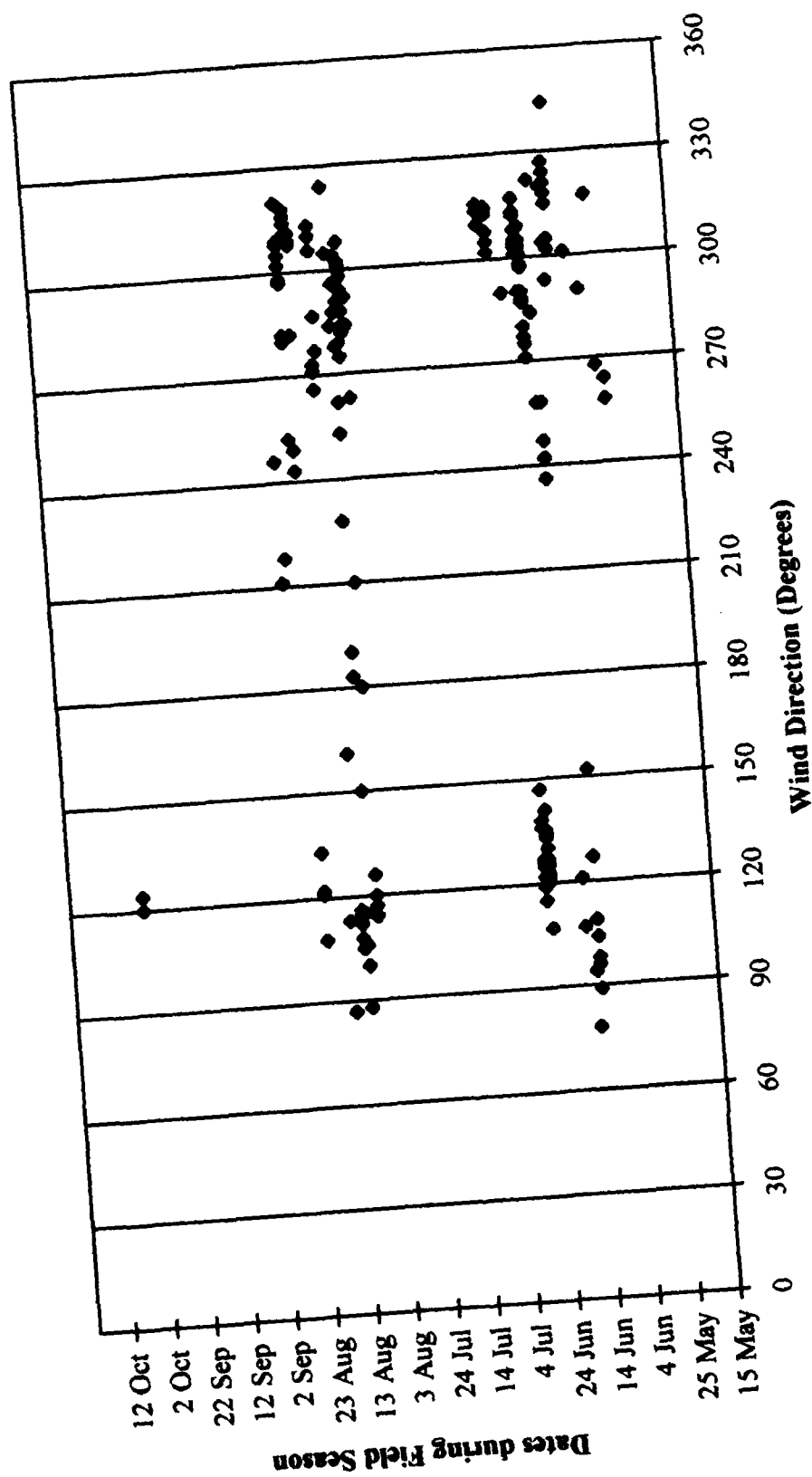


Figure 3. Plots of wind directions corresponding with all cloud events in which pH was measured.

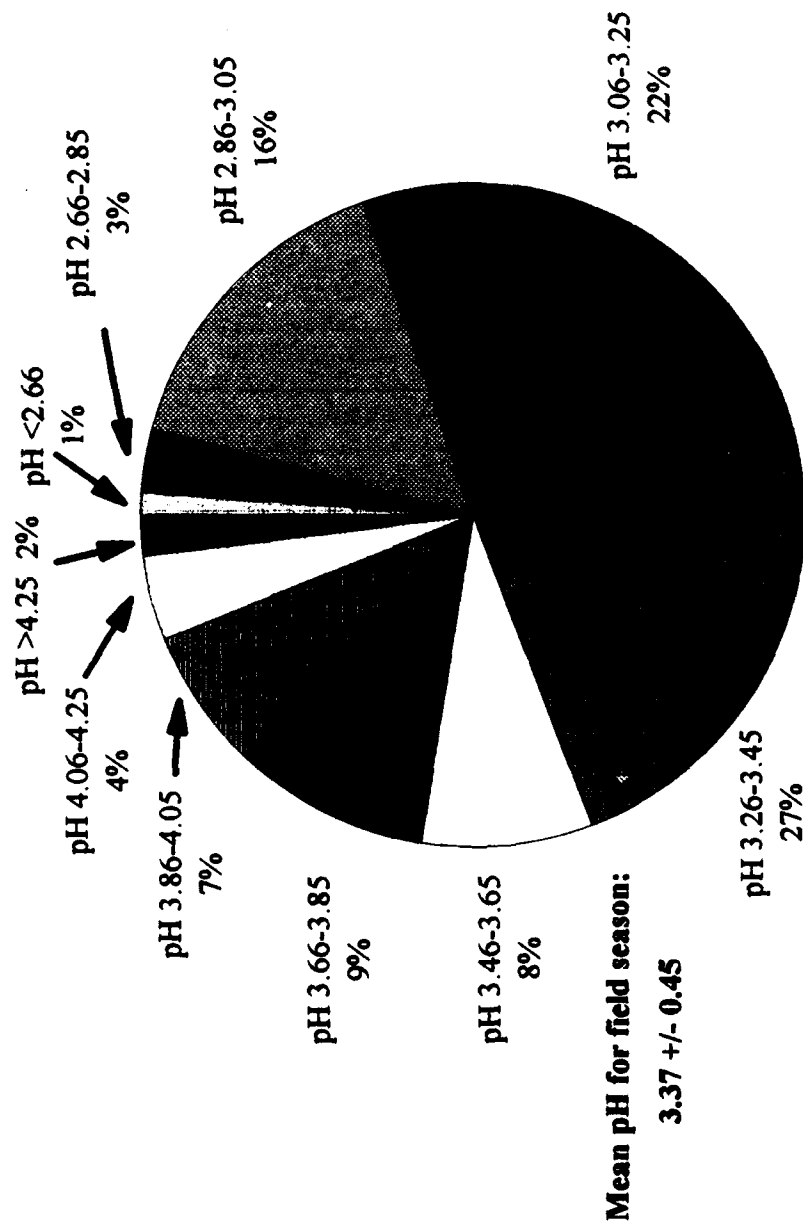


Figure 4. Relative frequencies of pH ranges for all cloud water samples retrieved during the entire 1993 field season.

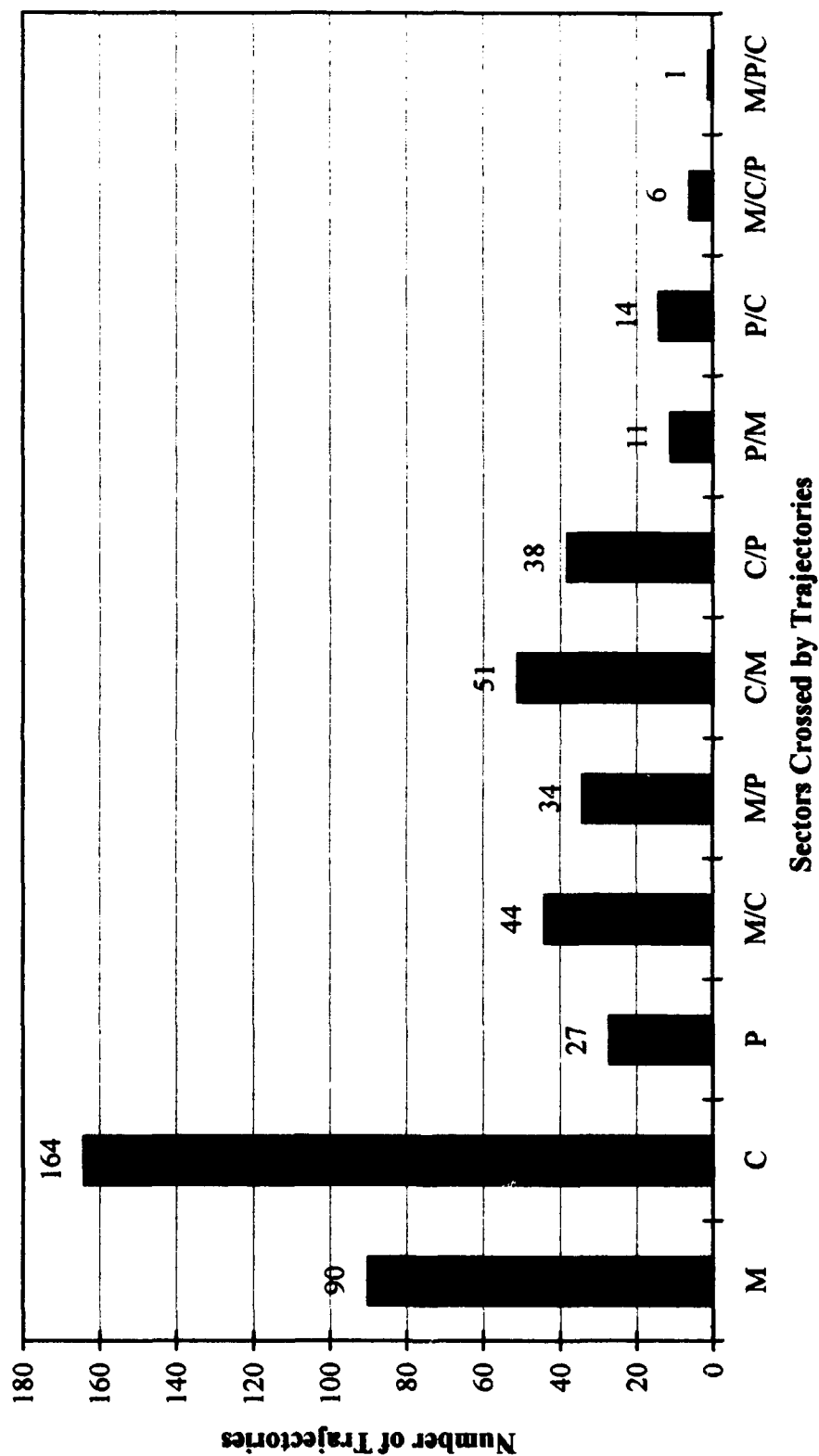


Figure 5a. HY-SPLIT model results of all pH-associated air mass trajectories calculated during cloud events for the entire 1993 field season.

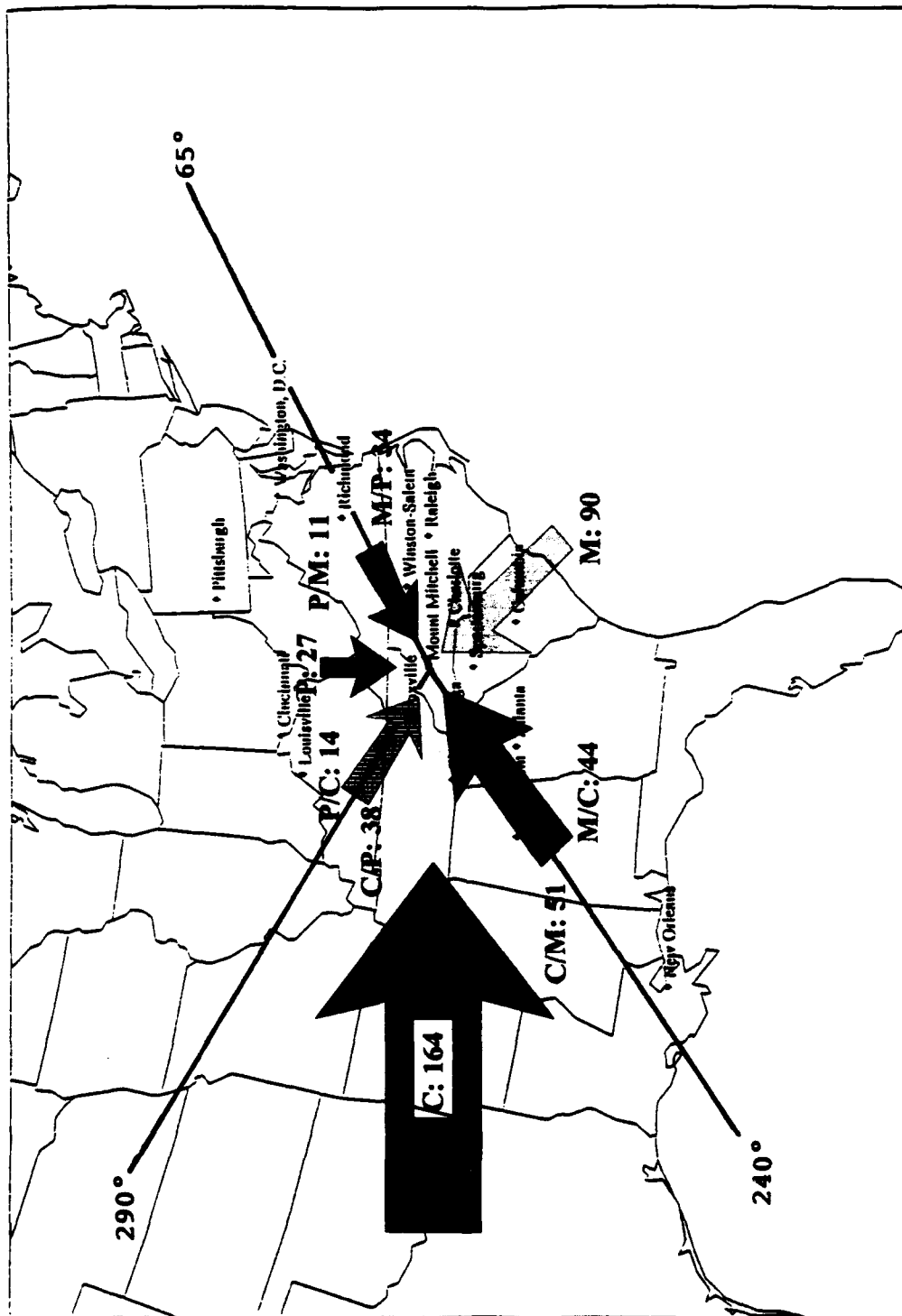


Figure 5b. Schematic diagram showing HY-SPLIT model results of all pH-associated trajectory calculations from the 1993 field season as in figure 5a, but with arrows representing relative numbers of trajectories in each category.

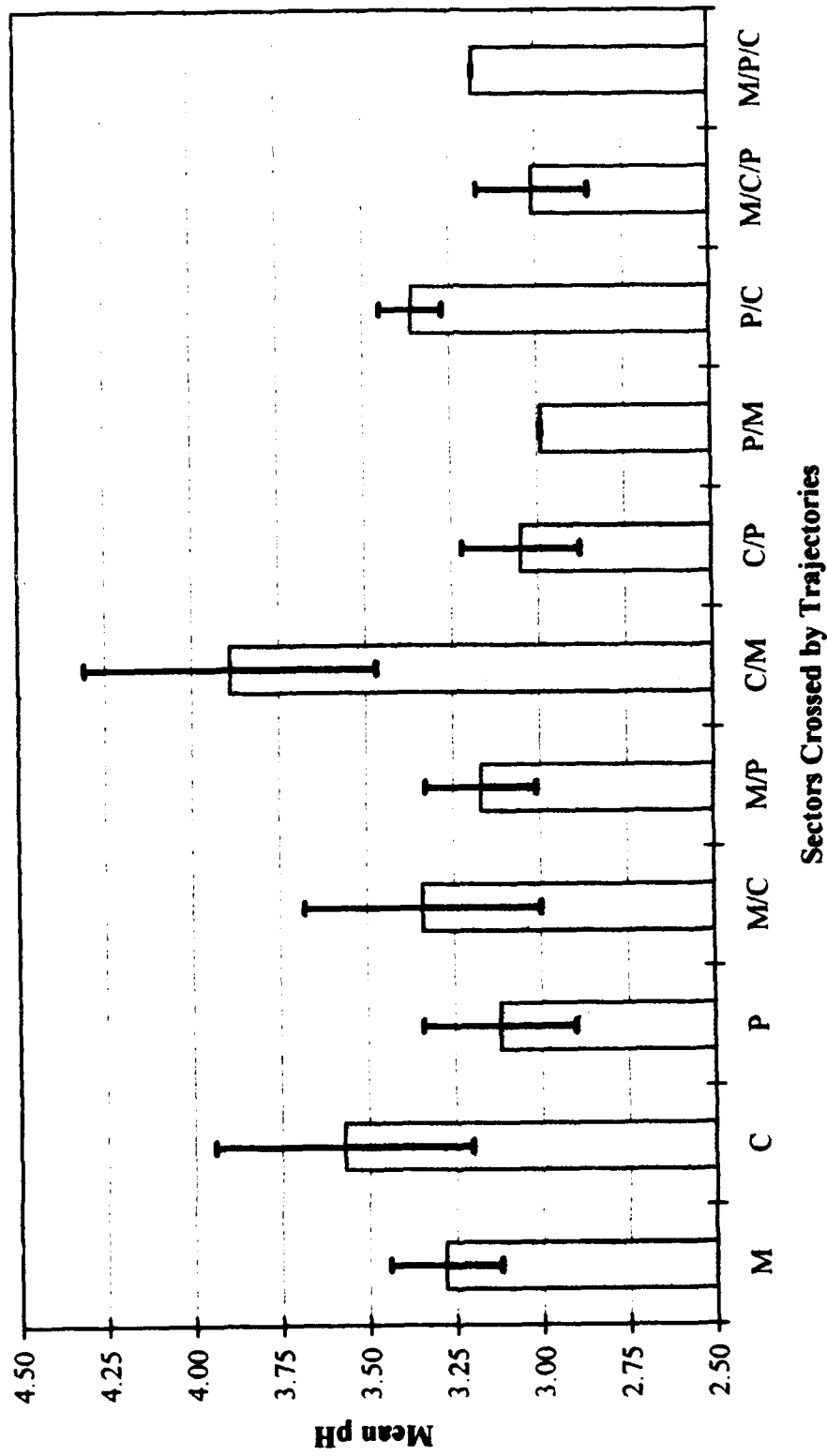


Figure 6. Mean pH versus HY-SPLIT trajectory category crossed for samples from the entire 1993 field season calculated in the DATA configuration. Error bars represent the standard deviations of the pH within each category.

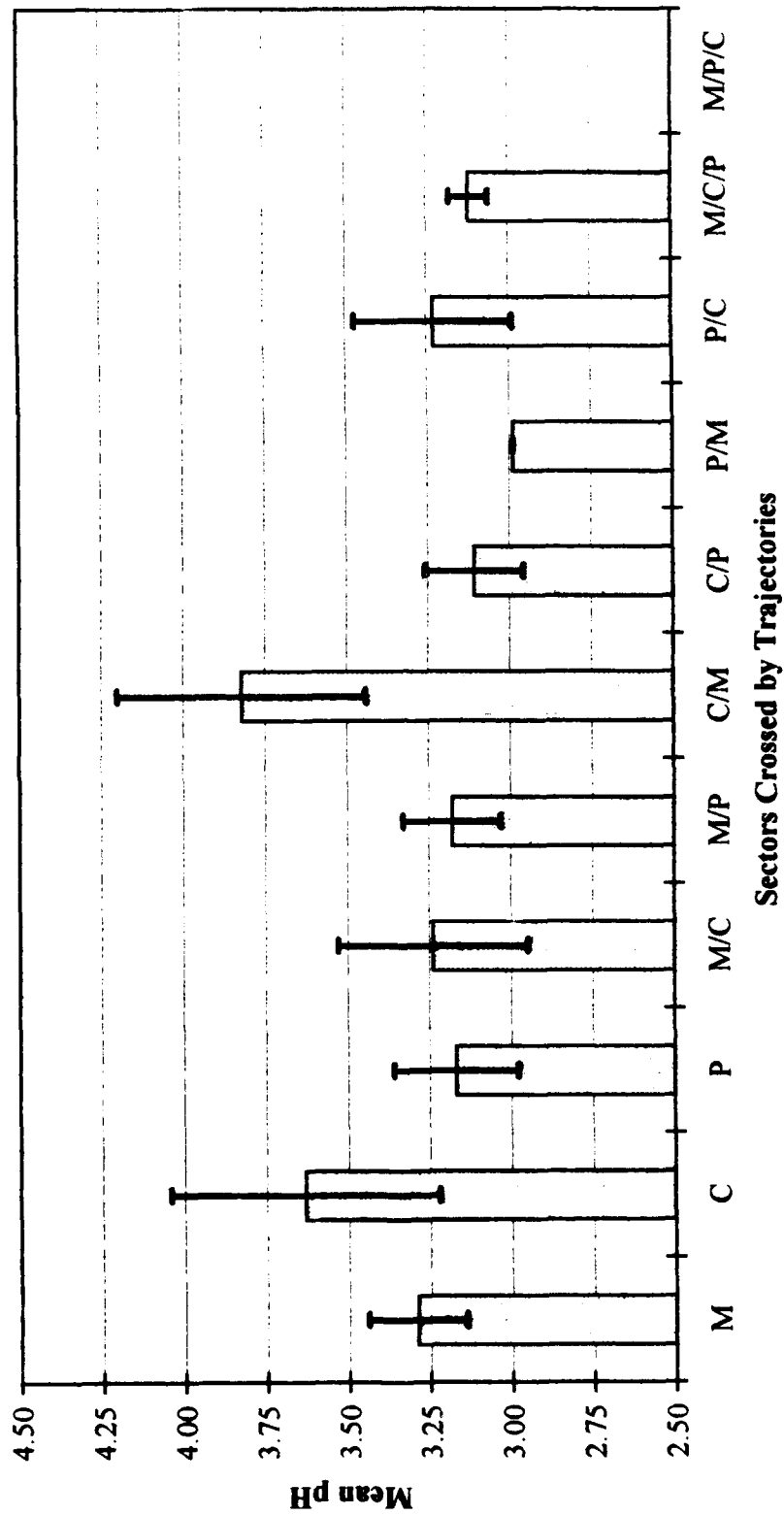


Figure 7. Mean pH versus HY-SPLIT trajectory category crossed for samples from the entire 1993 field season calculated in the ISOBARIC configuration. Error bars represent the standard deviations of the pH within each category.

**IMPACT OF EMISSIONS ON THE MICROSTRUCTURE,
CHEMICAL COMPOSITION, AND ALBEDO OF CLOUDS AT
MOUNT MITCHELL, NORTH CAROLINA**

K. L. Burns, V. K. Saxena*, J. C. Ulman, J. D. Grovenstein, and P. A. Durkee
North Carolina State University
Department of Marine, Earth, and Atmospheric Sciences
Raleigh, N.C. 27695-8208 U.S.A.

submitted for publication to
Journal of Climate

* To whom correspondence should be addressed

ABSTRACT

In situ cloud measurements were taken during 39 individual cloud events between June and October 1993 in Mount Mitchell State Park, North Carolina. Cloud droplet spectra, obtained using a Forward Scattering Spectrometer Probe (FSSP) were used to determine total droplet number concentration, average droplet radius, and liquid water concentration. A total of 113 hourly cases were recorded with simultaneous FSSP spectra, cloud water acidity, ionic content, and meteorological data. A positive correlation was detected between the cloud water pH and droplet radius ($r^2 = 0.47$). Also, a negative correlation was detected between the cloud water pH and droplet number concentration ($r^2 = 0.64$). The data were then sorted into three populations based on the pH: $\text{pH} < 3.0$ ($n = 18$), $3.0 \leq \text{pH} < 3.7$ ($n = 71$), and $\text{pH} \geq 3.7$ ($n = 24$). It was observed that lower pH values were associated, on average, with higher cloud droplet number concentrations and lower radii, and *vice versa*. For nine cases, cloud albedo was determined from measurements of the NOAA satellite-based Advanced Very High Resolution Radiometer (AVHRR). These albedos were shown to vary directly with the number concentrations of cloud droplets and cloud condensation nuclei (CCN) and inversely with the average droplet radius and cloud water pH. Cloud reflectivity values calculated from *in situ* cloud microphysical and meteorological measurements were found in agreement with the values obtained from the AVHRR within error limits. Air mass history of the nine cloud cases was determined from back trajectories calculated with the Hybrid Single-Particle Lagrangian Integrated Trajectories (HY-SPLIT) model. It was shown that the air mass trajectories were

consistent with the experimental values of cloud water pH and cloud water ionic content, the polluted air masses being associated with higher cloud albedos.

1. Introduction

There is currently significant interest in understanding the effect that pollutants present in cloud forming air masses have on the resulting cloud droplet sizes and number concentrations. Of particular interest are those pollutants which produce cooling effects upon the atmosphere that serve to counteract the greenhouse warming effects of CO_2 , and which are effective cloud condensation nuclei (CCN), such as SO_2 -derived sulfate (Hegg et al. 1984; Hegg et al. 1991). This interest has been fueled by the debate over anthropogenic climate forcing. Given the potential effects of climate change on human life, it is important that our fundamental theoretical understanding be supported by a wealth of field data that will quantitatively describe the relevant processes which produce both cooling and warming perturbations in climate on regional and global scales.

It is theoretically understood that pollution (natural and anthropogenic) can affect climate by altering the radiative transfer through the atmosphere. When released into the atmosphere, carbon dioxide and other greenhouse gases trap outgoing longwave radiation which results in heating of the earth-troposphere system. Since these greenhouse gases reside in the atmosphere for long times and are well mixed, increased concentrations should produce long-term climate warming on a global or regional scale.

Anthropogenic effluents such as SO_2 and NO_2 undergo gas-to-particle conversion and increase the aerosol loading of the atmosphere. Through single particle scattering of incoming solar radiation, increased aerosol reduce the total solar energy flux reaching the earth's surface (Charlson et al. 1992). It is also understood that low level clouds produce an indirect cooling effect by increasing the

planetary shortwave albedo (Twomey 1991). Increasing anthropogenic emissions can potentially enhance this cooling effect by changing the cloud droplet distribution, which largely determines the cloud optical depth and albedo. Since some anthropogenic aerosols form efficient cloud condensation nuclei, under identical conditions of cloud formation (e.g., a constant amount of cloud forming water vapor), elevated CCN levels should produce greater droplet concentration and reduced droplet size (Saxena 1991; Leaitch et al. 1992). Since aerosol production is very inhomogeneous over the earth's surface and residence times are only on the order of a few days, this cooling would be restricted to a regional or local scale and potentially vary widely over time.

Charlson et al. (1987) have asserted that to counteract the warming caused by atmospheric CO₂, an approximate doubling of CCN would be needed. It has also been estimated by Ghan et al. (1990), using the NCAR Community Climate Model One (CCM1), that in the absence of other moderating influences, the greenhouse warming of the earth-troposphere system caused by a doubling of carbon dioxide could be counteracted by a meager 1.7% increase in the shortwave albedo of global low level cloud cover. Slingo (1990) has similarly assessed the potential effects of increasing cloudiness, by showing that an approximate 15%-20% increase of the amount of low clouds would be sufficient to balance the warming caused by a doubling of CO₂ concentrations (see also Parungo et al. 1994). Charlson et al. (1992) have recently estimated the current climate forcing due to anthropogenic sulfate alone to be comparable in magnitude but opposite in sign to the current forcings due to greenhouse gases. They have shown that anthropogenic aerosols, in particular aerosol sulfate, are instrumental in this climate forcing by increasing the levels of CCN, which, in turn, increase the number and lifetime of clouds, while at

the same time reducing precipitation from those clouds (see also Fouquart and Isaka 1992; Parungo et al. 1994). Wigley (1991), and more recently Saxena and Grovenstein (1993), have shown that climate is sensitive to changes in both CO₂ and SO₂ emissions.

It is thus clearly pivotal to our understanding of anthropogenically driven climate change to show quantitative differences in microstructure and reflectivity between clouds formed in air masses with a variety of pollutant amounts. By comparing these various types of clouds, we can better determine the present anthropogenic climate perturbation, as well as make more precise predictions of future impacts. Although much more data is needed, several important field studies have been conducted that provide strong verification of many aspects of the proposed mechanisms for pollution induced increases in cloud albedo.

During project METROMEX (Metropolitan Meteorological Experiment), Braham (1974) has shown that anthropogenic effluents cause an increase in the number concentrations of droplets and precipitation in clouds formed downwind of urban-industrial regions. Alkezweeny et al. (1993) have found that clouds formed in urban plumes from metropolitan areas increased droplet concentrations and decreased the median volume diameter as compared with the clouds formed in nearby unpolluted air masses.

Based on the work previously discussed, it is now known that changes in the amounts of the CCN from which clouds form will have an impact on the climate by inducing changes in the cloud albedo (Fouquart and Isaka 1992). Despite the conclusions of Twomey (1977; 1984), who stated that the effects of increased anthropogenic pollutant levels in clouds should result in higher cloud droplet concentrations, decreased droplet sizes, and higher cloud albedo for all but the

thickest of clouds (see also Raga and Jonas 1993), it is still not known what impact these factors will have upon cloud albedo, i.e., whether the cloud albedo will subsequently increase or decrease. There has been research on this subject, but results have been contradictory, depending upon the geographical locations of the studies in question. Investigative work by Kondrat'yev et al. (1981) (see also Coakley et al. 1987), have shown that anthropogenic effluents emanating from urban areas tended to reduce the cloud albedo. However, Radke et al. (1989) have shown that anthropogenic effluents can significantly enhance cloud reflectivity. In investigations by Coakley et al. (1987) and during project FIRE [First ISCCP (International Satellite Cloud Climatology Project) Regional Experiment] airborne measurements were taken across ship tracks. The cloud reflectivity in both studies was determined from the AVHRR (Advanced Very High Resolution Radiometer) measurements aboard the NOAA-9 and NOAA-10 polar orbiting satellites, respectively. The results of both studies with ship tracks showed an increase in total droplet concentration, liquid water content, condensation nuclei (CN) concentration and cloud reflectivity for the ship track clouds compared to the surrounding uncontaminated clouds. If the ship exhaust was considered as a surrogate for anthropogenic pollution, the change in cloud reflectivity produced as a result of land-based emissions could cause considerable regional and perhaps global climate perturbations.

The objective of this paper is to describe how anthropogenic pollution affects cloud albedo through changes in cloud chemistry and microstructure at a remote rural site. To the authors' knowledge, this is the first time that *in situ* cloud microphysical and chemical measurements have been compared with satellite measured albedo over a land surface. As such, this paper should provide an

important first observational description of the entire cloud-climate feedback mechanism.

2. Methodology

Durkee et al. (1991) have asserted that satellite remote sensing, because it is inherently indirect, should be coupled with ground-based *in situ* observations of aerosol characteristics in order to gain a complete understanding of "the aerosol particle distribution". Both Twomey (1991) and Charlson et al. (1992) have suggested that remote sensing of cloud properties, in addition to ground-based observations, would help to delineate the primary properties of clouds and the precursor air masses, which may be affected by anthropogenic sulfates and/or other aerosols. Thus, based on their suggestions, as well as to help quantify some of the previously mentioned data disparities, *in situ* cloud measurements have been taken at Gibbs Peak (2,006 m MSL) in Mount Mitchell State Park (35° 44' 05" N, 82° 17' 15" W), in North Carolina, which is the highest mountain area east of the Mississippi River in the United States (2,038 m MSL). This site has several important advantages for the study of cloud microstructure and chemistry. The site, which extends into the free troposphere, is far from local pollution sources, allowing for the study of long range transport of both natural and anthropogenic aerosols. The site also experiences cloudiness on 71% of the days during the summer (Saxena et al. 1989). Thus, sufficient data is obtainable in a single season to allow for detailed analysis. Additionally, because of the similarity between the forest canopy, which from a satellite perspective is fairly smooth and consistent regarding the observed temperatures of its surface, and the sea surface, which has been utilized, up to this

point, as a primary area of remote sensing research into cloud chemical and microphysical characteristics, we can take advantage of the Advanced Very High Resolution Radiometer (AVHRR) satellite measurements of the cloud reflectivity. Finally, due to its position in mid-latitude, eastern North America, the clouds passing over the site vary in origin from heavily polluted to cleaner continental and marine air masses. Recently the site was designated a United Nations Biosphere Reserve, so that our measurements and others can be used over a very long time span to accurately gauge regional climate change.

a. Cloud droplet size spectra and in situ cloud albedo

Cloud droplet spectra were obtained using a Particle Measuring Systems Forward Scattering Spectrometer Probe (FSSP). The FSSP can accurately count and size particles from 0.5 to 47.0 μm . A description of the design and operation of the FSSP is given by Knollenberg (1981). Spectra were taken every 3 seconds during cloud events and later averaged over 5-minute and 1-hour intervals. From each 15-bin size spectrum, total droplet concentration (N , m^{-3}), average droplet radius (r_{avg} , μm), and cloud liquid water content (w , g m^{-3}) were easily computed. Then cloud optical depth was calculated as follows (Twomey 1977):

$$\tau = h (9 \pi w^2 N / 2 \rho^2)^{1/3} \quad (1)$$

where h is the cloud thickness in m , N is the cloud droplet number concentration in m^{-3} , w is the cloud liquid water content in g m^{-3} , and ρ is the density of liquid water

(1,000 kg m⁻³). After calculating τ , the cloud albedo was evaluated as (Lacis and Hansen 1974):

$$A_c = \tau / \tau + 7.7 \quad (2).$$

For identical cloud liquid water content, larger N implies larger optical thickness and thus higher cloud albedo.

b. Cloud water acidity and chemical composition

Cloud water samples were collected coincident with the FSSP spectra using a passive string impaction collector similar to that described by Kadlecek et al. (1983) and Mohnen and Kadlecek (1989). Samples were collected continuously and retrieved hourly. On site pH measurements were made for each sample immediately after retrieval. Samples were stored at 4 °C and later analyzed for chemical composition using a Dionex 2010i ion chromatograph.

c. Cloud condensation nuclei activation spectrum

A Horizontal Thermal Gradient Cloud Condensation Nucleus Spectrometer (Fukuta and Saxena 1979) was used to measure CCN activation spectra in the form

$$n = CS^k \quad (3)$$

where C represents the concentration parameter and is expressed in cm⁻³, k is the dimensionless slope parameter, and n is the cumulative number of CCN forming

cloud droplets at the ambient supersaturation S (usually expressed in percent). Knowing C , it is possible to correlate precursor CCN concentration in a cloud forming air mass with the actual cloud droplet concentration.

d. Air mass determination

Meteorological data (wind speed and direction, pressure, and temperature) were recorded and used for back trajectory analysis using the Hybrid Single-Particle Lagrangian Integration Trajectories (HY-SPLIT) model (Draxler 1992). Forty-eight hour 3-dimensional back trajectory graphs were generated for every cloud sample in which FSSP data were recorded, using high-resolution Nested Grid Model (NGM) data as the meteorological background source. The NGM data grid used for model calculations has a 183 km horizontal resolution and a 2-hour temporal resolution, with 10 vertical layers from the surface up to about 500 mb. The mathematics involved in the calculations of the trajectories are all based on finite differencing and interpolation approximations of the primary meteorological equations of motion and meteorological thermodynamics between NGM data grid points, and are explained thoroughly in Draxler (1992). All calculations of back trajectories of air masses used an option whereby the vertical motion along the trajectories was determined from the NGM background data itself. The model also produced skew T-log P diagrams for selected times during the events, which were used to estimate cloud base which represented saturation with respect to water.

e. Remotely sensed albedo

AVHRR measurements made from polar orbiting NOAA-10 and NOAA-11 satellites were used to determine the cloud reflectivity at the 0.63 μm wavelength. According to Durkee (1994), an approximation of the daytime reflectivity was accomplished by assuming that the clouds over the observation site were blackbodies at an 11.0 μm wavelength, with the temperature of the clouds found from the irradiance by the following equation, which is the Stefan-Boltzmann law:

$$F = \sigma T^4 \quad (4).$$

F is the irradiance from the cloud in W m^{-2} , σ is the Stefan-Boltzmann constant having the value of $5.67 \times 10^{-8} \text{ W m}^{-2} \text{ K}^{-4}$, and T is the effective temperature of the cloud in K. The irradiance was assumed to be known from the satellite instrument observations. Thus, in order for the cloud reflectance to be accurately determined, the cloud top temperature for the 11.0 μm wavelength was derived using (4) above and the emitted component of the 0.63 μm wavelength was estimated and removed, leaving the 0.63 μm reflectivity. The direct albedo measurements were then compared to values calculated from the droplet distributions.

3. Results and Discussion

Measurements were made during 39 individual cloud events between June and October 1993. Out of this data, 113 cases were available with simultaneous FSSP spectra, cloud water acidity and ionic composition data, and meteorological

data. Twenty-one CCN spectra were taken. Nine cases coincided with AVHRR retrievals.

Figure 1 shows frequency distributions of the 113 hourly cases for cloud acidity and microstructure measurements. The number of cases for each measurement interval is split up to indicate the contribution from each air mass regime. The following coding scheme has been employed: 'p' refers to back trajectories passing through polluted areas, 'mp' refers to back trajectories crossing both marine and polluted areas, 'm' refers to back trajectories confined to marine regimes, 'cp' refers to back trajectories crossing both continental and polluted areas, 'cmp' refers to back trajectories crossing all three areas, and 'c' refers to back trajectories confined to continental areas. It is seen that cloud water pH, cloud droplet number concentration, radius, and liquid water concentration all varied significantly. More explicitly, pH ranged from 2.51 to 4.78, droplet number concentration ranged from 30 to 939 cm^{-3} , cloud droplet radius ranged from 1.9 to 8.4 μm , and liquid water concentration ranged from 0.01 to 0.65 g m^{-3} . It can be concluded from figure 1 that these data represent a good variety of air mass origin, pollution content and cloud microstructure cases.

a. Cloud microstructure and acidity

When a cloud forms in a polluted air mass, the concentration of cloud droplets will be high, due to elevated concentrations of CCN. Then limited available liquid water guarantees that r_{avg} will remain small. To investigate the relationships between pH and N and between pH and r_{avg} , we calculated correlation coefficients and produced scatter plots using the corresponding data pairs for all 113 available

cases. Figure 2 shows that pH decreased with increasing cloud droplet number concentration ($r^2 = 0.64$). Figure 3 shows the positive relationship between pH and average droplet radius ($r^2 = 0.47$). The r^2 value for pH and w (not shown) was less than 0.01; therefore pH is independent of cloud liquid water content. Thus cloud water pH is strongly correlated with both droplet size and concentration. Since the clouds formed at the site were essentially moisture-limited, these results were expected. When a larger number of droplets are present, they must compete for the available water and the moisture is depleted while the droplets are still small. The droplets form solutions of acidic sulfates and nitrates which comprise the CCN. Since the droplets are small and have little liquid water to dilute the solution, acidity remains high and the pH remains low.

To further investigate the dependence of pH on cloud microstructure and provide a bulk quantification, the 113 cases were sorted into three populations: $\text{pH} < 3.0$ ($n = 18$), $3.0 \leq \text{pH} < 3.7$ ($n = 71$), and $\text{pH} \geq 3.7$ ($n = 24$). The average values for N , r_{avg} , w , and pH are shown for each population in Table 1. The \pm values represent standard errors. It is seen that low pH values were associated, on average, with higher number concentrations and lower average radii; high pH values were associated, on average, with lower number concentrations and higher average radii; intermediate pH values were associated, on average, with intermediate values of both number concentration and average radii; while liquid water content was statistically consistent across populations.

b. Cloud albedo and cloud microphysics

Our primary objective was to determine the effect of pollution content on cloud albedo. Nine cases coincided with satellite passage such that AVHRR retrievals allowed direct measurement of the visible albedo of the overlying cloud cover at the site. These events, which were all from short orographic cloud events, except for one, covered a large range of pH values and thus represented clouds formed in air masses with a variety of pollutant levels. Each of the three pH populations given above is represented by one or more cases.

Summaries of the pH, cloud microphysical parameters, CCN, and cloud thickness (h) versus cloud reflectance (AVHRR and *in situ*) instances are given in table 2. Using the data in table 2, we have subsequently derived plots of both AVHRR and *in situ* reflectivity values [calculated from (1) and (2)] versus cloud droplet number concentration and average droplet radius in figures 4 and 5. Error bars in the x-direction in figure 4 reflect the standard instrument error potential of the satellite measuring platform (here indicated to be an across-the-board 5% instrument error potential for all values) and the y-direction error bars are the result of assuming a standard, across-the-board 17% error possibility for both droplet number concentration and average radius (Baumgardner 1983), as calculated from the FSSP data. No error bars for the *in situ* albedos in figure 5 were calculated due to high error probability of the cloud thicknesses from table 2. In figure 4, a direct proportionality between reflectivity and number concentration is indicated, while a similar but reversed trend is observable for albedo versus average radius. The regression statistics for N versus the AVHRR albedo are: slope = 29.57, intercept = -910.93, and $r^2 = 0.79$. For r_{avg} vs. AVHRR albedo we have the slope = -0.19,

intercept = 13.65, and $r^2 = 0.97$. Figure 5 shows very similar characteristics to figure 4 for calculated albedos using (1) and (2). Here, the regression statistics for N versus the *in situ* albedo are: slope = 24.62, intercept = -715.70, and $r^2 = 0.76$. For r_{avg} versus *in situ* albedo we have the slope = -0.16, intercept = 12.17, and $r^2 = 0.89$. All of the observations as given in figures 4 and 5 are consistent with the findings of Coakley et al.'s (1987) ship-track observations, which showed that elevated levels of pollutants in clouds will result in higher reflectivity, which in turn tends to increase cloud droplet number concentrations and decrease average droplet radii, assuming a constant amount of available liquid water.

Again from table 2, we generated plots of pH and CCN concentrations versus the nine cases of AVHRR and *in situ* albedo in figures 6 and 7, respectively. For instances of pH versus AVHRR reflectivity in figure 6, there is a clear inverse relationship between the pH and albedo (slope = -0.06, intercept = 6.25, $r^2 = 0.83$), and a good positive correlation between CCN concentration and albedo (slope = 35.09, intercept = -1023.50, $r^2 = 0.70$). Figure 7 shows the same parameters as figure 6 measured against the *in situ* albedo, with similar trends (slope = -0.05, intercept = 5.74, $r^2 = 0.72$, for pH versus albedo, and slope = 29.85, intercept = -821.85, $r^2 = 0.70$ for CCN concentration versus albedo). All error bars in these two figures represent 5% instrument error potentials for the pH probe, CCN spectrometer, and the AVHRR satellite platform. For some of the cases no actual CCN measurements were available. For these cases, CCN values were selected from other cases with similar pH. The CCN relationships from both figures 6 and 7 give strong evidence that heavily polluted air masses produce clouds with higher albedos than cleaner air masses. The clouds formed in air masses with high CCN concentrations have correspondingly high cloud droplet number concentrations,

while the droplet size remains small, compared to clouds formed in lower CCN air masses. This distinction in droplet size distribution results in lower pH, higher albedo clouds for the more polluted clouds compared with the cleaner clouds.

c. Air mass history of AVHRR cases and cloud water chemistry

The results of each of the trajectory calculations corresponding to the nine cases are shown graphically in figure 8. Continental air masses were, for most calculations, associated with elevated pH levels (except for the June 8 case), while trajectories crossing more than one area were associated with highly variable results. Marine air masses were in all cases shown to cross other areas as well, giving a wide variety of results, but for the 19 June case, the only one in which the trajectory was mainly marine, the corresponding pH value was fairly high (3.77 ± 0.18). The two cases where polluted trajectories were represented (18 and 19 August) were associated with low pH values, which would be expected. It is also evident that the calculation indicated a small amount of polluted influence for 14 June, which appears to be reflected in the low pH value. Only the 8 and 14 June satellite coincident cases resulted in conflicting or contradictory results when comparing air mass history with cloud water pH. The 8 June case was shown to have continental air mass history, but was paired with a pH value more indicative of polluted character. The 14 June case was almost impossible to prioritize concerning the air mass history because a wide variety of air mass emission characteristics were shown to be crossed, but the pH value for this case indicates that polluted areas contributed significantly to the pH reduction.

Except where mentioned above, strong corroboration with the back trajectories as well as the observed pH values is provided by the various concentration values of cloud water ionic species in table 3, where high sulfate, nitrate and ammonium concentrations are allied with polluted influence. Similarly, very low concentrations of these ions were indicated for the 19 June and 6 August cases, where the air masses were shown to consist of marine and continental passage. High concentrations of chloride and sodium ions, which would normally be associated with marine origin, were indeed matched with marine inclusive air masses. Calcium and magnesium ions, usually associated with continental air masses, were shown to have their highest values associated with a variety of air mass combinations, but the highest calcium receipt was associated with polluted/continental passage from 18 August. The potassium ion receipts were all very low, but the highest values were found with air masses containing marine history, which would be expected, since this ion is often in chemical combination as KCl. Again, all of the preceding discussion must exclude the 8 June case, where elevated concentrations of all ions were observed from what was shown to be a continental air mass. It is possible that early-season chemical measurement errors may have contributed to the apparent anomalies for this case. No ionic data for the 3 October case was available, and due to the time of the season in which this case was observed and the extreme value of the observed pH, no suitable substitute from the preceding times during the field season could be used. A few other cases in table 3 also had no associated ionic constituency data, but in those cases ionic data from the same cloud event with very similar pH values were substituted.

4. Conclusions

Cloud pH, microstructure, and albedo are closely related to the CCN loading, and hence the pollution content of the cloud forming air mass. Cloud pH is largely controlled by cloud droplet size. For a given liquid water content, the average droplet radius is limited by the droplet concentration, which is controlled by the amount of CCN present in the cloud-forming air mass. Pollutants, primarily acidic sulfates and nitrates, undergo gas-to-particle conversion and form efficient CCN. Thus the amount of pollution present in the cloud forming air mass will affect the droplet size distributions. Since droplets themselves are the source of cloud reflectivities, cloud albedo is controlled by the droplet distribution and varies inversely with pH. With greater initial CCN concentration, low pH, high albedo clouds form and limit the flux of solar radiation reaching the earth's surface. Averaged over space and time, by increasing the mean cloud cover albedo, anthropogenic effluents produce an important cooling effect on regional climate. Due to the inhomogeneous emission of aerosol precursor gases over the earth's surface, and due to the short residence time of aerosol in the atmosphere, this effect is expected to vary perhaps greatly over time and region. We have shown for the first time over a continental land mass that anthropogenically produced CCN have a direct effect on cloud albedo and, by extrapolation, produce an important cooling perturbation on regional climate.

Acknowledgments-- This study was supported through the Southeast Regional Center of the National Institute for the Global Environmental Change by the U.S. Department of Energy under cooperative agreement No. DE-FCO3-90ER61010. Dr W. Robarge was responsible for the chemical analysis of the cloudwater samples and for the QA/QC of the data. We are indebted to Dr Roland R. Draxler at the NOAA Air Resources Laboratory for providing the trajectory model code, meteorological background data, and for useful hints and discussions which aided in the production of the back trajectories.

REFERENCES

- Alkezweeny, A. J., D. A. Burrows, C. A. Grainger, 1993: Measurements of cloud-droplet-size distributions in polluted and unpolluted stratiform clouds. *J. Appl. Meteor.*, **32**, 106-115.
- Baumgardner, D., 1983: An analysis and comparison of five water droplet measuring instruments. *J. Climate*, **22**, 891-910.
- Braham, R. R., Jr., 1974: Cloud physics of urban weather modification - a preliminary report. *Bull. Amer. Meteor. Soc.*, **55**, 100-106.
- Coakley, J. A., Jr., R. L. Bernstein, and P. A. Durkee, 1987: Effect of ship-stack effluents on cloud reflectivity. *Science*, **237**, 1020-1022.
- Charlson, R. J., J. E. Lovelock, M. O. Andreae, and S. G. Warren, 1987: Oceanic phytoplankton, atmospheric sulfur, cloud albedo and climate. *Nature*, **326**, 655-661.
- Charlson, R. J., S. E. Schwartz, J. M. Hales, R. D. Cess, J. A. Coakley, Jr., J. E. Hansen, and D. J. Hofmann, 1992: Climate forcing by anthropogenic aerosols. *Nature*, **255**, 423-430.
- Draxler, R. R., 1992: *Hybrid Single-Particle Lagrangian Integrated Trajectories (HY-SPLIT): Version 3.0--User's Guide and Model Description*. NOAA Technical Memorandum ERL ARL-195, Air Resources Laboratory, Silver Spring, MD, U.S.A., 26 pp.
- Durkee, P. A., F. Pfeil, E. Frost, and R. Shema, 1991: Global analysis of aerosol particle characteristics. *Atmos. Environ.*, **25A**, 2457-2471.
- Durkee, P. A., 1994: Cloud-climate feedback mechanisms: impact of the reduction of fossil fuel emissions--A science report for a sub-contract to the North Carolina State University. Unpublished.
- Fouquart, Y., and H. Isaka, 1992: Sulfur emission, CCN, clouds and climate: a review. *Ann. Geophys.*, **10**, 462-471.
- Fukuta, N., and V. K. Saxena, 1979: A horizontal thermal gradient cloud condensation nucleus spectrometer. *J. Appl. Meteor.*, **18**, 1352-1362.

- Ghan, S. J., K. E. Taylor, J. E. Penner, and D. J. Erickson, III, 1990: Model test of CCN-cloud albedo climate forcing. *Geophys. Res. Lett.*, **17**, 607-610.
- Hegg, D. A., P. V. Hobbs, and L. F. Radke, 1984: Measurements of the scavenging of sulfate and nitrate in clouds. *Atmos. Environ.*, **18**, 1939-1946.
- Hegg, D. A., L. F. Radke, and P. V. Hobbs, 1991: Measurements of Aitken nuclei and cloud condensation nuclei in the marine atmosphere and their relation to the DMS-cloud-climate hypothesis. *J. Geophys. Res.*, **96**, 18,727-18,733.
- Kadlecek, J., S. McLaren, N. Camarota, V. A. Mohnen, and J. Wilson, 1983: Cloud water chemistry at Whiteface Mountain. In: H. R. Pruppacher, R. G. Semonin and W. G. Slinn (Editors), *Precipitation Scavenging, Dry Deposition and Resuspension*. Elsevier, New York, NY, pp. 103-114.
- Knollenberg, R. G., 1981: Techniques for probing cloud microstructure. In: P. V. Hobbs and A. Deepak (Editors), *Clouds: Their Formation, Optical Properties, and Effects*. Academic Press, Inc., San Diego, CA, pp. 15-19.
- Kondrat'yev, K. Y., V. I. Binenko, and O. P. Petrenchuk, 1981: Radiative properties of clouds influenced by a city. *Izv. Acad. Sci. USSR Atmos. and Oceanic Phys. (English Translation)*, **17**, 122-127.
- Lacis, A. A., and J. E. Hansen, 1974: A parameterization of the absorption of solar radiation in the earth's atmosphere. *J. Atmos. Sci.*, **31**, 118-133.
- Leaitch, W. R., G. A. Isaac, J. W. Strapp, C. M. Banic, and H. A. Wiebe, 1992: The relationship between cloud droplet number concentrations and anthropogenic pollution: observations and climatic implications. *J. Geophys. Res.*, **97**, 2463-2474.
- Mohnen, V. A., and J. A. Kadlecek, 1989: Cloud chemistry research at Whiteface Mountain. *Tellus*, **41B**, 79-91.
- Parungo, F., J. F. Boatman, H. Sievering, S. W. Wilkison, and B. B. Hicks., 1994: Trends in global marine cloudiness and anthropogenic sulfur. *J. Climate*, **7**, 434-440.
- Radke, L. F., J. A. Coakley, Jr., and M. D. King, 1989: Direct and remote observations of the effect of ships on clouds. *Science*, **246**, 1146-1149.

- Raga, G. B., and P. R. Jonas, 1993: On the link between cloud-top radiative properties and sub-cloud aerosol concentrations. *Quart. J. Roy. Meteor. Soc.*, **119**, 1419-1425.
- Saxena, V. K., 1991: Climate forcing due to non-sea-salt sulfates. In: *Proceedings of the International Symposium on Glaciers-Ocean-Atmosphere Interactions, September, 1990*. IAHS-208, St. Petersburg, FL, pp. 243-255.
- Saxena, V. K., R. E. Stogner, A. H. Hendler, T. P. DeFelice, J.-Y. K. Yeh, and N.-H. Lin, 1989: Monitoring the chemical climate of the Mount Mitchell State Park for evaluation of its impact on forest decline. *Tellus*, **41B**, 92-109.
- Saxena, V. K., and J. D. Grovenstein, 1993: Impact of changes in sulfate aerosol loading on greenhouse warming. In: *Proceedings of the 1993 U.S. EPA/A&WMA International Symposium on Measurement of Toxic and Related Air Pollutants*. VIP-34, Air and Waste Management Association, Pittsburgh, PA, pp. 464-469.
- Slingo, A., 1990: Sensitivity of earth's radiation budget to changes in low clouds. *Nature*, **343**, 49-51.
- Twomey, S. A., 1977: The influence of pollution on the shortwave albedo of clouds. *J. Atmos. Sci.*, **34**, 1149-1152.
- Twomey, S. A., M. Piepgrass, and T. L. Wolfe, 1984: An assessment of the impact of pollution on global cloud albedo. *Tellus*, **36B**, 356-366.
- Twomey, S. A., 1991: Aerosols, clouds, and radiation. *Atmos. Environ.*, **25A**, 2435-2442.
- Wigley, T. M. L., 1991: Could reducing fossil-fuel emissions cause global warming? *Nature*, **349**, 3503-3505.

Table 1. Population mean microphysical and chemical parameters for three pH intervals. The \pm values represent standard errors.

	pH < 3.0	3.0 \leq pH < 3.7	3.7 \leq pH
Number of Cases	18	71	24
pH min-max	2.51-2.99	3.01-3.68	3.74-4.74
N (cm ⁻³)	793 \pm 36	589 \pm 21	282 \pm 22
r _{avg} (μ m)	3.35 \pm 0.14	3.77 \pm 0.08	4.99 \pm 0.24
w (g m ⁻³)	0.29 \pm 0.03	0.29 \pm 0.01	0.30 \pm 0.02
pH	2.86 \pm 0.03	3.28 \pm 0.02	3.98 \pm 0.04
[NO ₃ ⁻] (μ eq l ⁻¹)	98 \pm 8	53 \pm 3	9 \pm 2
[SO ₄ ²⁻] (μ eq l ⁻¹)	1428 \pm 127	691 \pm 375	132 \pm 15

Table 2. Cloud pH, microphysical parameters, CCN, and albedos for nine cases coincident with AVHRR satellite reflectivity data. \pm values represent various instrument error possibilities (5% for pH, CCN, and AVHRR albedo, 17% for N and r_{avg} , and 34% for w). Cloud thicknesses (h) were estimated from skew T-log p plots.

Date	pH	N (# cm ⁻³)	r_{avg} (μ m)	w (g m ⁻³)	CCN (# cm ⁻³)	h (m)	AVHRR Albedo (%)	<i>In Situ</i> Albedo (%)
1993								
8 Jun	3.07 \pm 0.15	771 \pm 131	2.79 \pm 0.47	0.16 \pm 0.06	940 \pm 47	140	53.0 \pm 2.7	54.0
14 Jun	2.84 \pm 0.14	823 \pm 140	2.88 \pm 0.49	0.18 \pm 0.06	1100 \pm 55	150	57.5 \pm 2.9	59.0
19 Jun	3.77 \pm 0.18	218 \pm 37	4.51 \pm 0.77	0.19 \pm 0.06	300 \pm 15	160	47.0 \pm 2.4	50.0
5 Aug	3.65 \pm 0.18	226 \pm 38	4.78 \pm 0.81	0.15 \pm 0.05	200 \pm 10	140	45.0 \pm 2.3	43.0
6 Aug	3.79 \pm 0.19	171 \pm 29	6.77 \pm 1.15	0.34 \pm 0.11	300 \pm 15	50	34.0 \pm 1.7	30.0
18 Aug	2.97 \pm 0.15	750 \pm 128	3.22 \pm 0.58	0.16 \pm 0.06	850 \pm 43	150	53.0 \pm 2.7	56.0
19 Aug	3.08 \pm 0.15	634 \pm 108	4.08 \pm 0.69	0.27 \pm 0.09	950 \pm 48	100	48.5 \pm 1.5	53.0
24 Aug	3.42 \pm 0.17	515 \pm 88	4.37 \pm 0.74	0.27 \pm 0.09	700 \pm 35	110	49.5 \pm 2.5	53.5
3 Oct	4.74 \pm 0.24	39 \pm 7	8.10 \pm 1.38	0.19 \pm 0.06	100 \pm 5	130	30.0 \pm 1.5	31.5

Table 3. Concentrations ($\mu\text{eq l}^{-1}$) of ionic constituents from the cloud water samples which corresponded with the observations of AVHRR satellite data. All quantities shown have a 5% instrument error potential.

Event/Satellite Case	$\mu\text{eq l}^{-1}$ SO ₄ ⁼	$\mu\text{eq l}^{-1}$ NO ₃ ⁻	$\mu\text{eq l}^{-1}$ NH ₄ ⁺	$\mu\text{eq l}^{-1}$ Cl ⁻	$\mu\text{eq l}^{-1}$ Na ⁺	$\mu\text{eq l}^{-1}$ Ca ⁺⁺	$\mu\text{eq l}^{-1}$ Mg ⁺⁺	$\mu\text{eq l}^{-1}$ K ⁺
8 Jun 93	720.63	45.30	277.19	61.21	60.29	70.08	31.72	15.86
14 Jun 93	664.17	40.73	155.61	31.88	26.05	20.91	12.18	7.77
19 Jun 93	162.08	24.76	73.22	39.21	51.59	23.35	13.74	6.98
* 5 Aug 93	319.17	24.61	121.39	34.67	5.26	25.95	4.94	2.97
6 Aug 93	164.65	9.42	23.06	2.83	1.91	3.12	1.23	0.00
# 18 Aug 93	1716.88	84.14	357.53	51.33	9.90	103.27	17.94	3.40
& 19 Aug 93	1110.21	107.11	218.33	38.87	3.91	30.79	9.54	2.48
24 Aug 93	589.58	64.50	190.00	38.76	52.15	35.28	18.51	6.47
3 Oct 93	N/A	N/A	N/A	N/A	N/A	N/A	N/A	N/A

Notes: * -- 5 Aug 93/0450 GMT ionic data was substituted.

-- 18 Aug 93/0250 GMT ionic data was substituted.

& -- 19 Aug 93/1155 GMT ionic data was substituted.

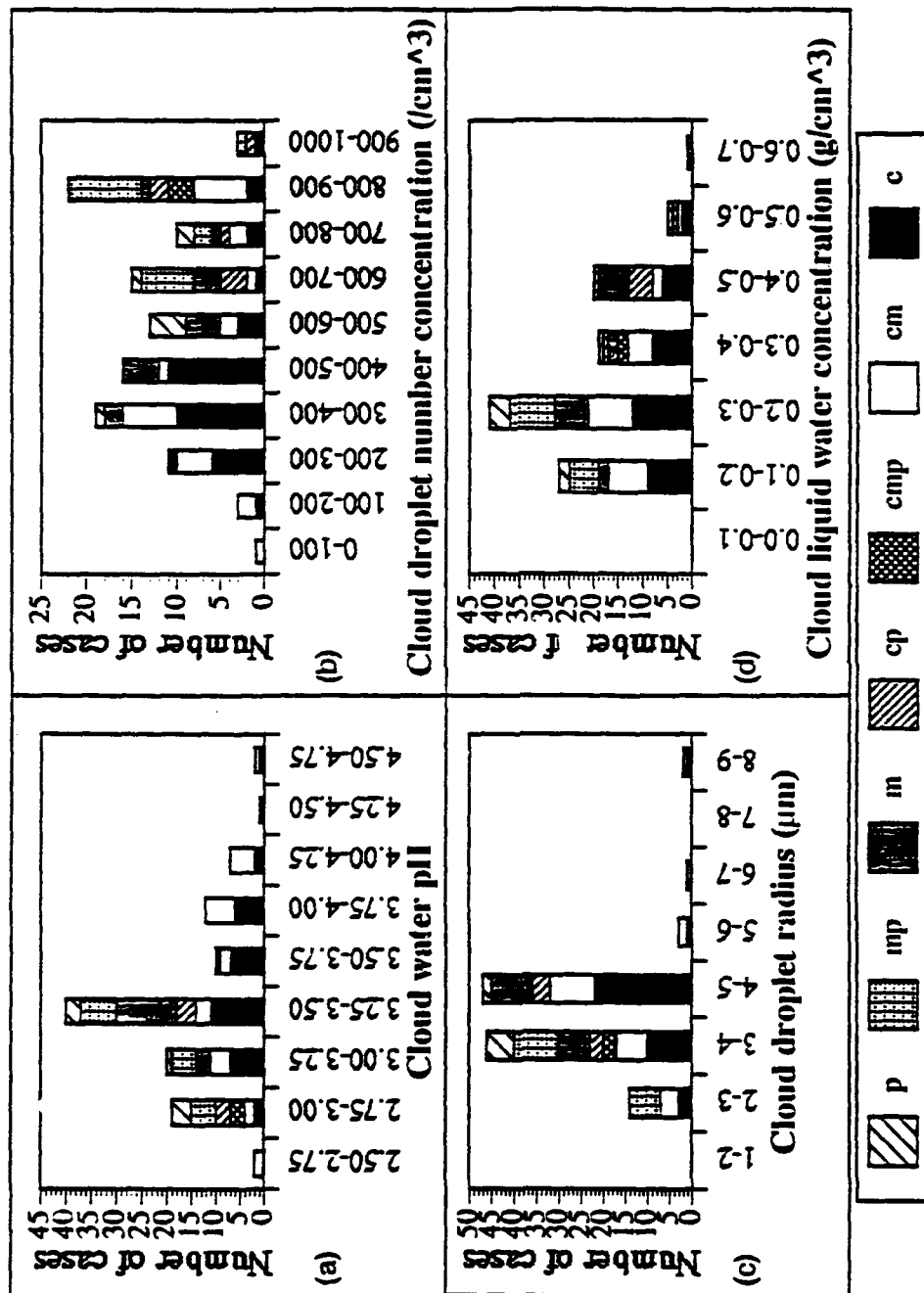


Figure 1. Frequency distributions of the 113 hourly cases for cloud acidity and microstructure measurements, subdivided to show the relative contributions from the various air mass sector origins.

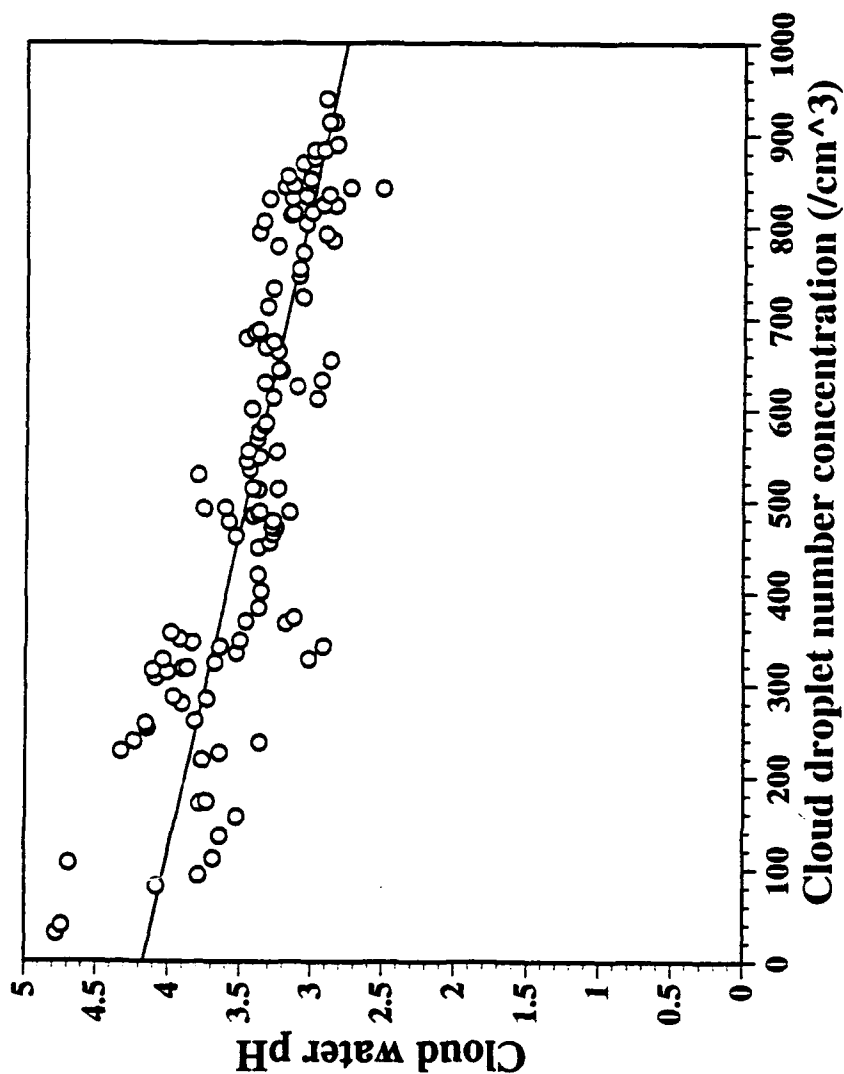


Figure 2. Cloud water pH versus cloud droplet number concentration (cm^{-3}). Least square line fit is shown (slope= -1.4×10^{-3} , intercept=4.2, $r^2=0.64$). Error bars are omitted for clarity. Cloud water pH measurements are assumed accurate to within five percent and cloud droplet number concentrations are assumed accurate to within seventeen percent.

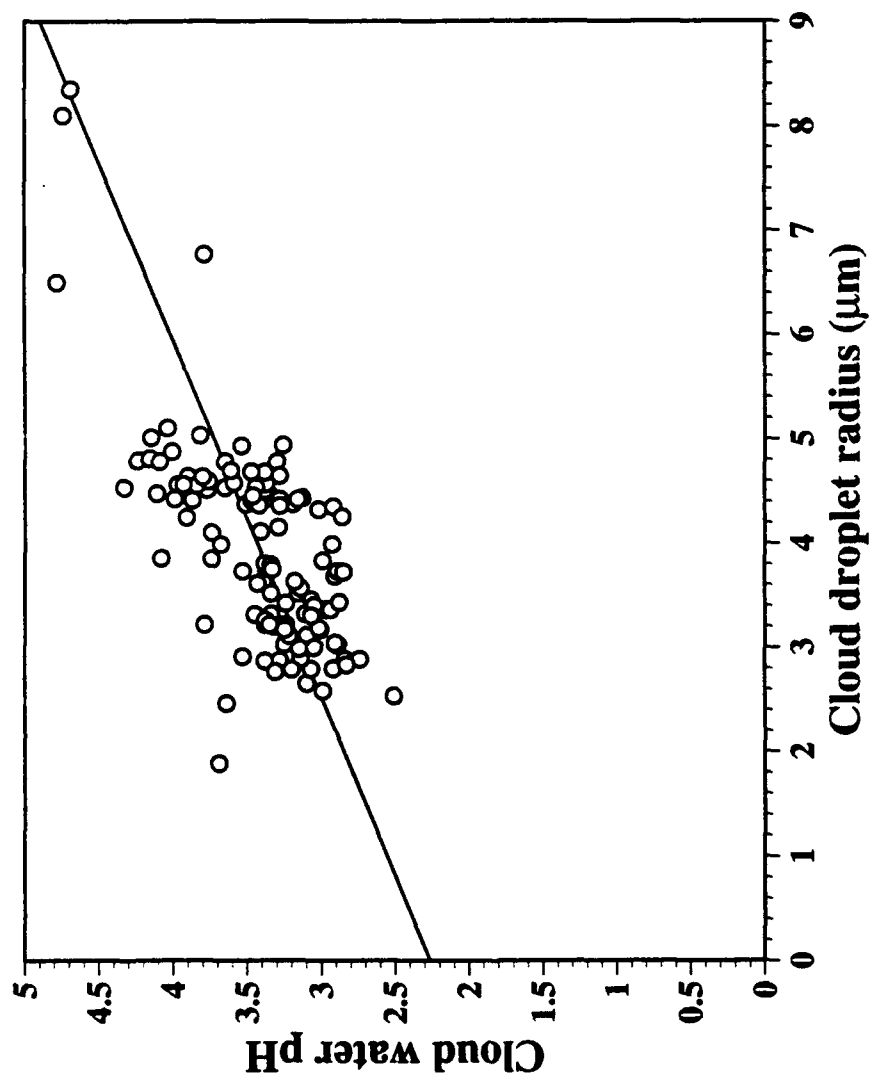


Figure 3. Cloud water pH versus cloud droplet radius (μm). Least square line fit is shown (slope=0.29, intercept=2.3, $r^2=0.47$). Error bars are omitted for clarity. Cloud water pH measurements are assumed accurate to within five percent and cloud droplet radius concentrations are assumed accurate to within seventeen percent.

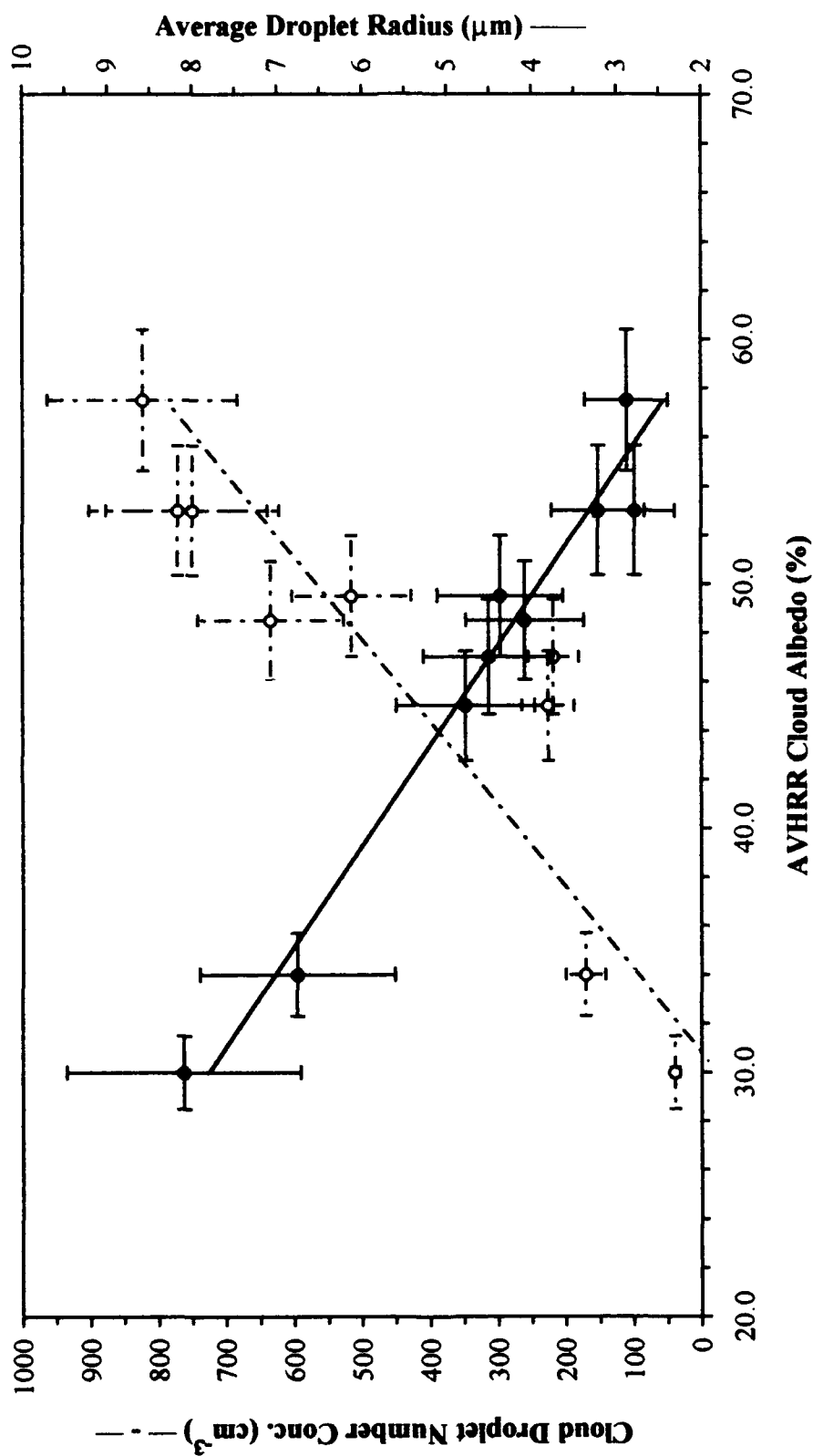


Figure 4. AVHRR cloud albedo vs. cloud droplet number concentration (cm^{-3}) and average droplet radius (μm) for nine cases from the 1993 field season. Error bars represent instrument errors (5% for AVHRR albedo and 17% for both cloud droplet number concentration and average radius).

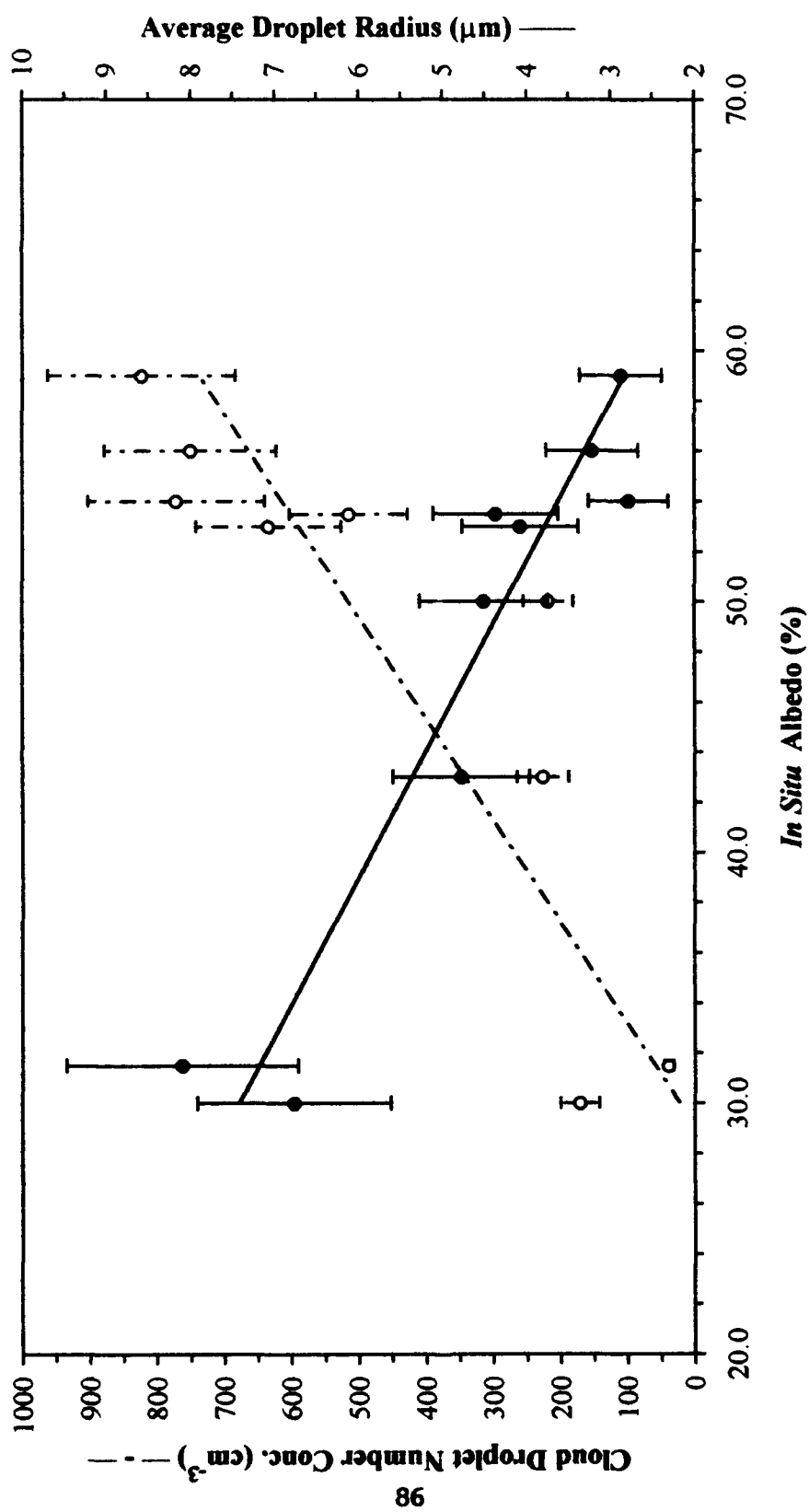


Figure 5. *In situ* cloud albedo vs. cloud droplet number concentration (cm^{-3}) and average droplet radius (μm) for nine cases from the 1993 field season. Error bars represent instrument errors (17% for both cloud droplet number concentration and average radius).

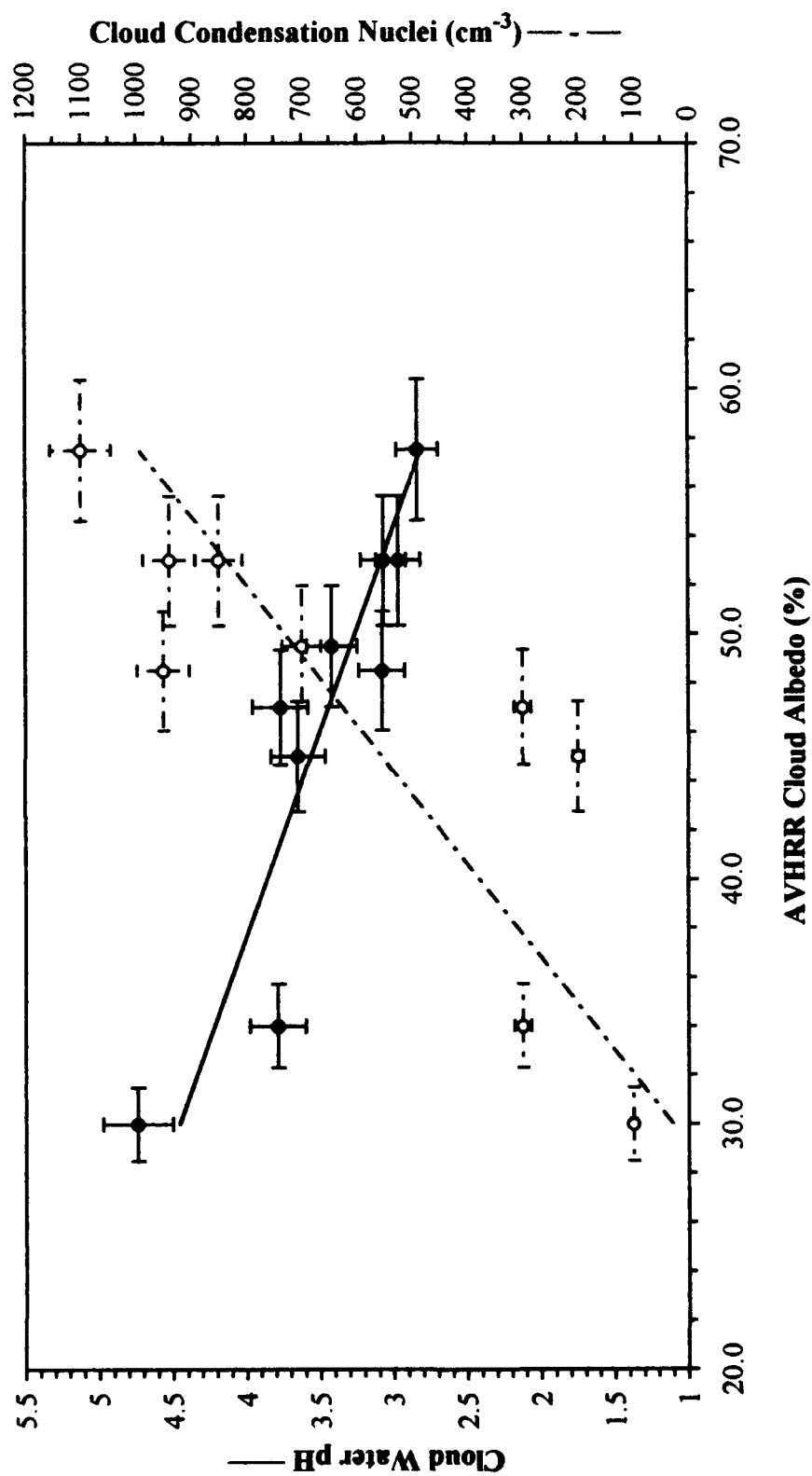


Figure 6. AVHRR cloud albedo vs. cloud water pH and cloud condensation nucleus concentration (cm⁻³) for nine cases from the 1993 field season. Error bars represent instrument errors (5% for all quantities).

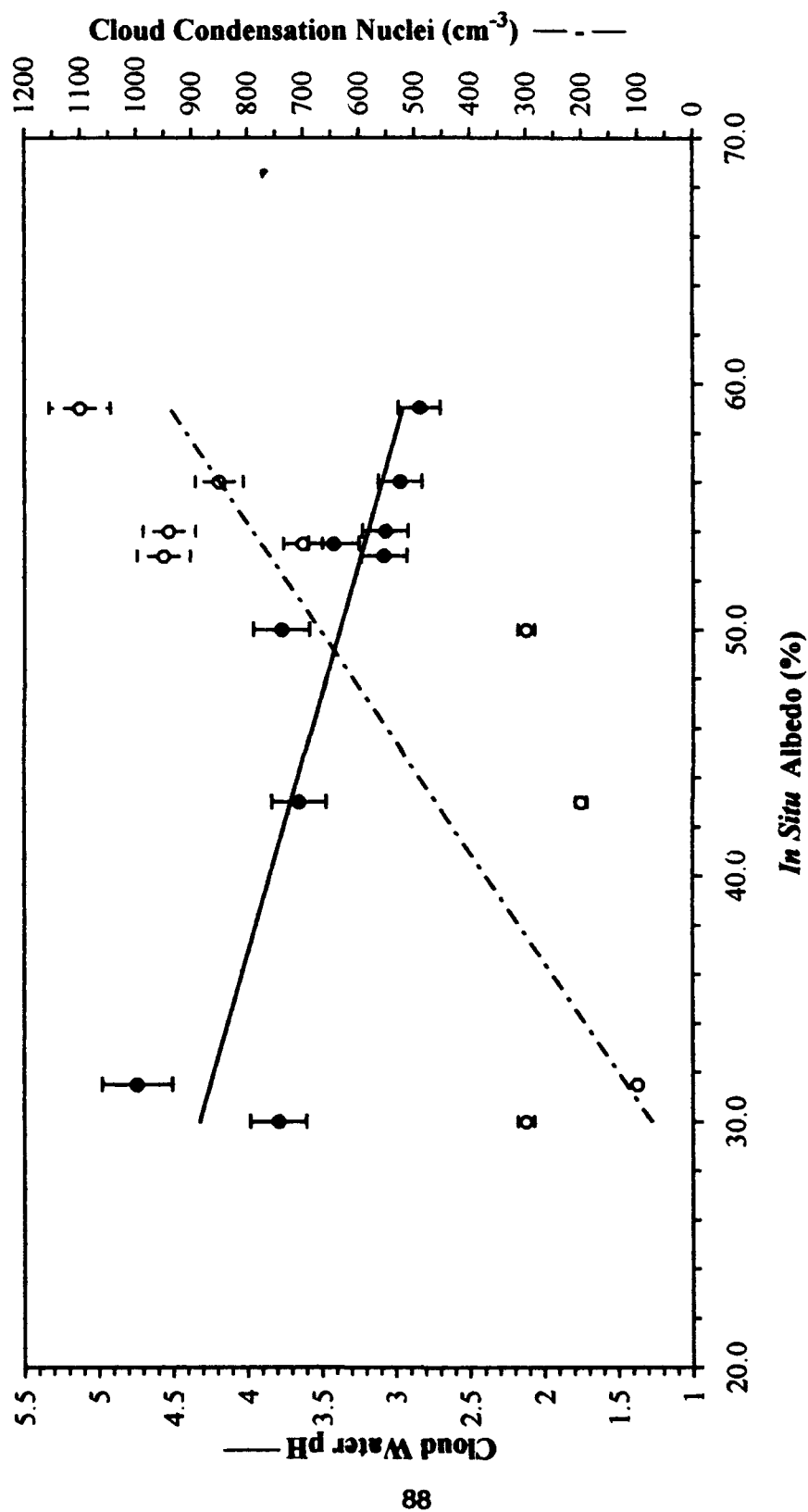


Figure 7. *In situ* cloud albedo vs. cloud water pH and cloud condensation nucleus concentration (cm^{-3}) for nine cases from the 1993 field season. Error bars represent instrument errors (5% for both pH and CCN concentrations).

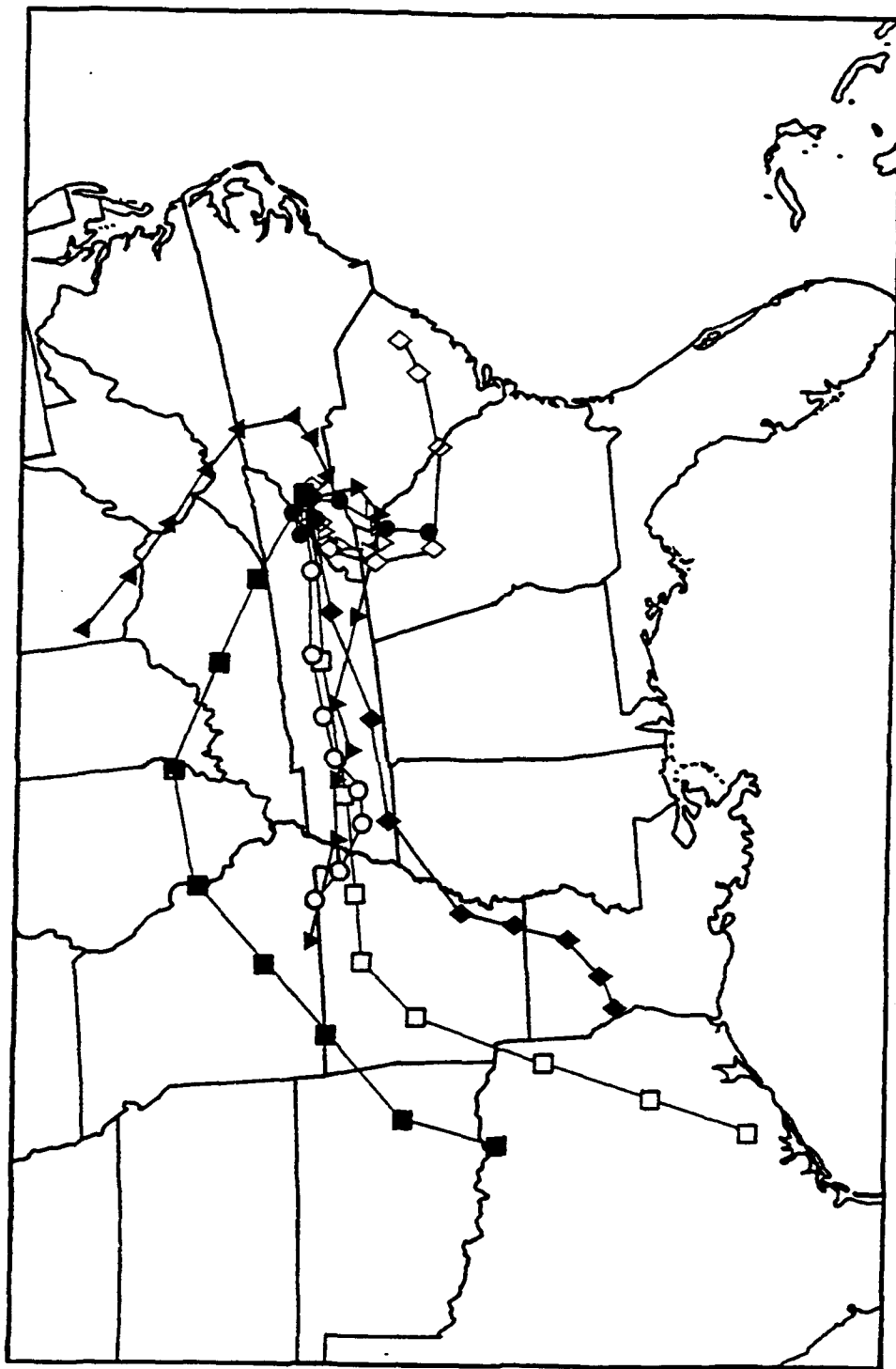


Figure 8. 48-hour back trajectories of the nine cases of cloud albedo derived from the AVHRR satellite during the 1993 field season. Plot symbols represent 6-hour time increments along the trajectory.

APPENDIX

Appendix The following tables and figures are all cross-referenced with material from Section I. They mainly provide data and diagrams concerning individual assessments of air mass history versus cloud water chemistry for each of the main months of sampling from the 1993 field season. Thus, most of the data are specifically concerned with analysis from either June or August of 1993.

Table A1. File of input parameters for running the HY-SPLIT trajectory model.

01	# TIME STEP; TRAJECTORY ADVECTION STEP (hrs)
BACK	# DIRECTION; OPTIONS (FWRD or BACK)
DATA	# VERTICAL MOTION; OPTIONS (ISOB DATA DIVG ISOS)
06	# STARTING MONTH; ZERO USES CURRENT DATA FILE
08	# DAY; RELATIVE IF MONTH ZERO
02	# HOUR; IF <0 THEN POSITION METEO BUT NO EMISSIONS
03	# DAYS TO RUN; ALWAYS IN WHOLE DAYS REGARDLESS OF START HOUR
JUN93.001	# METEO FILE; SUFFIX (BIN) OPTIONAL
35.73	# ORIGIN LATITUDE; USE NEGATIVE FOR SH (deg and frac)
82.29	# LONGITUDE; WEST IS POSITIVE (deg and frac)
808.0P	# HEIGHT; METERS FOR AGL OR MB FOR MSL (use suffix P)
0.0	# SOURCE VALUE; ARBITRARY UNITS PER HOUR
1	# EMISSION HOURS; PER INTERVAL SPECIFIED
9999	# INTERVAL; HOURS BETWEEN REPEAT OF EMISSION HOURS
01	# OUTPUT/AVERAGING PERIOD; APPLIES TO ALL MAPS OR FILES (hrs)
0	# OFFSET TIME; TIME OF FIRST OUTPUT (gmt hour)
1	# CONCENTRATION INDEX; INDEX NUMBER FOR OUTPUT (0 for deposition)
1	# HEIGHT OF INDEX; IN METERS ZERO DEFAULTS TO METEO GRID HEIGHTS
STEP	# DISK OUTPUT OF ENDPOINTS; OPTIONS (READ WRITE MOD STEP NONE)
NONE	# CONCENTRATION; OPTIONS (WRITE MOD NONE)
TRAJ	# MAP OUTPUTS; OPTIONS (TRAJectory SNAPshots CONCentration NONE)
NONE	# RUNTIME GRAPHICS; OPTIONS (NONE YES)
NUL	# ASCII PRINTER; OPTIONS (CONsole LPT FILE NUL)
45.0	# MAPLAT UPPER RIGHT; IN DEGREES AND FRACTION
27.0	# LAT LOWER LEFT; POSITIVE AND NEGATIVE AS ORIGIN
77.0	# LON UPPER RIGHT; SIZE DETERMINED BY VERTICAL HEIGHT
103.0	# LON LOWER LEFT; WIDTH ALWAYS 1.3 TIMES HEIGHT

Table A2. Cloud water pH ranges with corresponding mean values of ionic constituents ($\mu\text{eq l}^{-1}$) for the June, 1993 field season.

pH Range	Number of samples	Ionic Constituents									
		$\mu\text{eq l}^{-1}$ SO ₄ =	$\mu\text{eq l}^{-1}$ NO ₃ -	$\mu\text{eq l}^{-1}$ NH ₄ ⁺	$\mu\text{eq l}^{-1}$ Cl-	$\mu\text{eq l}^{-1}$ Na ⁺	$\mu\text{eq l}^{-1}$ Ca ⁺⁺	$\mu\text{eq l}^{-1}$ Mg ⁺⁺	$\mu\text{eq l}^{-1}$ K ⁺		
pH < 2.66	1	Mean 1889.79	157.10	476.72	117.35	90.00	174.75	50.68	20.05		
		St. Dev. 0.00	0.00	0.00	0.00	0.00	0.00	0.00	0.00		
pH 2.66-2.85	3	Mean 822.50	60.69	185.61	54.91	32.64	133.13	23.61	16.50		
		St. Dev. 366.80	34.11	57.73	24.51	22.65	201.33	24.21	10.36		
pH 2.86-3.05	12	Mean 883.81	59.62	230.74	37.17	17.49	52.87	13.70	7.97		
		St. Dev. 790.29	42.58	208.09	26.84	11.41	64.26	12.33	5.24		
pH 3.06-3.25	24	Mean 898.68	66.91	260.64	73.27	44.27	47.44	23.57	12.08		
		St. Dev. 351.59	30.42	112.87	49.85	47.97	19.45	12.30	9.39		
pH 3.26-3.45	46	Mean 597.31	45.74	189.40	50.73	32.73	31.94	16.01	7.01		
		St. Dev. 230.55	18.90	96.60	30.53	26.24	16.64	8.68	3.06		
pH 3.46-3.65	9	Mean 447.66	35.66	163.33	50.65	28.11	20.72	11.78	6.64		
		St. Dev. 185.21	13.90	88.01	26.01	12.99	6.91	6.69	3.06		
pH 3.66-3.85	8	Mean 163.72	11.52	37.74	12.27	17.88	11.69	6.95	7.05		
		St. Dev. 45.71	10.44	35.08	20.20	18.34	9.75	5.34	8.22		
pH 3.86-4.05	14	Mean 112.88	4.71	17.25	5.82	10.67	9.19	4.66	4.54		
		St. Dev. 18.87	1.89	3.30	11.10	3.25	12.30	7.16	5.24		
pH 4.06-4.25	21	Mean 65.82	3.06	11.02	0.58	7.28	5.39	2.16	2.48		
		St. Dev. 11.54	1.16	2.21	0.76	4.62	1.98	0.86	1.50		
pH > 4.25	0	Mean 0.00	0.00	0.00	0.00	0.00	0.00	0.00	0.00		
		St. Dev. 0.00	0.00	0.00	0.00	0.00	0.00	0.00	0.00		

Total number of observations = 138

Table A3. Cloud water pH ranges with corresponding mean values of ionic constituents ($\mu\text{eq l}^{-1}$) for the August, 1993 field season.

pH Range	Number of Samples	Ionic Constituents							
		$\mu\text{eq l}^{-1}$ SO ₄ =	$\mu\text{eq l}^{-1}$ NO ₃ -	$\mu\text{eq l}^{-1}$ NH ₄ +	$\mu\text{eq l}^{-1}$ Cl-	$\mu\text{eq l}^{-1}$ Na+	$\mu\text{eq l}^{-1}$ Ca++	$\mu\text{eq l}^{-1}$ Mg++	$\mu\text{eq l}^{-1}$ K+
pH < 2.66	0	Mean	0.00	0.00	0.00	0.00	0.00	0.00	0.00
		St. Dev.	0.00	0.00	0.00	0.00	0.00	0.00	0.00
pH 2.66-2.85	2	Mean	1829.48	79.77	382.19	45.43	10.55	91.02	16.74
		St. Dev.	49.35	0.46	0.20	15.26	0.03	1.76	1.22
pH 2.86-3.05	13	Mean	1458.48	107.17	343.91	54.30	12.85	70.79	16.33
		St. Dev.	424.11	19.75	95.35	14.04	9.69	40.27	8.23
pH 3.06-3.25	20	Mean	968.38	69.47	296.81	43.65	7.19	42.15	10.09
		St. Dev.	255.13	13.54	120.36	11.24	4.28	33.98	5.46
pH 3.26-3.45	27	Mean	594.56	50.15	178.49	33.24	11.53	34.27	8.24
		St. Dev.	125.99	15.03	63.41	16.47	17.37	25.49	6.32
pH 3.46-3.65	9	Mean	335.64	25.49	76.92	20.76	3.88	21.32	3.15
		St. Dev.	87.72	6.26	28.56	8.35	4.76	20.58	1.75
pH 3.66-3.85	9	Mean	241.19	17.29	66.10	16.84	4.19	14.13	3.08
		St. Dev.	55.30	5.31	36.45	11.31	4.04	7.18	1.27
pH 3.86-4.05	7	Mean	140.72	11.14	38.99	11.98	8.63	8.79	3.03
		St. Dev.	14.89	1.57	8.87	10.37	8.46	4.00	1.22
pH 4.06-4.25	4	Mean	96.63	5.56	22.99	3.35	2.58	2.48	0.84
		St. Dev.	14.20	0.38	1.62	1.14	1.17	1.09	0.10
pH > 4.25	3	Mean	43.58	3.59	15.22	30.90	21.52	4.79	1.45
		St. Dev.	36.36	1.48	6.12	36.56	36.21	6.83	1.73

Total number of observations = 94

Table A4. Statistical summary of mean concentrations, in $\mu\text{eq l}^{-1}$, of ionic constituents for trajectories calculated in the HY-SPLIT "Data" configuration for the June, 1993 field season.

Sectors Crossed by Trajectory										
Marine (N=40)	Field pH	SO₄=	NO₃-	NH₄+	Cl-	Na+	Ca++	Mg++	K+	
Mean	3.30	614.80	49.73	211.61	65.46	42.40	28.65	18.25	9.68	
Standard Deviation	0.16	368.06	30.13	127.72	43.39	29.67	14.06	9.94	5.16	
pH Range	2.93-3.57									
Continental (N=32)	Field pH	SO₄=	NO₃-	NH₄+	Cl-	Na+	Ca++	Mg++	K+	
Mean	3.60	388.84	28.20	102.83	26.08	18.79	41.54	11.59	6.79	
Standard Deviation	0.43	344.76	25.19	95.25	28.63	15.67	70.52	12.48	6.24	
pH Range	2.83-4.15									
Polluted (N=5)	Field pH	SO₄=	NO₃-	NH₄+	Cl-	Na+	Ca++	Mg++	K+	
Mean	3.17	1120.83	72.71	317.72	29.22	11.83	76.88	17.82	6.37	
Standard Deviation	0.22	709.88	39.72	215.41	18.00	3.26	45.47	8.87	3.45	
pH Range	2.92-3.39									
Marine/Contin. (N=14)	Field pH	SO₄=	NO₃-	NH₄+	Cl-	Na+	Ca++	Mg++	K+	
Mean	3.31	514.61	36.51	121.71	53.01	48.47	23.96	15.50	7.44	
Standard Deviation	0.29	348.74	21.54	81.32	40.47	44.68	17.14	12.97	6.43	
pH Range	2.74-3.82									
Marine/Polluted (N=13)	Field pH	SO₄=	NO₃-	NH₄+	Cl-	Na+	Ca++	Mg++	K+	
Mean	3.22	953.37	64.83	261.57	50.60	12.08	36.19	13.47	10.91	
Standard Deviation	0.15	459.63	20.00	98.04	17.31	5.87	16.99	7.15	10.56	
pH Range	2.88-3.38									

Table A4. (continued)

Contin./Marine (N=28)	Field pH	SO4=	NO3-	NH4+	Cl-	Na+	Ca++	Mg++	K+
Mean	3.89	179.17	9.88	35.72	6.70	11.58	11.55	4.28	3.43
Standard Deviation	0.40	347.87	29.65	92.59	22.31	16.47	32.15	9.20	3.50
pH Range	2.51-4.24								
Contin./Polluted (N=5)	Field pH	SO4=	NO3-	NH4+	Cl-	Na+	Ca++	Mg++	K+
Mean	3.21	947.17	77.00	296.99	47.39	11.93	67.14	26.98	4.75
Standard Deviation	0.07	137.14	15.00	29.46	12.46	1.94	10.28	4.26	0.62
pH Range	3.09-3.26								
Marine/Con./Poll. (N=1)	Field pH	SO4=	NO3-	NH4+	Cl-	Na+	Ca++	Mg++	K+
Mean	2.84	664.17	40.73	155.61	31.88	26.05	20.91	12.18	7.77
Standard Deviation	0.00	0.00	0.00	0.00	0.00	0.00	0.00	0.00	0.00
pH Range	2.84								

Notes: Polluted/Marine and Polluted/Continental sector categories had no trajectories which coincided with ionic data.

Samples might include liquid precipitation as well as cloud water.

Table A5. Statistical summary of mean concentrations, in $\mu\text{eq l}^{-1}$, of ionic constituents for trajectories calculated in the HY-SPLIT "Isobaric" configuration for the June, 1993 field season.

Sectors Crossed by Trajectory		Field pH	SO ₄ =	NO ₃ -	NH ₄ +	Cl-	Na+	Ca++	Mg++	K+
Marine (N=34)										
Mean		3.31	686.75	56.38	238.12	74.60	50.01	31.28	20.80	10.40
Standard Deviation		0.15	332.15	27.95	112.98	42.20	32.75	12.80	9.85	5.03
pH Range		3.01-3.57								
Continental (N=31)										
Mean		3.61	375.92	27.55	102.42	26.46	19.54	38.83	11.02	6.85
Standard Deviation		0.43	343.40	25.34	97.06	29.05	15.81	71.12	12.39	6.32
pH Range		2.83-4.15								
Polluted (N=6)										
Mean		3.18	1056.94	68.57	293.96	27.36	11.37	72.94	16.67	5.87
Standard Deviation		0.20	653.93	36.95	201.27	16.73	3.12	41.80	8.41	3.32
pH Range		2.92-3.39								
Marine/Contin. (N=19)										
Mean		3.24	429.46	30.38	107.27	45.33	40.63	22.34	13.71	7.52
Standard Deviation		0.29	364.59	23.15	97.63	38.09	40.51	17.06	12.04	6.26
pH Range		2.74-3.82								
Marine/Polluted (N=13)										
Mean		3.22	953.37	64.83	261.57	50.60	12.08	36.19	13.47	10.91
Standard Deviation		0.15	459.63	20.00	98.04	17.31	5.87	16.99	7.15	10.56
pH Range		2.88-3.38								

Table A5. (continued)

Contin./Marine (N=29)	Field pH	SO ₄ =	NO ₃ -	NH ₄ +	Cl-	Na+	Ca++	Mg++	K+
Mean	3.88	189.96	10.98	38.15	7.26	11.07	11.54	4.37	3.47
Standard Deviation	0.38	346.55	29.71	91.45	22.11	15.95	31.56	9.05	3.44
pH Range	2.51-4.24								
Contin./Polluted (N=6)	Field pH	SO ₄ =	NO ₃ -	NH ₄ +	Cl-	Na+	Ca++	Mg++	K+
Mean	3.22	890.69	70.75	268.88	42.92	11.89	71.28	26.93	5.19
Standard Deviation	0.07	184.88	20.37	73.72	15.61	1.74	13.70	3.81	1.21
pH Range	3.09-3.28								

Notes: Polluted/Marine and Polluted/Continental sector categories had no trajectories which coincided with ionic data.

Samples might include liquid precipitation as well as cloud water.

Table A6. Statistical summary of mean concentrations, in $\mu\text{eq l}^{-1}$, of ionic constituents for trajectories calculated in the HY-SPLIT "Data" configuration for the August, 1993 field season.

Sectors Crossed by Trajectory											
Marine (N=16)	Field pH	SO ₄ =	NO ₃ -	NH ₄ +	Cl-	Na+	Ca++	Mg++	K+		
Mean	3.24	730.29	78.64	247.70	45.01	15.38	26.96	10.73	5.32		
Standard Deviation	0.13	192.14	21.82	38.71	12.76	21.56	19.50	6.91	1.58		
pH Range	3.05-3.42										
Continental (N=37)	Field pH	SO ₄ =	NO ₃ -	NH ₄ +	Cl-	Na+	Ca++	Mg++	K+		
Mean	3.54	431.48	33.25	108.13	31.21	6.67	17.26	3.99	2.37		
Standard Deviation	0.32	251.82	21.33	71.86	20.43	11.09	11.76	2.48	2.55		
pH Range	3.02-4.33										
Polluted (N=1)	Field pH	SO ₄ =	NO ₃ -	NH ₄ +	Cl-	Na+	Ca++	Mg++	K+		
Mean	2.91	1242.71	137.82	272.28	47.48	10.27	30.14	8.39	4.19		
Standard Deviation	0.00	0.00	0.00	0.00	0.00	0.00	0.00	0.00	0.00		
pH Range	2.91										
Marine/Contin. (N=7)	Field pH	SO ₄ =	NO ₃ -	NH ₄ +	Cl-	Na+	Ca++	Mg++	K+		
Mean	3.41	919.65	51.33	323.66	28.62	6.23	59.02	12.11	2.78		
Standard Deviation	0.46	570.73	31.96	211.41	18.45	4.02	46.16	8.36	1.98		
pH Range	3.07-4.08										
Marine/Polluted (N=3)	Field pH	SO ₄ =	NO ₃ -	NH ₄ +	Cl-	Na+	Ca++	Mg++	K+		
Mean	2.99	1491.60	123.09	356.83	66.55	28.59	95.21	27.94	10.55		
Standard Deviation	0.09	169.41	10.22	7.42	14.61	4.01	4.78	1.69	0.46		
pH Range	2.89-3.04										

Table A6. (continued)

Contin./Marine (N=11)	Field pH	SO4=	NO3-	NH4+	Cl-	Na+	Ca++	Mg++	K+
Mean	3.91	346.01	19.75	86.87	11.65	3.65	15.76	3.69	0.87
Standard Deviation	0.50	653.83	27.76	155.41	14.40	3.40	33.01	5.36	1.20
pH Range	2.91-4.68								
Contin./Polluted (N=6)	Field pH	SO4=	NO3-	NH4+	Cl-	Na+	Ca++	Mg++	K+
Mean	2.92	1746.81	82.95	398.22	46.89	10.25	103.60	18.18	3.80
Standard Deviation	0.09	203.28	7.50	49.38	8.95	1.73	13.28	1.60	0.36
pH Range	2.85-3.09								
Polluted/Marine (N=1)	Field pH	SO4=	NO3-	NH4+	Cl-	Na+	Ca++	Mg++	K+
Mean	2.99	1110.21	107.11	218.33	38.87	3.91	30.79	9.54	2.48
Standard Deviation	0.00	0.00	0.00	0.00	0.00	0.00	0.00	0.00	0.00
pH Range	2.99								
Polluted/Contin. (N=8)	Field pH	SO4=	NO3-	NH4+	Cl-	Na+	Ca++	Mg++	K+
Mean	3.36	617.16	44.64	155.48	23.20	7.49	64.28	7.52	1.05
Standard Deviation	0.09	95.75	5.92	20.03	4.36	1.45	11.19	1.11	0.42
pH Range	3.28-3.47								
Marine/Con./Poll. (N=2)	Field pH	SO4=	NO3-	NH4+	Cl-	Na+	Ca++	Mg++	K+
Mean	3.09	1262.71	67.35	378.14	38.41	13.27	40.47	10.94	3.82
Standard Deviation	0.10	356.21	10.36	115.45	3.85	5.54	22.09	2.44	0.27
pH Range	3.02-3.16								
Marine/Poll./Con. (N=2)	Field pH	SO4=	NO3-	NH4+	Cl-	Na+	Ca++	Mg++	K+
Mean	3.18	929.17	61.69	276.36	31.20	13.33	27.62	8.89	3.27
Standard Deviation	0.00	19.45	0.09	0.04	1.95	0.03	0.53	0.00	0.11
pH Range	3.18								

Notes: Samples might include liquid precipitation as well as cloud water.

Table A7. Statistical summary of mean concentrations, in $\mu\text{eq l}^{-1}$, of ionic constituents for trajectories calculated in the HY-SPLIT "Isobaric" configuration for the August, 1993 field season.

Sectors Crossed by Trajectory		Field pH	SO ₄ =	NO ₃ -	NH ₄ +	Cl-	Na+	Ca++	Mg++	K+
Marine (N=13)										
Mean		3.22	725.76	79.11	253.50	43.90	5.44	18.99	7.68	4.75
Standard Deviation		0.13	204.93	23.81	38.29	13.39	1.38	3.15	1.58	1.00
pH Range		3.05-3.41								
Continental (N=43)										
Mean		3.64	386.88	30.65	99.76	28.57	7.71	16.90	4.29	2.29
Standard Deviation		0.40	266.43	22.60	73.73	21.27	13.78	14.01	4.30	2.62
pH Range		3.02-4.68								
Polluted (N=3)										
Mean		3.16	885.49	79.38	201.76	32.21	7.81	48.39	8.01	2.01
Standard Deviation		0.21	309.41	50.61	61.07	13.29	2.12	15.80	0.34	1.90
pH Range		2.91-3.28								
Marine/Polluted (N=5)										
Mean		3.07	1266.63	98.53	324.64	52.41	22.49	68.17	20.32	7.64
Standard Deviation		0.12	330.67	34.40	44.39	21.97	8.83	37.18	10.51	4.00
pH Range		2.89-3.18								
Contin./Marine (N=9)										
Mean		3.64	356.59	29.81	92.51	17.64	13.49	17.60	6.38	2.00
Standard Deviation		0.31	277.08	29.86	85.86	18.19	23.36	26.66	9.30	3.21
pH Range		3.26-4.08								

Table A7. (continued)

Contin./Polluted (N=9)	Field pH	SO4=	NO3-	NH4+	Cl-	Na+	Ca++	Mg++	K+
Mean	3.04	1531.78	76.36	458.12	42.85	8.66	92.78	17.44	3.97
Standard Deviation	0.14	397.23	11.34	59.71	10.16	2.27	18.19	2.59	0.54
pH Range	2.85-3.24								
Polluted/Marine (N=1)	Field pH	SO4=	NO3-	NH4+	Cl-	Na+	Ca++	Mg++	K+
Mean	2.99	1110.21	107.11	218.33	38.87	3.91	30.79	9.54	2.48
Standard Deviation	0.00	0.00	0.00	0.00	0.00	0.00	0.00	0.00	0.00
pH Range	2.99								
Polluted/Contin. (N=9)	Field pH	SO4=	NO3-	NH4+	Cl-	Na+	Ca++	Mg++	K+
Mean	3.23	994.86	57.91	227.76	30.63	8.84	81.44	11.23	1.95
Standard Deviation	0.24	662.47	643.54	129.60	23.15	3.97	40.29	5.86	44.45
pH Range	2.89-3.47								
Marine/Con./Poll. (N=2)	Field pH	SO4=	NO3-	NH4+	Cl-	Na+	Ca++	Mg++	K+
Mean	3.12	1154.58	65.51	325.53	39.31	15.18	29.34	10.08	3.67
Standard Deviation	0.06	203.29	7.74	41.05	5.13	2.83	6.35	1.22	0.49
pH Range	3.07-3.16								

Notes: Marine/Continental sector category had no trajectories which coincided with ionic data.

Samples might include liquid precipitation as well as cloud water.

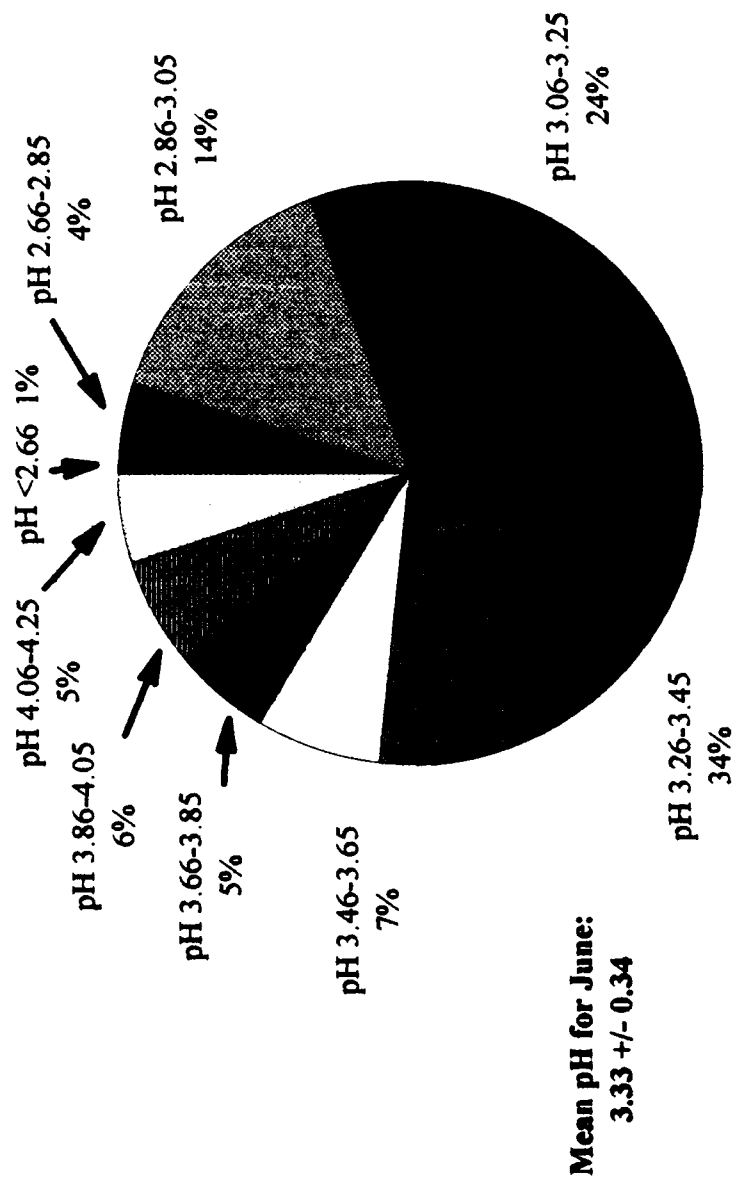


Figure A1. Relative frequencies of pH ranges for all samples retrieved during the June, 1993 field season.

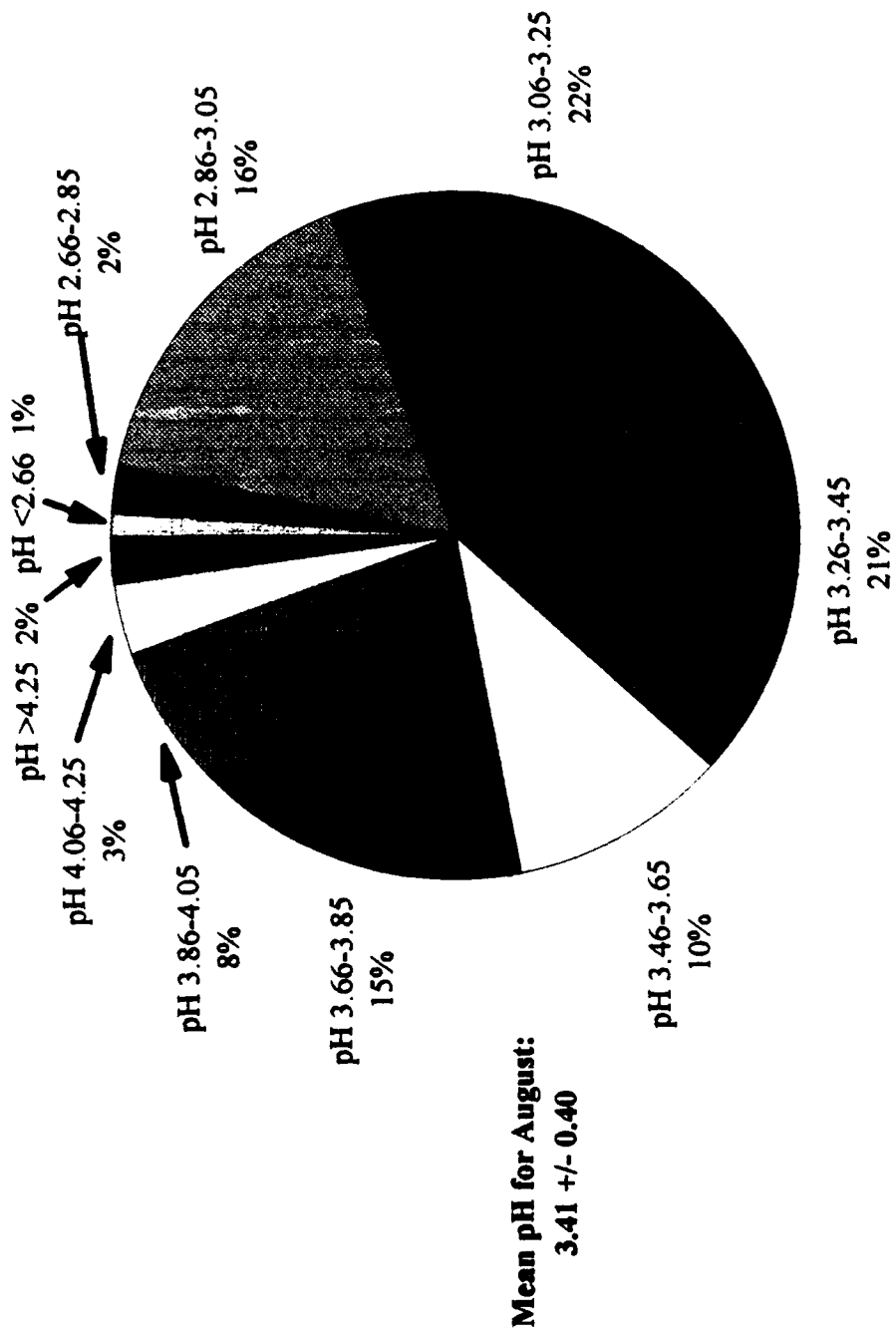


Figure A2. Relative frequencies of pH ranges for all samples retrieved during the August, 1993 field season.

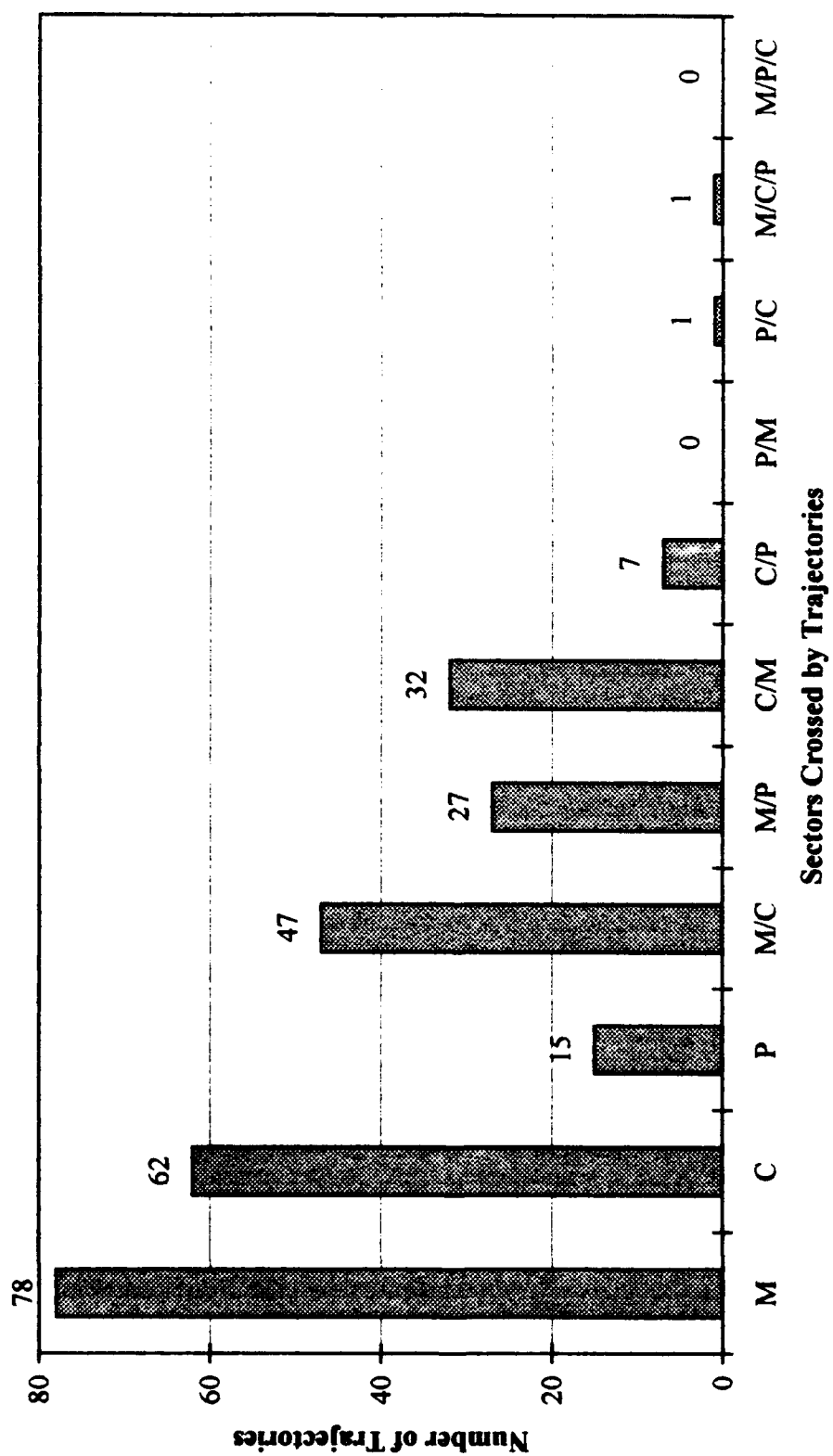


Figure A3. HY-SPLIT model results for all trajectories from the June, 1993 field season.

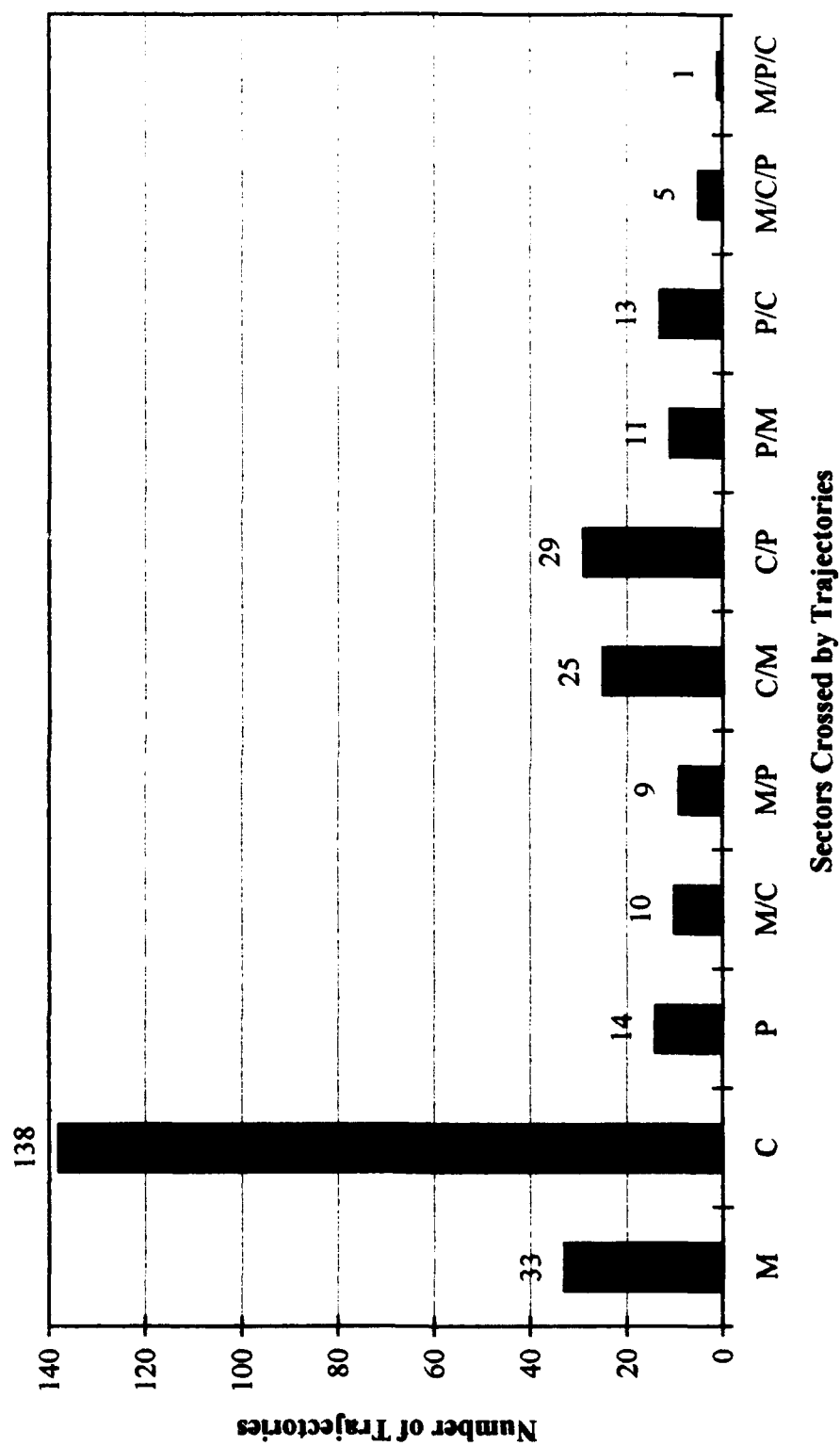


Figure A4. HY-SPLIT model results for all trajectories from the August, 1993 field season.

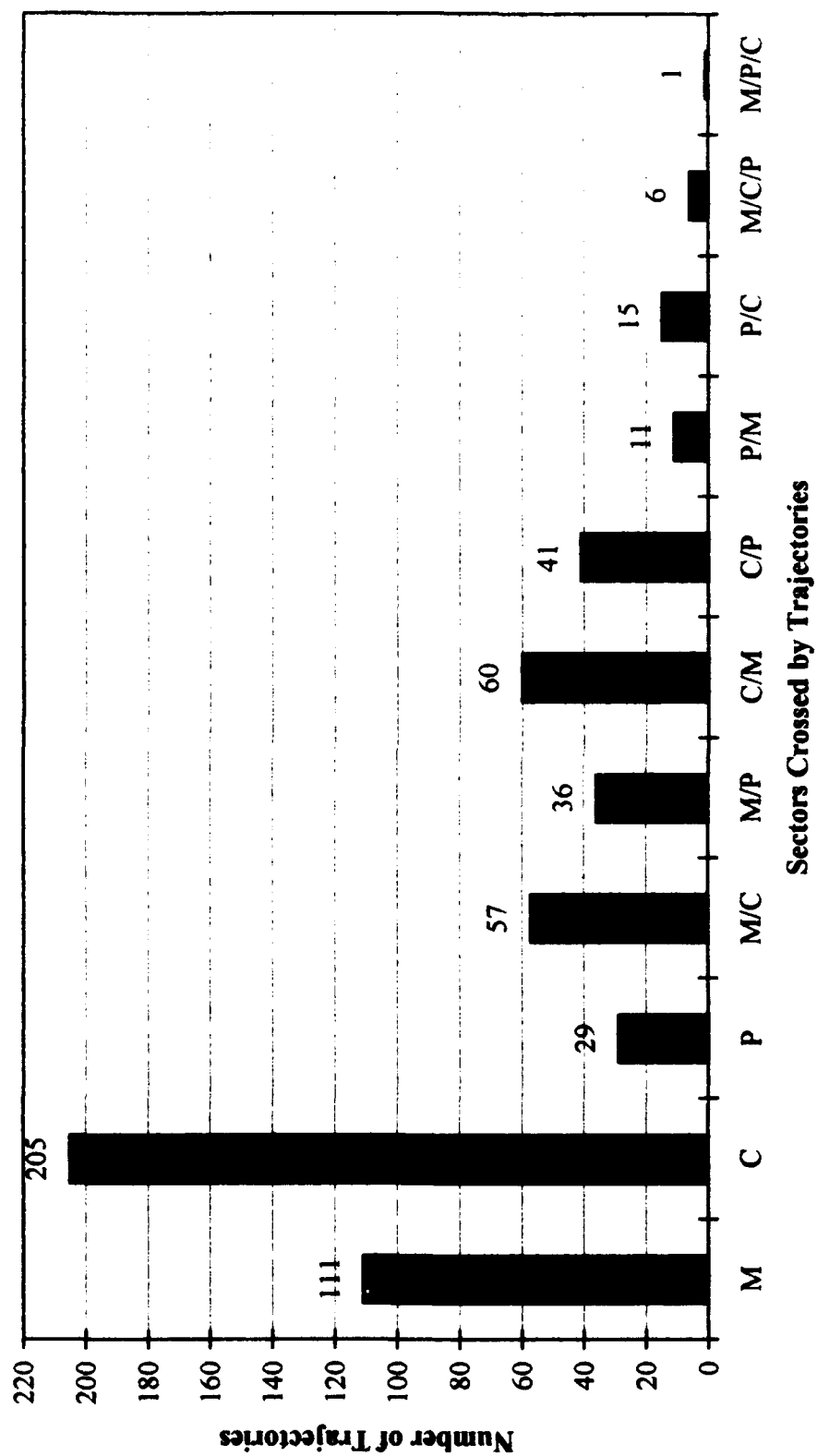


Figure A5. HY-SPLIT model results of all air mass trajectories calculated during cloud events for the entire 1993 field season.

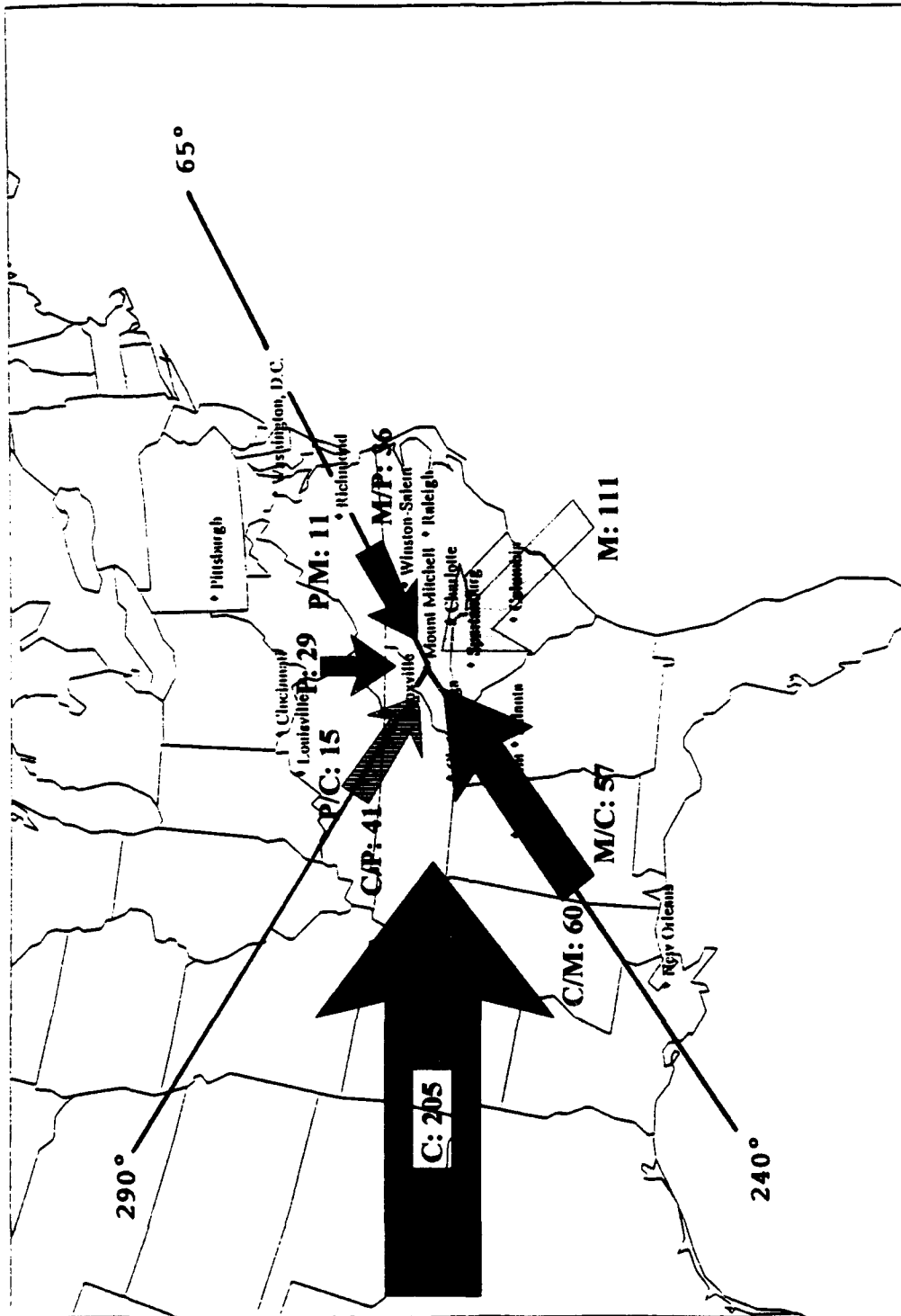


Figure A6 Schematic diagram showing HY-SPLIT model results of all trajectory calculations from the 1993 field season as in figure A5, but with arrows representing relative numbers of trajectories in each category.

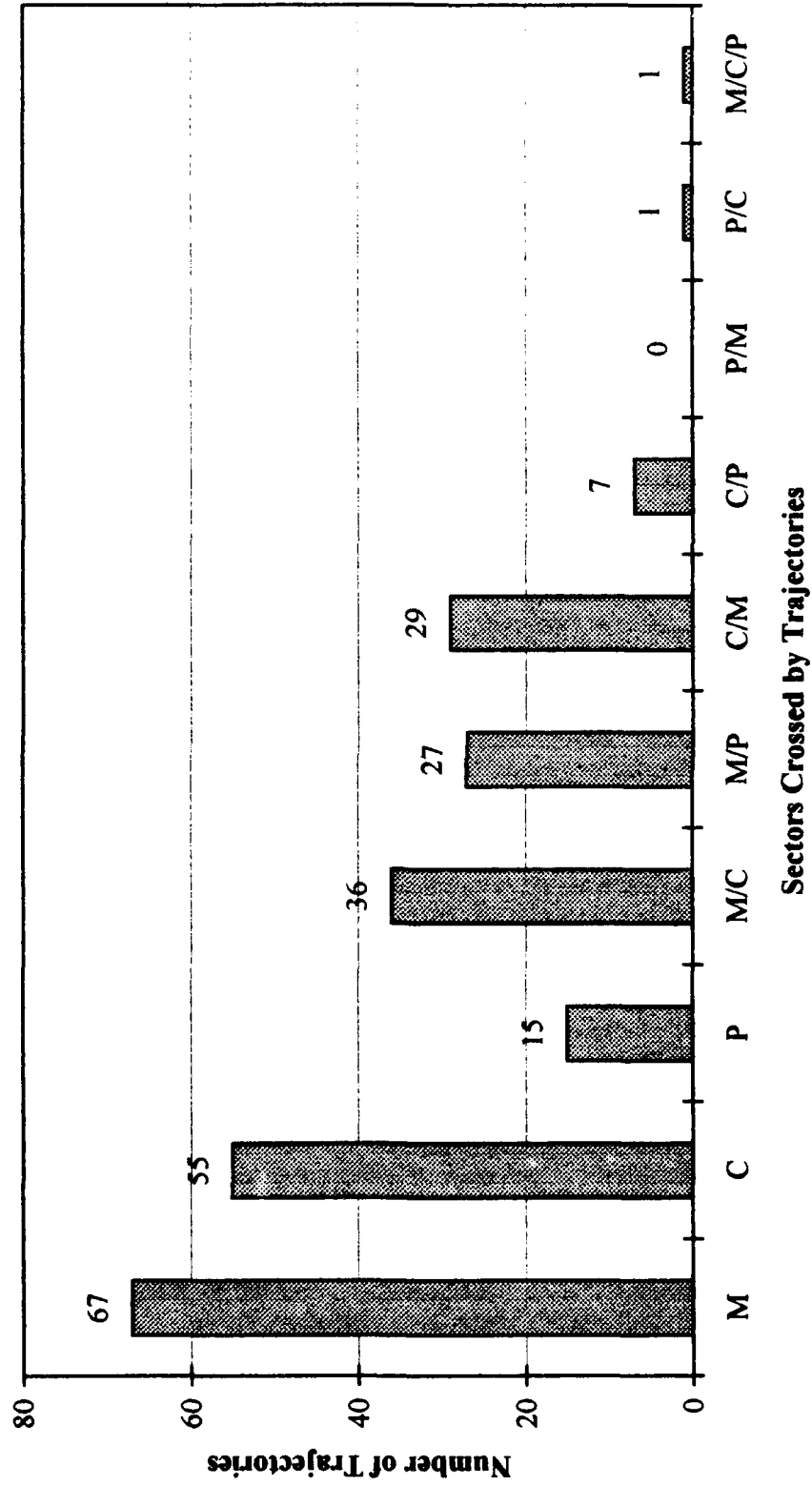


Figure A7. HY-SPLIT model results for all pH-associated trajectories from the June, 1993 field season.

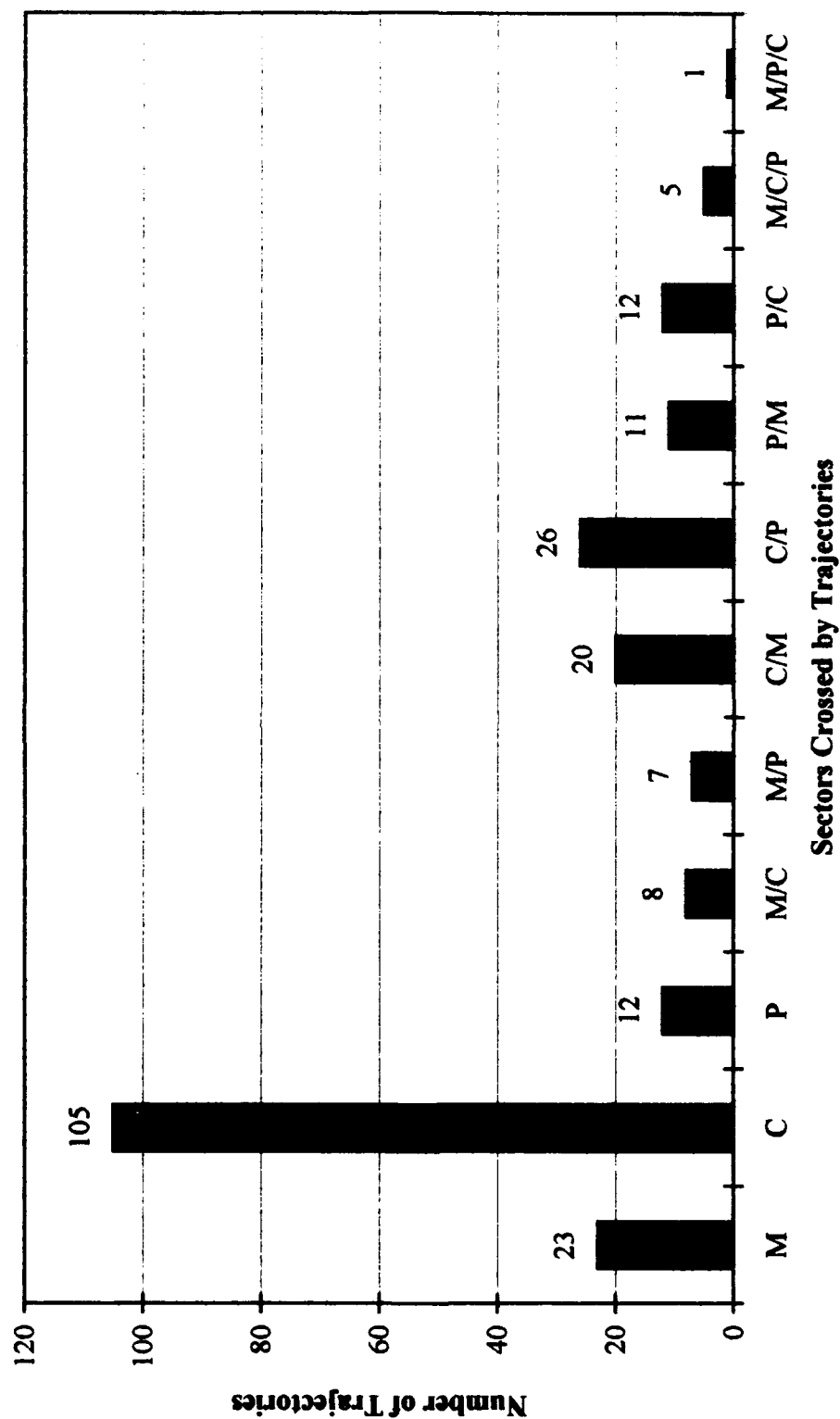


Figure A8. HY-SPLIT model results for all pH-associated trajectories from the August, 1993 field season.

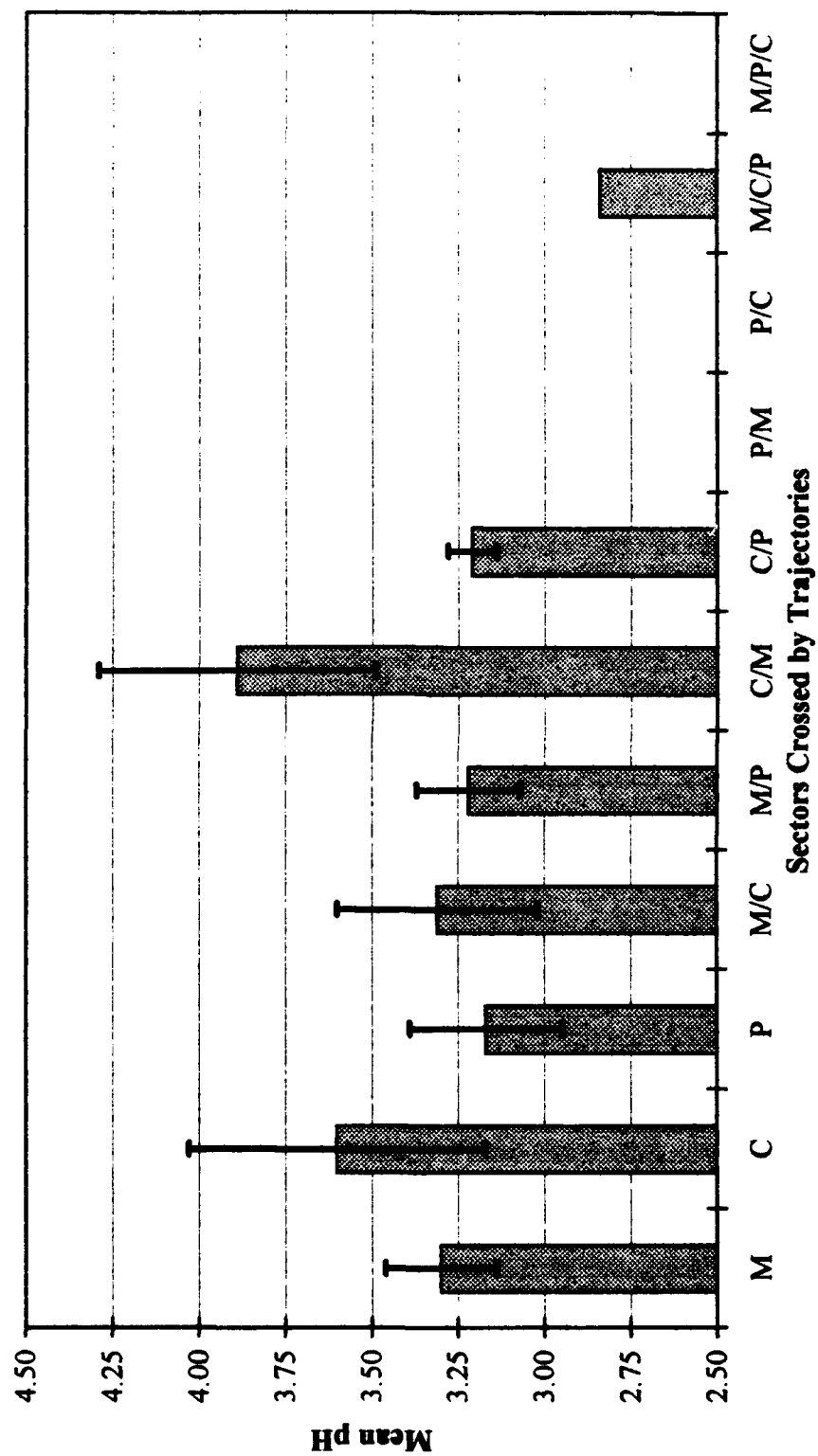


Figure A9. Mean pH versus HY-SPLIT trajectory category crossed for samples from the June, 1993 field season calculated in the DATA configuration. Error bars represent standard deviations of the pH within each category.

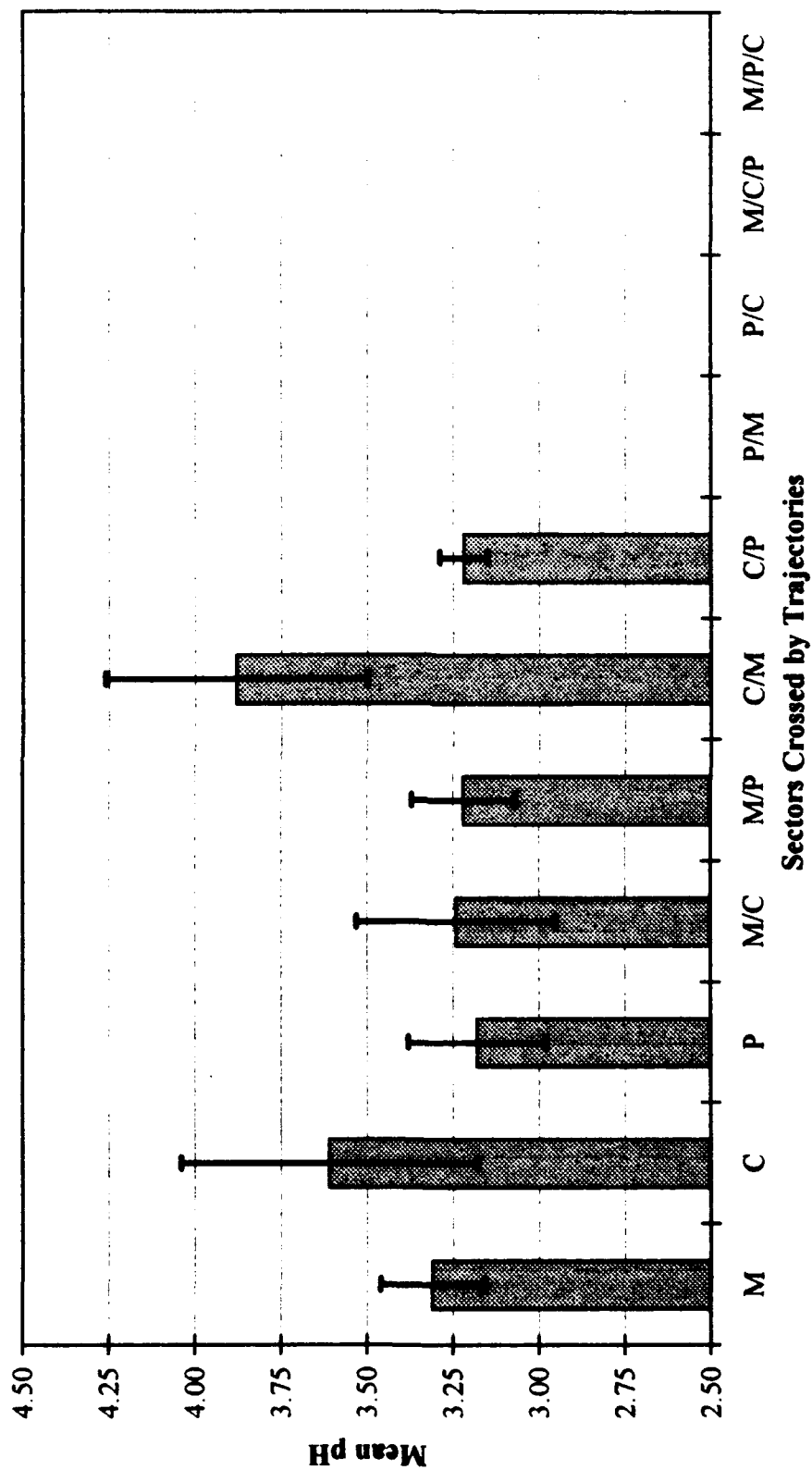


Figure A10. Mean pH versus HY-SPLIT trajectory category crossed for samples from the June, 1993 field season calculated in the ISOBARIC configuration. Error bars represent the standard deviations of the pH within each category.

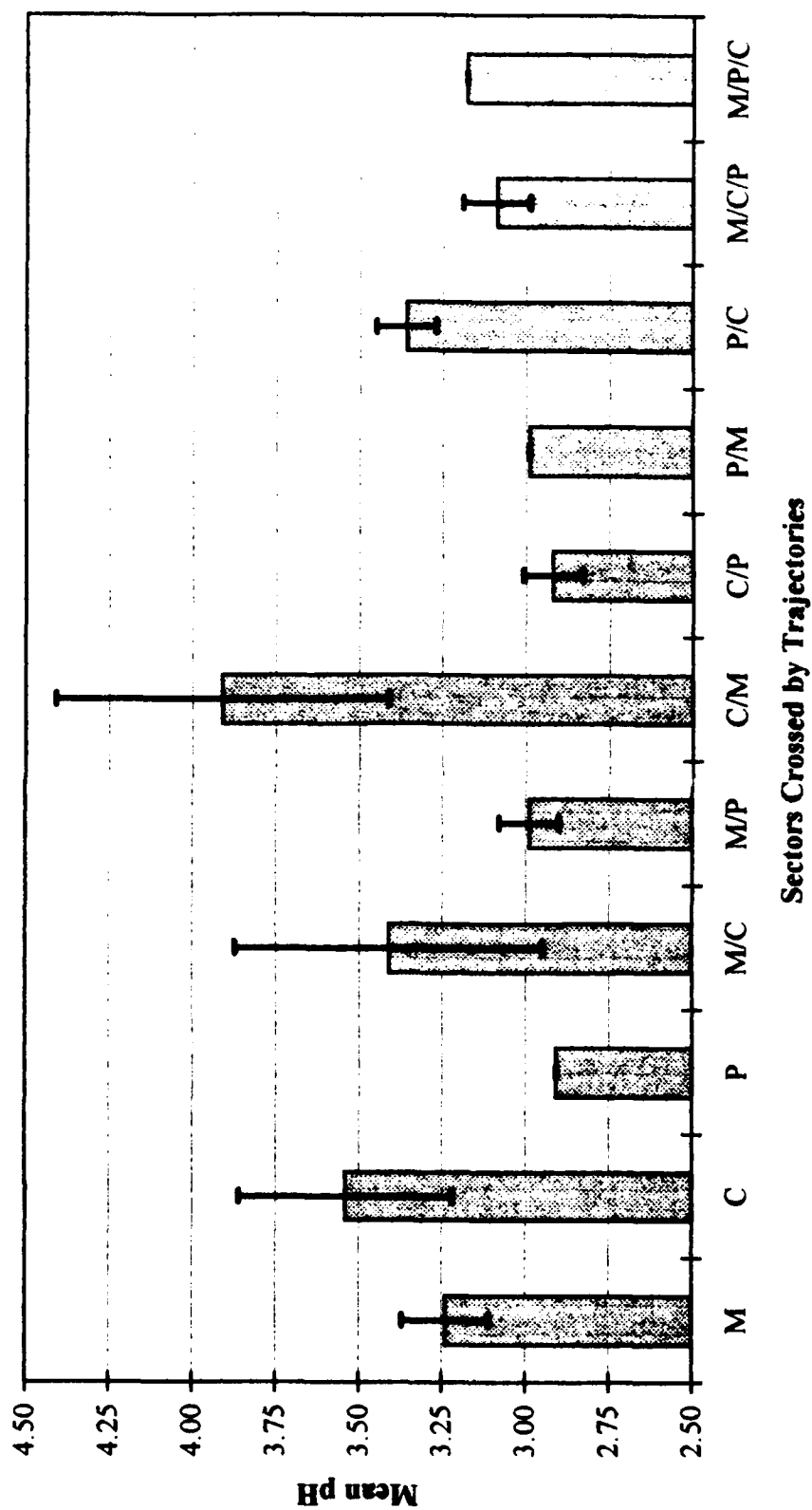


Figure A11. Mean pH versus HY-SPLIT trajectory category crossed for samples from the August, 1993 field season calculated in the DATA configuration. Error bars represent the standard deviation of the pH within each category.

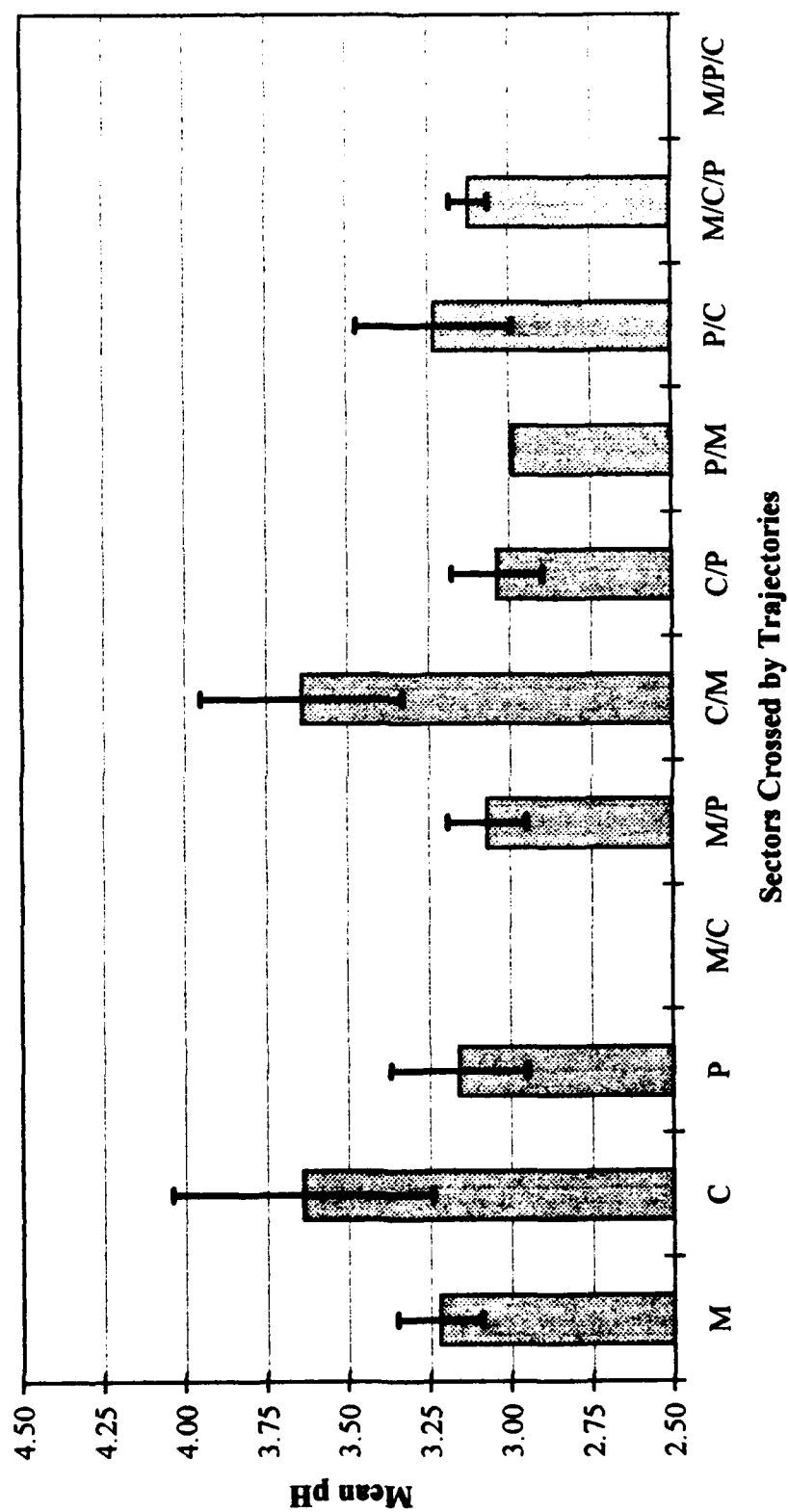


Figure A12. Mean pH versus HY-SPLIT trajectory category crossed for samples from the August, 1993 field season calculated in the ISOBARIC configuration. Error bars represent standard deviations of the pH within each category.

ABSTRACT

ULMAN, JAMES CHARLES. Impact of Air Mass History on the Chemical, Microphysical, and Radiative Properties of Clouds at Mount Mitchell, North Carolina. (Under the direction of Vinod K. Saxena and Viney P. Aneja.)

SECTION I. Cloud water acidity and ionic content, as measured at the Mount Mitchell State Park observing site (35° 44' 05" N, 82° 17' 15" W, 2038 m MSL--highest peak in the eastern U.S.), using a passive cloud water collector, are directly influenced by the trajectories of cloud forming air masses which pass over areas of varying levels of pollutant emission. Regions of the United States which are emitters of high levels of pollutants, such as SO_x and NO_x, will thus serve to reduce observed pH levels in cloud water samples and raise the levels of acidifying ions, such as sulfate and nitrate. Cloud water is one of the best indicators of pollution levels because all water soluble impurities in one cubic meter of air from an air mass are found condensed in typically one milliliter or less of the cloud water. The 48-hr backward trajectories for all 39 cloud events during the 1993 field season (15 May 1993 - 14 October 1993) were computed using the Hybrid Single-Particle Lagrangian Integrated Trajectories (HY-SPLIT) model. Three sectors, identified as the polluted sector, from 290° to 65° azimuth relative to the site, the continental sector, 240° to 290° azimuth, and the marine sector, 65° to 240° azimuth, were used to classify the cloud forming air masses. The polluted sector was associated with the lowest overall pH averages, with the marine sector following closely behind. The highest average pH values were received from air masses indicated as having crossed the continental and the marine sectors (in combination), with the

largest portions of those air mass trajectories passing through the continental sector (exclusively continental sector air masses were also the most frequent). These observations are in agreement with findings in Colorado where aerosols produced by wind erosion were responsible for neutralizing the precipitation acidity.

SECTION II. In situ cloud measurements were taken during 39 individual cloud events between June and October 1993 in Mount Mitchell State Park, North Carolina. Cloud droplet spectra, obtained using a Forward Scattering Spectrometer Probe (FSSP) were used to determine total droplet number concentration, average droplet radius, and liquid water concentration. A total of 113 hourly cases were recorded with simultaneous FSSP spectra, cloud water acidity, ionic content, and meteorological data. A positive correlation was detected between the cloud water pH and droplet radius ($r^2 = 0.47$). Also, a negative correlation was detected between the cloud water pH and droplet number concentration ($r^2 = 0.64$). The data were then sorted into three populations based on the pH: $\text{pH} < 3.0$ ($n = 18$), $3.0 \leq \text{pH} < 3.7$ ($n = 71$), and $\text{pH} \geq 3.7$ ($n = 24$). It was observed that lower pH values were associated, on average, with higher cloud droplet number concentrations and lower radii, and *vice versa*. For nine cases, cloud albedo was determined from measurements of the NOAA satellite-based Advanced Very High Resolution Radiometer (AVHRR). These albedos were shown to vary directly with the number concentrations of cloud droplets and cloud condensation nuclei (CCN) and inversely with the average droplet radius and cloud water pH. Cloud reflectivity values calculated from *in situ* cloud microphysical and meteorological measurements were found in agreement with the values obtained from the AVHRR within error limits. Air mass history of the nine cloud cases was determined from back trajectories calculated with the Hybrid Single-Particle Lagrangian Integrated

Trajectories (HY-SPLIT) model. It was shown that the air mass trajectories were consistent with the experimental values of cloud water pH and cloud water ionic content, the polluted air masses being associated with higher cloud albedos.

ABSTRACT

JAMES CHARLES ULMAN, Captain, USAF. 1994, 115 pp., Master of Science, North Carolina State University.

Impact of Air Mass History on the Chemical, Microphysical, and Radiative Properties of Clouds at Mount Mitchell, North Carolina.

Cloud water acidity and ionic content, as measured at the Mount Mitchell State Park observing site (35° 44' 05" N, 82° 17' 15" W, 2038 m MSL--highest peak in the eastern U.S.), using a passive cloud water collector, are directly influenced by the trajectories of cloud forming air masses which pass over areas of varying levels of pollutant emission. Regions of the United States which are emitters of high levels of pollutants, such as SO_x and NO_x, will thus serve to reduce observed pH levels in cloud water samples and raise the levels of acidifying ions, such as sulfate and nitrate. The 48-hr backward trajectories for all 39 cloud events during the 1993 field season (15 May 1993 - 14 October 1993) were computed using the Hybrid Single-Particle Lagrangian Integrated Trajectories (HY-SPLIT) model. Polluted trajectories were associated with the lowest overall pH averages, with the marine trajectories following closely behind. For nine cases, cloud albedo was determined from measurements of the NOAA satellite-based Advanced Very High Resolution Radiometer (AVHRR). Air mass histories of these cases were shown to be in good overall agreement with expected values of cloud water pH and cloud water ionic content, with polluted air masses indicated to be associated with higher cloud albedos than clouds formed in less polluted air masses. This was the first time over a continental land area that such a study has been accomplished.

REFERENCES

- Aneja V. P. and Kim D.-S. (1993) Chemical dynamics of clouds at Mount Mitchell, North Carolina. *J. Air & Waste Mgmt. Assoc.* **43**, 1074-1083.
- Castillo R. A., Justo J. E. and McLaren E. (1983) The pH and ionic composition of stratiform cloud water. *Atmos. Environ.* **17**, 1497-1505.
- Charlson R. J., Schwartz S. E., Hales J. M., Cess R. D., Coakley J. A., Jr., Hansen J. E. and Hofmann D. J. (1992) Climate forcing by anthropogenic aerosols. *Nature* **255**, 423-430.
- Collett J. L., Jr., Daube B. C., Jr., Munger J. W. and Hoffmann M. R. (1989) Cloudwater chemistry in Sequoia National Park. *Atmos. Environ.* **23**, 999-1007.
- Collett J. L., Jr., Daube B. C., Jr. and Hoffmann M. R. (1990) The chemical composition of intercepted cloudwater in the Sierra Nevada. *Atmos. Environ.* **24A**, 959-972.
- DeFelice T. P. and Saxena V. K. (1990) Temporal and vertical distributions of acidity and ionic composition in clouds: comparison between modeling results and observations. *J. Atmos. Sci.* **47**, 1117-1126.
- DeFelice T. P. and Saxena V. K. (1991) The characterizations of extreme episodes of wet and dry deposition of pollutants on an above cloud-base forest during its growing season. *J. Appl. Meteor.* **30**, 1548-1561.
- Dignon J. (1992) NO_x and SO_x emissions from fossil fuels: a global distribution. *Atmos. Environ.* **26A**, 1157-1163.
- Draxler R. R. (1992) Hybrid Single-Particle Lagrangian Integrated Trajectories (HY-SPLIT): Version 3.0--User's Guide and Model Description. NOAA Technical Memo ERL ARL-195, Air Resources Laboratory, Silver Spring, MD, U.S.A., 26 pp.
- Environmental Protection Agency (1993) Regional Emission Inventories (1987-1991): Volume II--Emission Summaries. Office of Air Quality Planning and Standards, Research Triangle Park, NC, 27711.
- Falconer R. E. and Falconer P. D. (1980) Determination of cloud water acidity at a mountain observatory in the Adirondack Mountains of New York state. *J. Geophys. Res.* **85**, 7465-7470.

- Fan A., Hopke P. K. and Raunemaa T. M. (1994) A study on the sources of air pollutants observed at Tjorn, Sweden. *J. Aerosol Sci.* **25** Supp. 1, S31-S32.
- Gorham E., Martin F. B. and Litzau J. T. (1984) Acid rain: ionic correlations in the eastern United States. *Science* **225**, 407-409.
- Hansen A. D. A., Artz R. S., Pszenny A. A. P., and Larson R. E. (1990) Aerosol black carbon and radon as tracers for air mass origin over the North Atlantic Ocean. *Global Biogeochemical Cycles* **4**, 189-199.
- Hegg D. A. and Hobbs P. V. (1979) The homogeneous oxidation of sulfur dioxide in cloud droplets. *Atmos. Environ.* **13**, 981-987.
- Hegg D. A. and Hobbs P. V. (1981) Cloud water chemistry and the production of sulfates in clouds. *Atmos. Environ.* **15**, 1597-1604.
- Hegg D. A., Hobbs P. V. and Radke L. F. (1984) Measurements of the scavenging of sulfate and nitrate in clouds. *Atmos. Environ.* **18**, 1939-1946.
- Hegg D. A., Radke L. F. and Hobbs P. V. (1991) Measurements of Aitken nuclei and cloud condensation nuclei in the marine atmosphere and their relation to the DMS-cloud-climate hypothesis. *J. Geophys. Res.* **96**, 18,727-18,733.
- Hopke P. K., Gao N. and Cheng M. D. (1993) Combining chemical and meteorological data to infer source areas of airborne pollutants. *Chemometrics and Intel. Lab. Sys.* **19**, 187-199.
- Kadlecek J., McLaren S., Camarota N., Mohnen V. A. and Wilson J. (1983) Cloud water chemistry at Whiteface Mountain. In: *Precipitation Scavenging, Dry Deposition and Resuspension* (edited by Pruppacher H. R., Semonin R. G. and Slinn W. G. N.) pp. 103-114. Elsevier, New York, NY.
- Kelly T. J., Tanner R. L., Newman L., Galvin P. J. and Kadlecek J. A. (1984) Trace gas and aerosol measurements at a remote site in the northeast U.S. *Atmos. Environ.* **18**, 2565-2576.
- Kim D.-S. and V. P. Aneja (1992) Chemical composition of clouds at Mount Mitchell, North Carolina. *Tellus* **44B**, 41-53.
- Knollenberg, R. G. (1981) Techniques for probing cloud microstructure. In: *Clouds: Their Formation, Optical Properties, and Effects* (edited by Hobbs P. V. and Deepak A.), pp. 15-19. Academic Press, Inc., San Diego, CA.

- Lazrus A. L., Haagenson P. L., Kok G. L., Huebert B. J., Kreitzberg C. W., Likens G. E., Mohnen V. A. and Wilson W. E. (1983) Acidity in air and water in a case of warm frontal precipitation. *Atmos. Environ.* **17**, 581-591.
- Lin N.-H. and V. K. Saxena (1991a) Short communication: interannual variability in acidic deposition on the Mount Mitchell area forest. *Atmos. Environ.* **25A**, 517-524.
- Lin N.-H. and V. K. Saxena (1991b) In-cloud scavenging and deposition of sulfates and nitrates: case studies and parameterization. *Atmos. Environ.* **25A**, 2301-2320.
- Malm W. C., Hohnson C.E. and Bresch J. F. (1986) Applications of principal component analysis for purpose of identifying source-receptor relationships. In: *Receptor Methods for Source Apportionment* (edited by Pace T. G.), pp. 127-148, Air Pollut. Control Assoc., Pittsburgh, PA.
- Markus M. J., Bailey B. H., Stewart R., and Samson P. J. (1991) Low-level cloudiness in the Appalachian region. *J. Appl. Meteor.* **30**, 1147-1162.
- Millero F. J. (1974) The physical chemistry of seawater. *Ann. Rev. Earth Planet Sci.* **2**, 101-150.
- Mohnen V. A., Leonard K., and Bailey B. H. (1987) Cap cloud frequency and chemistry at Whiteface Mountain, *Preprint of AMS Annual Meeting*, pp. 51-54, January 1987, New Orleans, LA. Amer. Met. Soc., Boston, MA.
- Mohnen V. A. (1990) An Assessment of Atmospheric Exposure and Deposition to High Elevation Forests in the eastern United States. Technical Report, EPA 600/3-90/058 (U.S. Environmental Protection Agency, Washington, D.C., U.S.A.).
- Nagamoto C. T., Parungo F., Reinking R., Pueschel R. and Gerish T. (1983) Acid clouds and precipitation in eastern Colorado. *Atmos. Environ.* **17**, 1073-1082.
- Ogren J. and Rohde H. (1986) Measurements of the chemical composition of cloudwater at a clean air site in central Scandinavia. *Tellus* **38B**, 190-196.
- Pack D. H., Ferber G. J., Heffter J. L., Telegadas K., Angell J. K., Hoecker W. H. and Machta L. (1978) Meteorology of long-range transport. *Atmos. Environ.* **12**, 425-444.

- Parungo F., Boatman J. F., Sievering H., Wilkison S. W. and Hicks B. B. (1994) Trends in global marine cloudiness and anthropogenic sulfur. *J. Climate* **7**, 434-440.
- Petrenchuk O. P. and Drozdova V. M. (1966) On the chemical composition of cloud water. *Tellus* **18**, 280-286.
- Saxena V. K. and Lin N.-H. (1989) Contribution of acidic deposition on high elevation forest canopy to the hydrologic cycle. In: *Acidic Deposition*, pp. 193-201, Publ. No. 179. International Association of Hydrological Sciences (IAHS).
- Saxena V. K., Stogner R. E., Hendler A. H., DeFelice T. P., Yeh J.-Y. R. and Lin N.-H. (1989) Monitoring the chemical climate of the Mount Mitchell State Park for evaluation of its impact on forest decline. *Tellus* **41B**, 92-109.
- Saxena V. K. and J.-Y. R. Yeh (1989) Temporal variability in cloud water acidity: physico-chemical characteristics of atmospheric aerosols and windfield. *J. Aerosol Sci.* **19**, 1207-1210.
- Saxena V. K. and Lin N.-H. (1990) Cloud chemistry measurements and estimates of acidic deposition on an above cloudbase coniferous forest. *Atmos. Environ.* **24A**, 329-352.
- Twomey S. A. and Wojciechowski T. A. (1969) Observations of the geographical variation of cloud nuclei. *J. Atmos. Sci.* **26**, 684-688.
- Waldman J. M., Munger J. W., Jacob D. J., and Hoffmann M. R. (1985) Chemical characterization of stratus cloudwater and its role as a vector for pollutant deposition in a Los Angeles pine forest. *Tellus* **37B**, 91-108.
- Yeh, J.-Y. R. (1988) Measurements of cloud water acidity and windfield for evaluating cloud-canopy interactions in Mt. Mitchell State Park. MS thesis (available from D. H. Hill Library, North Carolina State University).

REFERENCES

- Alkezweeny, A. J., D. A. Burrows, C. A. Grainger, 1993: Measurements of cloud-droplet-size distributions in polluted and unpolluted stratiform clouds. *J. Appl. Meteor.*, **32**, 106-115.
- Baumgardner, D., 1983: An analysis and comparison of five water droplet measuring instruments. *J. Climate*, **22**, 891-910.
- Braham, R. R., Jr., 1974: Cloud physics of urban weather modification - a preliminary report. *Bull. Amer. Meteor. Soc.*, **55**, 100-106.
- Coakley, J. A., Jr., R. L. Bernstein, and P. A. Durkee, 1987: Effect of ship-stack effluents on cloud reflectivity. *Science*, **237**, 1020-1022.
- Charlson, R. J., J. E. Lovelock, M. O. Andreae, and S. G. Warren, 1987: Oceanic phytoplankton, atmospheric sulfur, cloud albedo and climate. *Nature*, **326**, 655-661.
- Charlson, R. J., S. E. Schwartz, J. M. Hales, R. D. Cess, J. A. Coakley, Jr., J. E. Hansen, and D. J. Hofmann, 1992: Climate forcing by anthropogenic aerosols. *Nature*, **255**, 423-430.
- Draxler, R. R., 1992: *Hybrid Single-Particle Lagrangian Integrated Trajectories (HY-SPLIT): Version 3.0—User's Guide and Model Description*. NOAA Technical Memorandum ERL ARL-195, Air Resources Laboratory, Silver Spring, MD, U.S.A., 26 pp.
- Durkee, P. A., F. Pfeil, E. Frost, and R. Shema, 1991: Global analysis of aerosol particle characteristics. *Atmos. Environ.*, **25A**, 2457-2471.
- Durkee, P. A., 1994: Cloud-climate feedback mechanisms: impact of the reduction of fossil fuel emissions—A science report for a sub-contract to the North Carolina State University. Unpublished.
- Environmental Protection Agency, 1993: *Regional Emission Inventories (1987-1991): Volume II—Emission Summaries*. Office of Air Quality Planning and Standards, Research Triangle Park, NC, 27711.
- Fouquart, Y., and H. Isaka, 1992: Sulfur emission, CCN, clouds and climate: a review. *Ann. Geophys.*, **10**, 462-471.

- Fukuta, N., and V. K. Saxena, 1979: A horizontal thermal gradient cloud condensation nucleus spectrometer. *J. Appl. Meteor.*, **18**, 1352-1362.
- Ghan, S. J., K. E. Taylor, J. E. Penner, and D. J. Erickson, III, 1990: Model test of CCN-cloud albedo climate forcing. *Geophys. Res. Lett.*, **17**, 607-610.
- Hegg, D. A., P. V. Hobbs, and L. F. Radke, 1984: Measurements of the scavenging of sulfate and nitrate in clouds. *Atmos. Environ.*, **18**, 1939-1946.
- Hegg, D. A., L. F. Radke, and P. V. Hobbs, 1991: Measurements of Aitken nuclei and cloud condensation nuclei in the marine atmosphere and their relation to the DMS-cloud-climate hypothesis. *J. Geophys. Res.*, **96**, 18,727-18,733.
- Kadlecek, J., S. McLaren, N. Camarota, V. A. Mohnen, and J. Wilson, 1983: Cloud water chemistry at Whiteface Mountain. In: H. R. Pruppacher, R. G. Semonin and W. G. Slinn (Editors), *Precipitation Scavenging, Dry Deposition and Resuspension*. Elsevier, New York, NY, pp. 103-114.
- Kim, D.-S., and V. P. Aneja, 1992: Chemical composition of clouds at Mount Mitchell, North Carolina. *Tellus*, **44B**, 41-53.
- Knollenberg, R. G., 1981: Techniques for probing cloud microstructure. In: P. V. Hobbs and A. Deepak (Editors), *Clouds: Their Formation, Optical Properties, and Effects*. Academic Press, Inc., San Diego, CA, pp. 15-19.
- Kondrat'yev, K. Y., V. I. Binenko, and O. P. Petrenchuk, 1981: Radiative properties of clouds influenced by a city. *Izv. Acad. Sci. USSR Atmos. and Oceanic Phys. (English Translation)*, **17**, 122-127.
- Lacis, A. A., and J. E. Hansen, 1974: A parameterization of the absorption of solar radiation in the earth's atmosphere. *J. Atmos. Sci.*, **31**, 118-133.
- Leaitch, W. R., G. A. Isaac, J. W. Strapp, C. M. Banic, and H. A. Wiebe, 1992: The relationship between cloud droplet number concentrations and anthropogenic pollution: observations and climatic implications. *J. Geophys. Res.*, **97**, 2463-2474.
- Lin, N.-H., and V. K. Saxena, 1991: In-cloud scavenging and deposition of sulfates and nitrates: case studies and parameterization. *Atmos. Environ.*, **25A**, 2301-2320.
- Mohnen, V. A., and J. A. Kadlecek, 1989: Cloud chemistry research at Whiteface Mountain. *Tellus*, **41B**, 79-91.

- Parungo, F., J. F. Boatman, H. Sievering, S. W. Wilkison, and B. B. Hicks., 1994: Trends in global marine cloudiness and anthropogenic sulfur. *J. Climate*, **7**, 434-440.
- Radke, L. F., J. A. Coakley, Jr., and M. D. King, 1989: Direct and remote observations of the effect of ships on clouds. *Science*, **246**, 1146-1149.
- Raga, G. B., and P. R. Jonas, 1993: On the link between cloud-top radiative properties and sub-cloud aerosol concentrations. *Quart. J. Roy. Meteor. Soc.*, **119**, 1419-1425.
- Saxena, V. K., 1991: Climate forcing due to non-sea-salt sulfates. In: *Proceedings of the International Symposium on Glaciers-Ocean-Atmosphere Interactions, September, 1990*. IAHS-208, St. Petersburg, FL, pp. 243-255.
- Saxena, V. K., R. E. Stogner, A. H. Hendler, T. P. DeFelice, J.-Y. R. Yeh, and N.-H. Lin, 1989: Monitoring the chemical climate of the Mount Mitchell State Park for evaluation of its impact on forest decline. *Tellus*, **41B**, 92-109.
- Saxena, V. K., and J.-Y. R. Yeh, 1989: Temporal variability in cloud water acidity: physico-chemical characteristics of atmospheric aerosols and windfield. *J. Aerosol Sci.*, **19**, 1207-1210.
- Saxena, V. K., and J. D. Grovenstein, 1993: Impact of changes in sulfate aerosol loading on greenhouse warming. In: *Proceedings of the 1993 U.S. EPA/A&WMA International Symposium on Measurement of Toxic and Related Air Pollutants*. VIP-34, Air and Waste Management Association, Pittsburgh, PA, pp. 464-469.
- Slingo, A., 1990: Sensitivity of earth's radiation budget to changes in low clouds. *Nature*, **343**, 49-51.
- Twomey, S. A., 1977: The influence of pollution on the shortwave albedo of clouds. *J. Atmos. Sci.*, **34**, 1149-1152.
- Twomey, S. A., M. Piepgrass, and T. L. Wolfe, 1984: An assessment of the impact of pollution on global cloud albedo. *Tellus*, **36B**, 356-366.
- Twomey, S. A., 1991: Aerosols, clouds, and radiation. *Atmos. Environ.*, **25A**, 2435-2442.
- Wigley, T. M. L., 1991: Could reducing fossil-fuel emissions cause global warming? *Nature*, **349**, 3503-3505.